JASCO
APPLIED SCIENCES

Johan Castberg Passive Acoustic Monitoring

Marine Mammal Acoustic Occurrence and Soundscape Analysis

Submitted to:

Jűrgen Weissenberg
Equinor ASA
Contract: 4503836271

Authors:

Julien J-Y. Delarue
Jessica B. Winters
Katie K. Kowarski
S. Bruce Martin

9 September 2020

P001533-001
Document 02053
Version 2.1

Suggested citation:

Delarue, J. J-Y, J.B. Winters, K.K. Kowarski, and S.B. Martin. 2020. *Johan Castberg Passive Acoustic Monitoring: Marine Mammal Acoustic Occurrence and Soundscape Analysis*. Document 02053, Version 2.1. Technical report by JASCO Applied Sciences for Equinor ASA.

Disclaimer:

The results presented herein are relevant within the specific context described in this report. They could be misinterpreted if not considered in the light of all the information contained in this report. Accordingly, if information from this report is used in documents released to the public or to regulatory bodies, such documents must clearly cite the original report, which shall be made readily available to the recipients in integral and unedited form.

Contents

Figures

Tables

Executive Summary

Acoustic data were recorded at the Johan Castberg oil field in the southern Barents Sea at three locations from October 2018 until June 2019 to assess the presence of marine mammals and characterize the underwater soundscape. The marine mammal analysis was focused on two stations as the third one stopped recording early and the data suffered from poor audio quality.

Five marine mammal species were detected during the study: fin, humpback, killer, sperm whales and a dolphin species whose signals were tentatively attributed to white-beaked dolphins on the basis of sighting records in the area and habitat preference of this species. These species were generally detected at similar levels at PAMEast and PAMNorth, except for dolphins which were more common at PAMNorth. Dolphins showed a pronounced seasonal pattern of occurrence, with very few detections in winter. Killer whale occurred sporadically, their occurrence peaking in November and March, possibly coinciding with that of prey species. Along with dolphins, sperm and fin whales were the most commonly detected species, occurring throughout the study, albeit slightly less frequently in late winter than during the rest of the year. Humpback whale detections peaked in March, which may be associated with the transit of migrating animals through the area as they return to feed on spring spawning herring.

Sound levels at Johan Castberg were generally higher than in other areas of the North Atlantic previously monitored by JASCO, particularly at low frequencies and in absence of sustained anthropogenic activity. A significant contribution to the soundscape at low frequencies is that of fin whale song notes, centered around 20 Hz. Considering other North Atlantic areas during the month of November when fin whale songs are near their peak, the power spectral density levels measured at Johan Castberg were more comparable to other North Atlantic locations. Because of generally elevated noise levels, the detection range of the detected species under average conditions were between a few hundred meters to a few kilometers, indicating that the results provide a good characterization of marine mammal occurrence inside, and in close proximity to, the Johan Castberg oil field. Vessels were detected on 36-40% of days but only 4-5% of recording hours. Their contribution to the soundscape was therefore limited. Besides vessels, the only other anthropogenic activity detected were seismic airgun sounds recorded on 10–12 and 16–21 May 2019 and associated with a seabed profiling survey for a fiber optic cable route that operated briefly near the outer edges of the oil field.

Because of the limited anthropogenic activity recorded in the study area, the results presented in this report provide a good baseline against which to assess the occurrence of marine mammals in the study area in the future. It is harder to reconcile the relatively high noise levels with the low levels of human activity in the area. It is possible that the extended fin whale detection period (compared to what is typical for the species) and higher source levels of their calls in this area resulted in higher acoustic energy around 20 Hz. However, noise levels were also higher than in other comparable areas at higher frequencies. Although all efforts have been made to ensure that the calibration curves were correctly applied to the data to produce accurate sound measurements, issues with calibration or the recorders cannot be entirely ruled out by JASCO.

1. Introduction

This report presents the results of an analysis of underwater acoustic data recorded off Northern Norway, in the southwestern Barents Sea. Three acoustic recorders were deployed in the Johan Castberg oil field, jointly held by Equinor Energy AS (50%), Var Energy AS (30%), and Petoro AS (20%). The objective of this passive acoustic monitoring (PAM) program was to characterize the underwater soundscape and the occurrence of vocalizing marine mammals.

1.1. Background on the Study Area

The study area is located in the southwestern Barents Sea. The Barents Sea is a marginal sea of the Arctic Ocean characterized by a relatively shallow shelf (~230 m) and year-round open water. The area is known for its productivity and supports the largest cod fishery and one of the largest herring fisheries in the world (Ottersen and Stenseth 2001). This productivity is driven in part by the mixing of several water masses: the northern termination of the Gulf Stream with its warm and saline Atlantic water, cold arctic water from the north, and coastal water characterized by relatively high temperatures but low salinity (Loeng 1991) (Figure 1). The influx of warm Atlantic water explains why the southern Barents Sea is largely devoid of sea ice, even in winter, with sea surface temperature remaining near or above 5°C year-round. The southern edge of the ice pack generally reaches the area near Bear Island, about 200 km to the north of the Johan Castberg oil field. The eastern and northern Barents Sea are considering arctic warming hotspots, a process driven by increased flux from Atlantic water and decreasing sea ice import from the Arctic interior, leading to lower stratification and ultimately unknown consequences for the productivity of the Barents Sea as a whole (Lind et al. 2018).
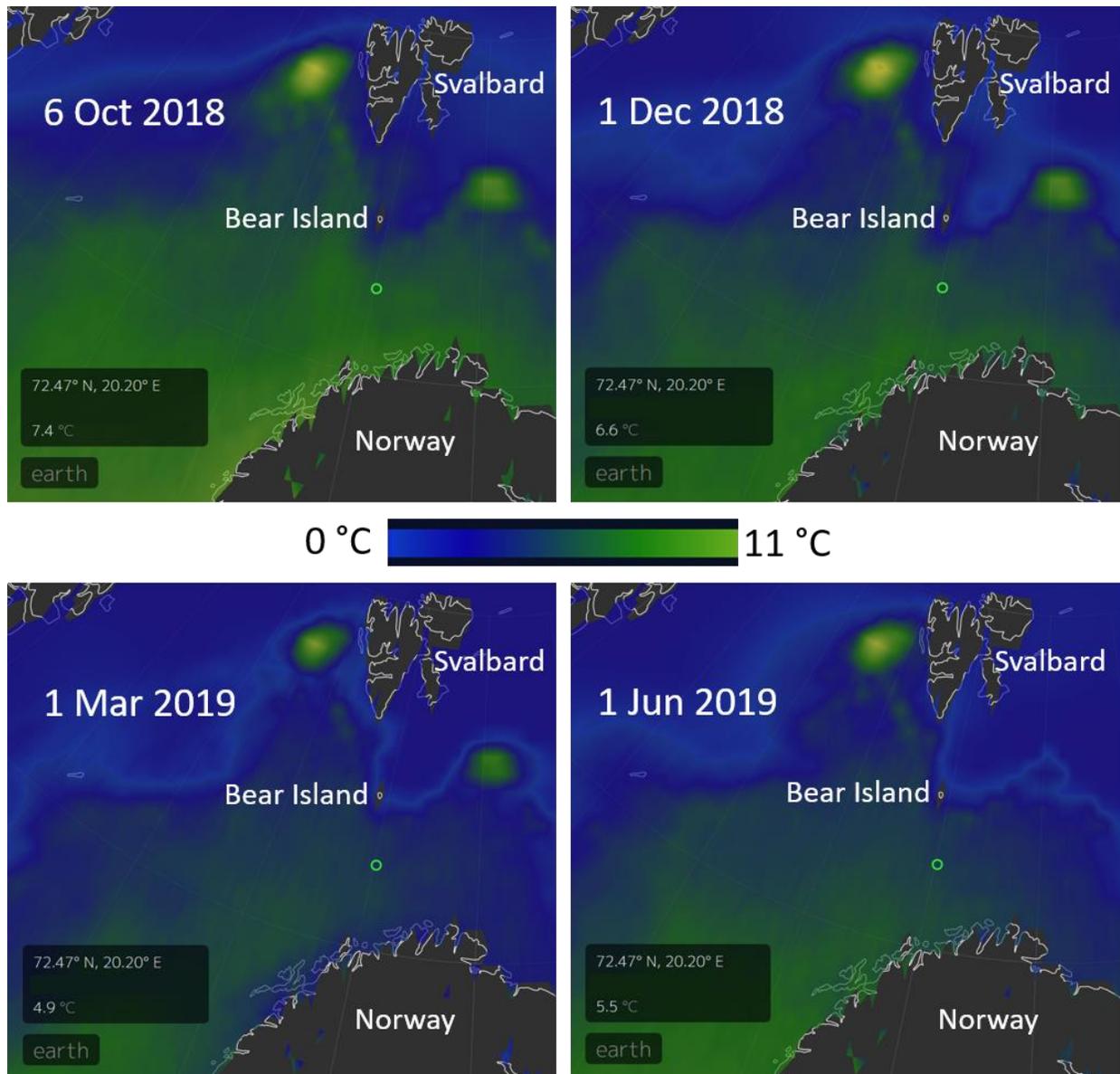
Figure 1. View of the North Atlantic and Barents Sea showing sea surface temperature during the recording period. It highlights the boundary between warm Atlantic water (green) and cold arctic water (blue). The green circle shows the location of the study area (source: earth.nullschool.net 2020).

1.2. Soniferous Marine Life and Acoustic Monitoring

Passive Acoustic Monitoring (PAM) is increasingly preferred as a cost-effective and efficient survey method. It is less dependent on weather conditions than visual surveys and is unaffected by visibility. Most importantly, it is nonintrusive. It relies on the premise that the monitored species produce detectable sounds. For a marine mammal vocalization to be detected, the received amplitude of the vocalization at the monitoring location must be above background noise levels in at least one of vocalization's frequency bands. The distance over which it can be detected depends on background noise levels, source levels of the vocalization, depth of the animal, and acoustic propagation properties of the environment. Background or ambient noise levels vary due to fluctuations in natural sounds (e.g., seismic and biological activity, wind, precipitation, and waves) and anthropogenic sounds (mainly vessels). Acoustic

propagation also varies seasonally due to physical properties of the water column. Seasonal and sex- or age-biased differences in sound production, as well as signal frequency, source level, and directionality all influence the applicability and merit of PAM, and its effectiveness must be considered separately for each species. Ultimately, a lack of detections of marine mammal vocalizations cannot be strictly interpreted as an absence of a species of interest but rather as a lack of vocalizing animals, which may or may not indicate physical absence from an area.

Marine mammals are the main biological contributors to the underwater soundscape, particularly in deep water and at high latitudes, and they sometimes introduce substantial amounts of energy. For instance, fin whale (*Balaenoptera physalus*) songs can raise noise levels in the 18–25 Hz band by 15 dB for extended durations (Simon et al. 2010). Marine mammals, cetaceans in particular, rely almost exclusively on sound for navigating, foraging, breeding, and communicating (Clark 1990, Edds-Walton 1997, Tyack and Clark 2000). Although species differ widely in their vocal behavior, many can be reasonably expected to produce sounds on a regular basis. Most odontocetes perform foraging dives multiple times a day, producing echolocation clicks to detect their prey. Whistles are also used throughout the day to maintain group cohesion and for communication. In baleen whales, the most intense period of sound production coincides with the breeding season, usually from fall to spring, when males advertise their breeding conditions via the use of long, stereotyped displays called songs (Helweg et al. 1998, Croll et al. 2002, Stafford et al. 2007, Morano et al. 2012, Herman et al. 2013). Outside the breeding season, vocal output decreases in most species, however, most still produce social and feeding sounds. For several species such as fin, blue (*B. musculus*) and sei (*B. borealis*) whales, increased overlap in spectral features of signals produced (mainly) during the feeding season complicates their identification and use for PAM (Ou et al. 2015). In some areas, some species are remarkably cryptic acoustically. This is the case of minke whales (*B. acutorostrata*) in the North Atlantic, for instance (Delarue et al. 2017). Many pinnipeds also display pronounced seasonal variations in their acoustic output. Bearded seals (*Erignathus barbatus*)can dominate the underwater soundscape during the Arctic winter and spring, but their vocalizations are rarely heard in late spring and early summer (MacIntyre et al. 2013). Sound production is high year-round in gregarious species such as walruses (*Odobenus rosmarus*) (Hannay et al. 2013). It is generally low in grey seals outside of the breeding seasons, except near coastal haul-outs.

Knowledge of the acoustic signals of the marine mammals expected in the study area varies across species. These sounds can be split into two broad categories: Tonal signals (including baleen whale moans, delphinid whistles, and some pinniped vocalizations) and echolocation clicks (produced by all odontocetes mainly for foraging and navigating). Although the signals of most species have been described to some extent, these descriptions are not always sufficient for reliable systematic identification, let alone to design automated detectors to process large data sets (Table 2). This is particularly true for harp (*P. groenlandica)* and hooded (*Cystophora cristata)* seals. In general, baleen whale signals produced as part of their songs can be reliably identified to the species level. However, the tonal signals produced by blue, fin, and sei whales tend to show greater overlap in late spring and summer, which limits our ability to identify and monitor these species acoustically. These issues are considered and discussed on a case-by-case basis.

In non-mammalian aquatic species, the practical use of acoustic monitoring to date has been largely limited to fish, although a number of crustaceans and other aquatic invertebrates are known to produce sounds (Staaterman et al. 2011, Lillis and Mooney 2016). Many fish species produce sound during the breeding season or when engaged in agonistic behaviors (Amorim 2006). Several species of gadids (cod family), such as the Northern cod (*Gadus morhua*) and haddock (*Melanogrammus aeglefinus*), form spawning aggregations that have been detected acoustically (Nordeide and Kjellsby 1999, Hawkins et al. 2002). The acoustic monitoring of fish is hindered by a limited understanding of their acoustic repertoire and behavior. Nevertheless, the stereotypical nature of acoustic signals produced by some species have led to the development of dedicated acoustic detectors (e.g., cod; see Urazghildiiev and Van Parijs 2016). Regardless of species identity, fish choruses can raise ambient noise levels and therefore influence local soundscapes (Erbe et al. 2015).

The biological focus of this study was on marine mammals. Eleven cetacean species are known or thought to occur in the study area (Table 1). The total number of cetacean species found in the Barents Sea is higher, but several are only associated with sea ice or coastal areas surrounding Svalbard and other large islands and are therefore not found in the southern Barents Sea (Kovacs et al. 2009). Among

the baleen whales, minke, fin, and humpback (*Megaptera novaeangliae*) whales are the most common species ((Kovacs et al. 2009, Skern-Mauritzen et al. 2011). They occur seasonally during summer and fall. Blue whales may also occur in the study area, based on small number of sightings between Bear Island and Svalbard (Kovacs et al. 2009) and evidence for increasing numbers around Svalbard (Storrie et al. 2018). Modern records of sei whales off northern Norway are rare, but they were hunted off Finmark during the industrial whaling era (Prieto et al. 2012). Recent sightings near Svalbard (Storrie et al. 2018) suggest that the species may be returning to historical feeding grounds and could be encountered in the study area.

Odontocetes likely to occur in the study area include killer (*Orcinus orca*), long-finned pilot (*Globicephala melas*), and sperm (*Physeter macrocephalus*) whales as well as white-beaked dolphins (*Lagenorhynchus albirostris*), harbor porpoises (*Phocoena phocoena*), and northern bottlenose whales (*Hyperoodon ampullatus)* (Kovacs et al. 2009). They are regularly sighted in the Barents Sea (Øien 1996). Killer whales are abundant in Norwegian waters as far north as Bear Island and Svalbard although their relative use of inshore vs offshore waters is unclear. Sperm whales are thought to occur in Norwegian waters primarily along the continental slope and, as such, they may not be particularly common in the study area, located 200 km east of the continental shelf break (see Figure 7). Based on their cold-water preference and the fact that the study area remains ice-free year-round, white-beaked dolphins may be year-round residents in the study area. Northern bottlenose whales are believed to share a similar distribution as sperm whales. Historical catch and sighting records suggest a core distribution between Iceland and Svalbard, with a number of records distributed along the continental slope to the west of the Barents Sea shelf. Incidental sightings on the continental shelf suggest that their occasional presence cannot be ruled out in the study area (Øien and Hartvedt 2011, Storrie et al. 2018). Long-finned pilot whales are an abundant species in the northeast Atlantic but are rarely sighted off northern Norway (Kovacs et al. 2009). Their preference for deep continental slope waters suggest that they are likely rare in the study area. Harbor porpoise are abundant in the Barents Sea and occur as far north as Svalbard but are predominantly found in shallow coastal areas around Svalbard and along the Norwegian coast (Bjørge et al. 1991, Storrie et al. 2018). Movements between these areas may result in a sporadic occurrence in the study area. It is possible that delphinid species usually encountered in more temperate areas, such as white-sided (*L. acutus*), long-beaked common (*Delphinus delphis*), and bottlenose (*Tursiops truncatus*) dolphins, occur on the Barents Sea shelf in summer. A few sightings have been recorded in the southern Barents Sea along the continental shelf break, but these observations are considered to be of vagrant individuals (Kovacs et al. 2009).

Of the seven pinniped species known to occur in the Barents Sea, four are not expected in the study area because they exhibit year-round association with sea ice (ringed seal (*Pusa hispida*)) or coastal, shallow waters (grey (*Halichoerus grypus*) and harbor seals (*Phoca vitulina*)), or due to their need for shallow (<80 m) productive waters in proximity to suitable haul-out platforms (sea ice or coastline; walrus). Bearded seals are benthic feeders and are generally found on shallow shelves within range of the pack ice. However, juveniles can wander away from the typical population range and are not uncommon along the northern coast of mainland Norway in summer (Kovacs et al. 2009). In addition, the species can be found in deep waters (> 500 m) off West Greenland and in the Canadian Arctic (Frouin-Mouy et al. 2017). Therefore, bearded seals could occasionally occur in the study area. Harp seals may occur occasionally, as they transit between whelping or molting areas in the southeastern Barents Sea and summer feeding grounds along the receding ice edge in the northern Barents Sea (Kovacs et al. 2009). However, the study area appears to lie at the edge of or outside their migration corridors. Northeast Atlantic hooded seals breed off northeast Greenland and perform extensive foraging trips in summer, including along the edge of the continental shelf between Norway and Svalbard (Kovacs et al. 2009). One can therefore not rule out that some Northeast Atlantic hooded seals may be found in the study area.

Table 1. List of cetacean and pinniped species known to occur (or possibly occurring) in the study area.

Species	Scientific name	Occurrence
Mysticetes		
Fin whales	*Balaenoptera physalus*	Common
Humpback whales	*Megaptera novaeangliae*	Common
Minke whales	*Balaenoptera acutorostrata*	Common
Blue whales	*Balaenoptera musculus*	Rare
Sei whales	*Balaenoptera borealis*	Rare
Odontocetes		
White-beaked dolphins	*Lagenorhynchus albirostris*	Common
Killer whales	*Orcinus orca*	Common
Long-finned pilot whales	*Globicephala melas*	Common
Harbor porpoises	*Phocoena*	Common
Sperm whales	*Physeter macrocephalus*	Common
Northern bottlenose whales	*Hyperoodon ampullatus*	Rare
Pinnipeds		
Harp seals	*Pagophilus groenlandica*	Rare
Bearded seals	*Erignathus barbatus*	Rare
Hooded seals	*Cystophora cristata*	Rare

Table 2. Acoustic signals used for identification and automated detection of the species expected off northern Norway and supporting references.

Species	Identification signal	Automated detection signal	Reference
Minke whales	Pulse train	Pulse train	(Risch et al. 2013)
Sei whales	Tonal downsweep	Tonal downsweep	(Baumgartner et al. 2008)
Blue whales	A-B vocalization, tonal downsweep	A-B vocalization	Mellinger and Clark (2003), Berchok et al. (2006)
Fin whales	20-Hz pulse, tonal downsweep	20-Hz pulse	Watkins (1981), Watkins et al. (1987)
Humpback whales	Moan, grunt	Moan	Dunlop et al. (2008), Kowarski et al. (2018)
White-beaked dolphins	Burst pulses, clicks	Whistles, clicks	(Rasmussen and Miller 2002)
Killer whales	Whistle, pulsed vocalization	Tonal signal <6 kHz	Ford (1989), Deecke et al. (2005)
Long-finned pilot whales	Whistle, pulsed vocalization	Tonal signal <6 kHz	(Nemiroff and Whitehead 2009)
Harbor porpoises	Click	Click	(Au et al. 1999)
Sperm whales	Click	Click	Møhl et al. (2000), (2003)
Northern bottlenose whales	Click	Click	Hooker and Whitehead (2002), Wahlberg et al. (2012)
Harp seal	Diverse	N/A	(Terhune 1994)
Bearded seal	Trills	Trills	(Risch et al. 2007)
Hooded seal	Diverse	N/A	(Ballard and Kovacs 1995)

1.3. Ambient Ocean Soundscape

The ambient, or background, sound levels that create the ocean soundscape are comprised of many natural and anthropogenic sources (Figure 2). The main environmental sources of sound are wind, precipitation, and sea ice. Wind-generated noise in the ocean is well-described (e.g., Wenz 1962, Ross 1976), and surf sound is known to be an important contributor to near-shore soundscapes (Deane 2000). In polar regions, sea ice can produce loud sounds that are often the main contributor of acoustic energy in the local soundscape, particularly during ice formation and break up. Precipitation is a frequent noise source, with contributions typically concentrated at frequencies above 500 Hz. At low frequencies (<100 Hz), earthquakes and other geological events contribute to the natural soundscape (Figure 2).
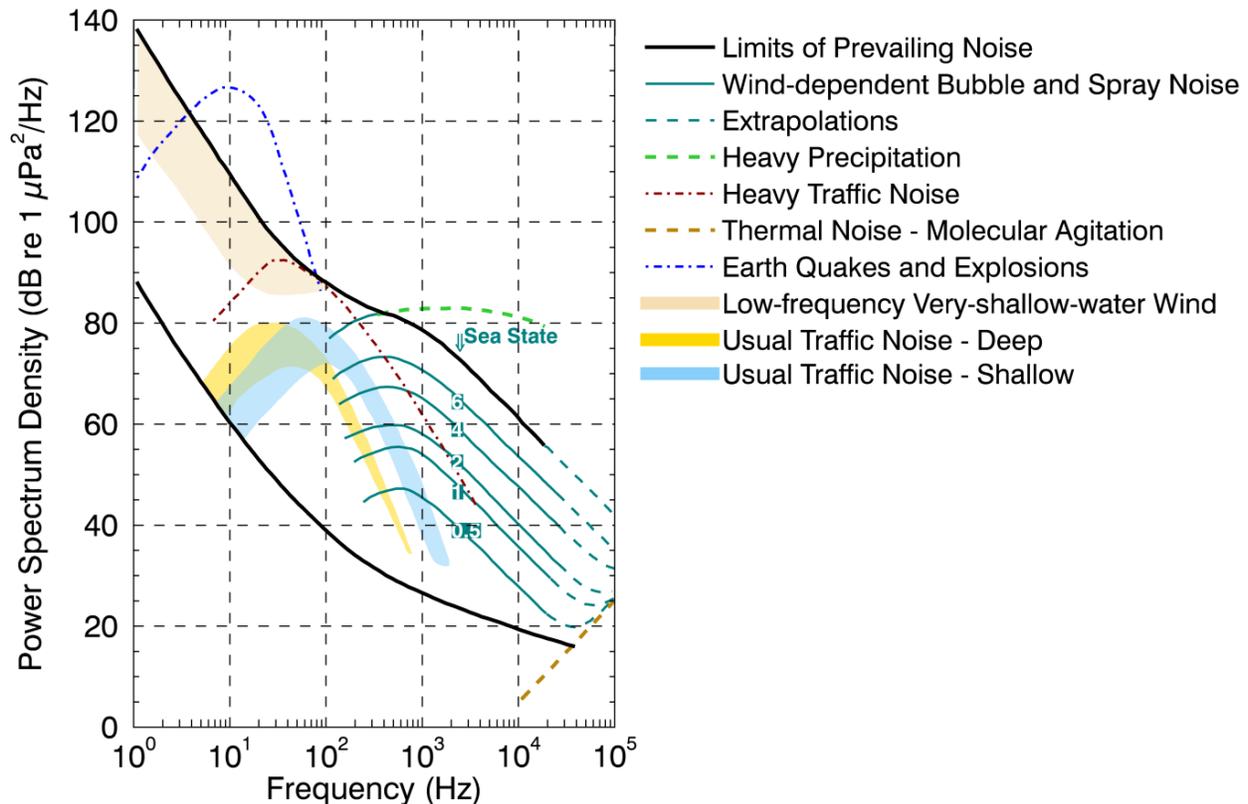
Figure 2. Wenz curves describing pressure spectral density levels of marine ambient sound from weather, wind, geologic activity, and commercial shipping (adapted from NRC 2003, based on Wenz 1962). Thick lines indicate limits of prevailing ambient sound.

1.4. Anthropogenic Contributors to the Soundscape

Anthropogenic (human-generated) sound can be a by-product of vessel operations, such as engine sound radiating through vessel hulls and cavitating propulsion systems, or it can be a product of active acoustic data collection with seismic surveys, military sonars, echosounders as the main contributors. Marine construction projects often involve nearshore blasting and pile driving that can produce high levels of impulsive-type noise that can be heard at 100 km or further. The contribution of anthropogenic sources to the ocean soundscape has increased greatly from the 1950s to 2010, largely driven by greater maritime shipping traffic (Ross 1976, Andrew et al. 2011). Recent trends suggest that global sound levels are leveling off or potentially decreasing in some areas (Andrew et al. 2011, Miksis-Olds and Nichols 2016). Oil and gas exploration with seismic airguns, marine pile driving and oil and gas production platforms elevate sound levels over radii of 10 to 1000 km when present (Bailey et al. 2010, Miksis-Olds

and Nichols 2016, Delarue et al. 2018).The extent of seismic survey sounds has increased substantially following the expansion of oil and gas exploration into deep water, and seismic sounds can now be detected across ocean basins (Nieukirk et al. 2004).

1.4.1. Vessel Traffic and Fishing activity

Figure 3 shows the marine traffic in the project area derived from vessel broadcasting on the Automated Identification System (AIS). The location of the Johan Castberg field is shown in the figure. The distance between the Johan Castberg field and the nearest shipping lanes along the Norwegian coastline is approximately 150 km. There is limited shipping traffic in the immediate vicinity of the Johan Castberg field. Most of the traffic in offshore waters is associated with fishing vessels, particularly around Bear Island (north of the Johan Castberg field) and along the slope of the continental shelf to the west of the Johan Castberg field. The four areas of denser traffic to the south of the field are presumably associated with localized fishing activities.

Figure 4 shows the tracks of fishing vessels around Johan Castberg out to 70 km. Vessels operated in the vicinity of the recorders in all months but were closest to them in late winter and spring.
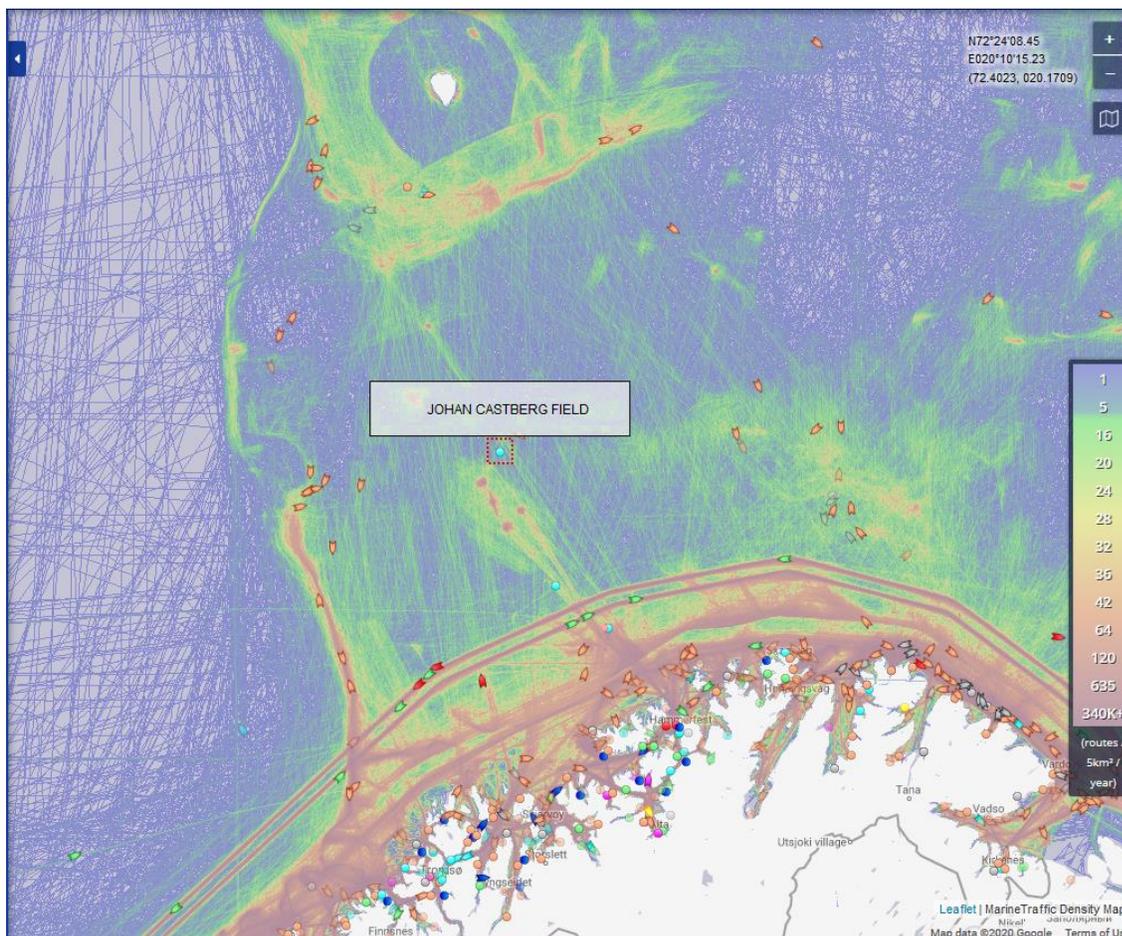
Figure 3. Vessel traffic off northern Norway in 2017 (source: marinetraffic.com; accessed 4 May 2020).
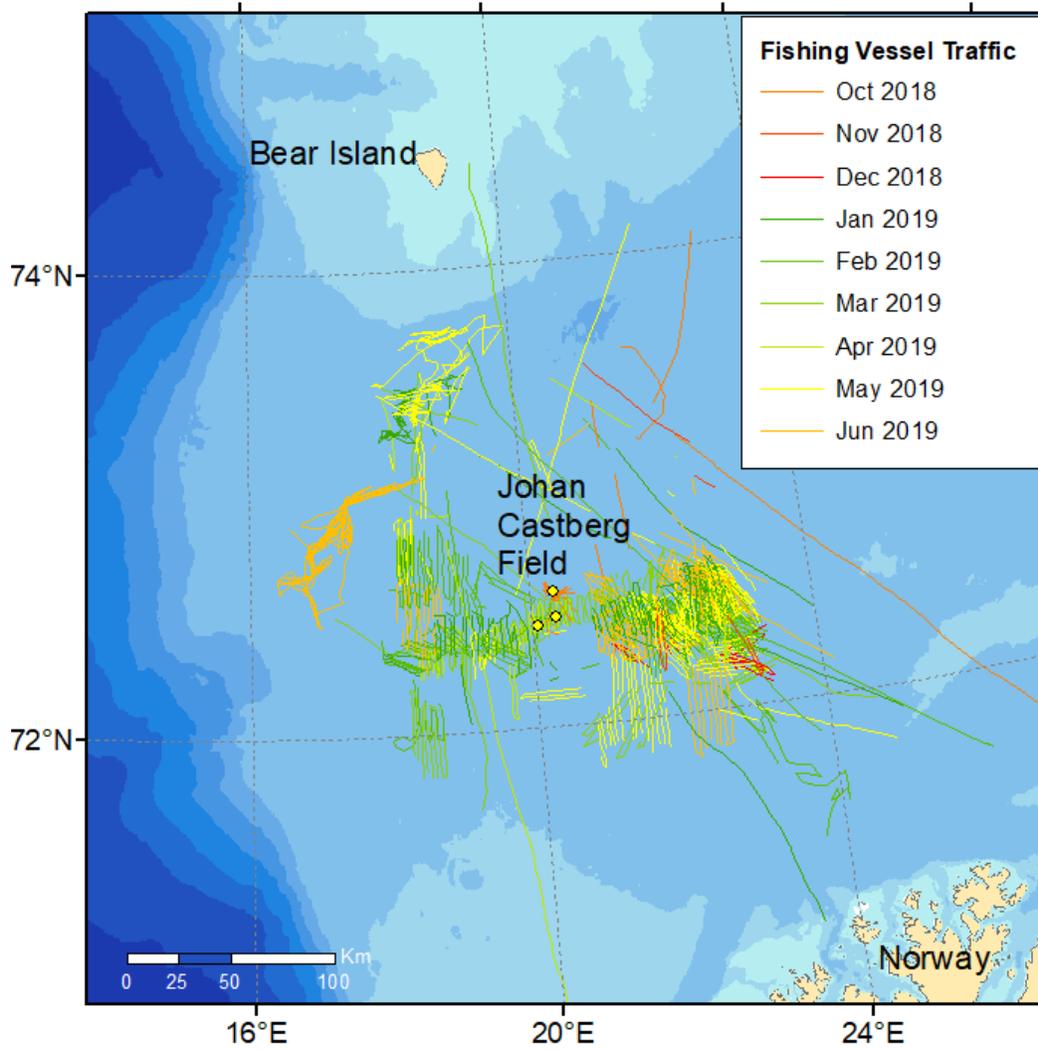
Figure 4. Presumed fishing vessel traffic on the Johan Casterg field and out to 70 km from October 2018 until June 2019 recorded by Norway's Fiskeridirektoratet. The three yellow dots show the location of the acoustic recorders deployed during the study over the same period.

1.4.2. Oil and Gas Activities

Norway's oil and gas activities are distributed across the North Sea, the Norwegian Sea, and the southern Barents Sea (Figure 5). The latter is the most recently developed but is considered to have the largest potential for oil and gas. It has seen several oil and gas discoveries in recent years (Figure 6). There are two fields actively producing south of Johan Castberg, namely Snøhvit and Goliat, and a number of newly discovered fields awaiting further assessment. The Johan Castberg oil field was discovered and proven between 2011 and 2013. It is currently under development, and production is expected to start in 2022 (https://www.norskpetroleum.no/en/facts/field/johan-castberg/).
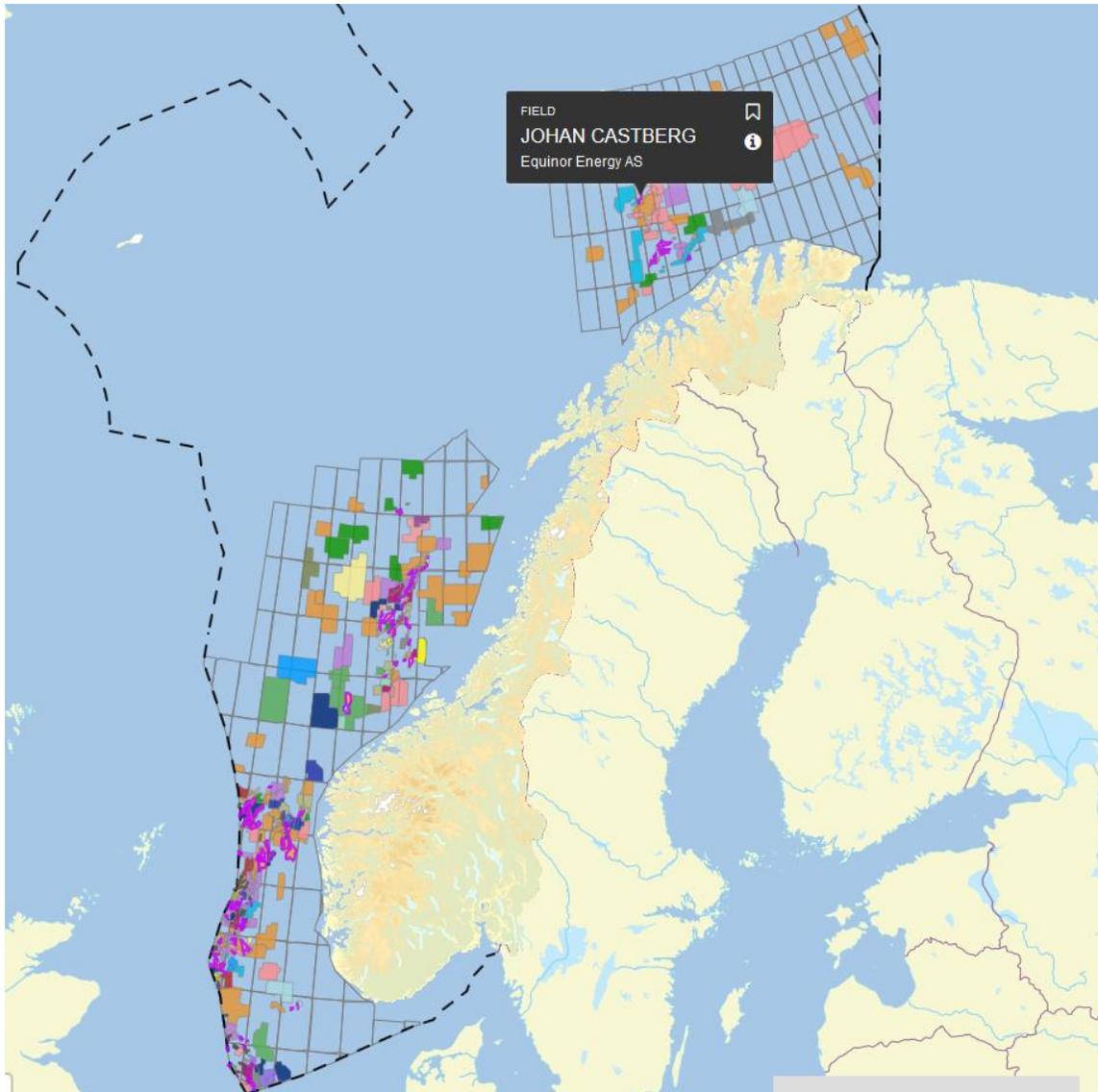
Figure 5. Norway's oil and gas resources (source: https://www.norskpetroleum.no/en/interactive-map-quick-downloads/interactive-map/; accessed 6 May 2020)
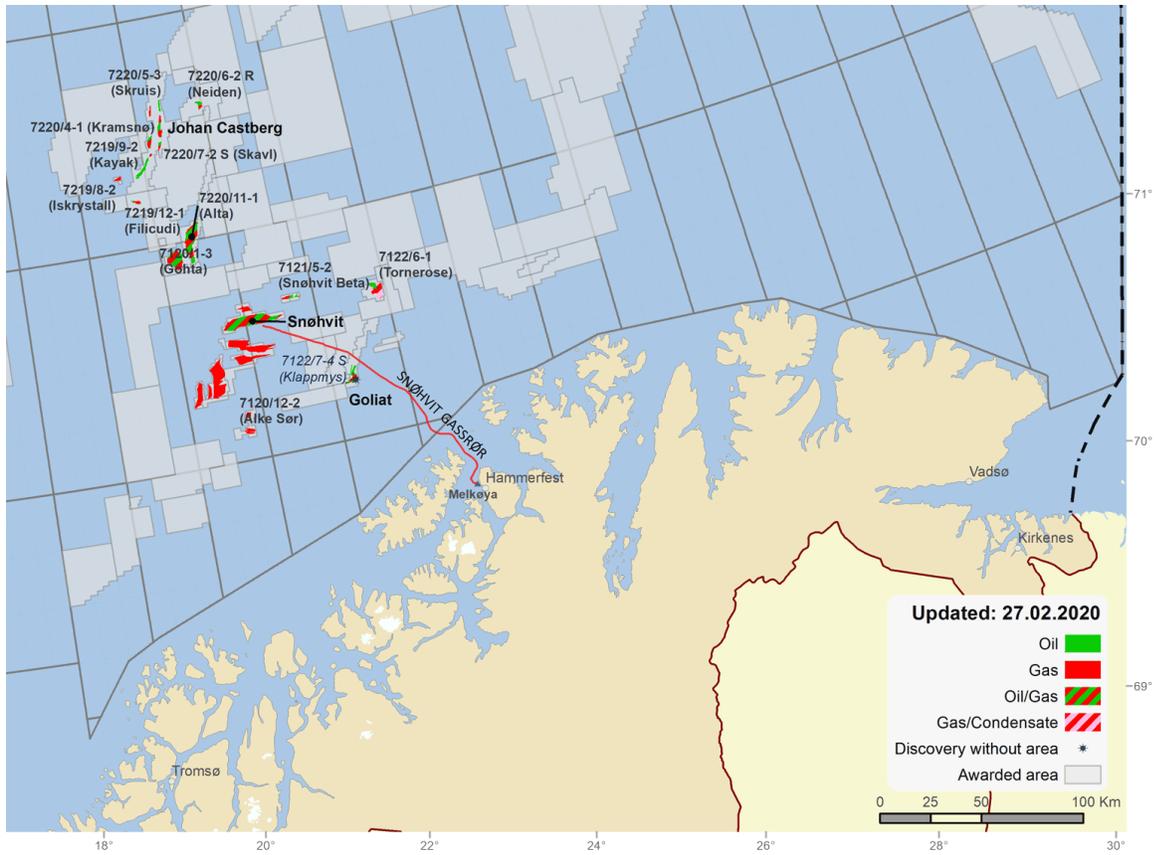
Figure 6. Norway's southern Barents Sea oil and gas resources (source: https://www.norskpetroleum.no/en/interactive-map-quick-downloads/quick-downloads/; accessed 7 May 2020).

2. Methods

2.1. Data Acquisition

The acoustic data were provided to JASCO by Equinor. The data were recorded using RTsys recorders (RTsys 2020). Three locations (PAMEast, PAMNorth, and PAMWest) in the Barents Sea were monitored for up to 257 days starting in October 2018 (Table 3; Figure 7). A system failure with the recorder deployed at PAMWest resulted in a shorter recording duration than at the other two stations.

Accurate noise measurements rely on precise calibration of the recording systems. Based on information provided by Equinor, calibrations were performed during the last overhaul of the recorders at the RTsys office in June 2018 and not before and after the deployment, according to ISO standard. The recorders were equipped with Aguatech hydrophones with sensitivity of −162 dB re 1µPa/V and a bandwidth 2 Hz to 80 kHz (Jürgen Weissenberger, personal communication).

Calibration curves provided to JASCO by Equinor show a relatively flat frequency response from ~15 Hz to 20 kHz. Above 20 kHz, the signal decays rapidly. The headers of the RTsys .wav files specified a hydrophone sensitivity of -160 dB re 1 µPa/V for the PAMEast and PAMNorth recorders as well as -170.4 dB re 1 µPa/V for PAMWest; these values were employed for the final analysis. Similarly, the file headers specified different gain values and gain corrections; these values were employed for the analysis.

Table 3. Location, depth, and operation period of the RTSys recorders deployed for this study.

Station	Latitude	Longitude	Depth (m)	Deployment	Record end	Duration (Days)
PAMEast	72.46501	20.34738	358	2018 Oct 5	2019 May 26	233
PAMNorth	72.57413	20.34345	405	2018 Oct 5	2019 Jun 19	257
PAMWest	72.43361	20.09079	360	2018 Oct 11	2019 Jan 30	111
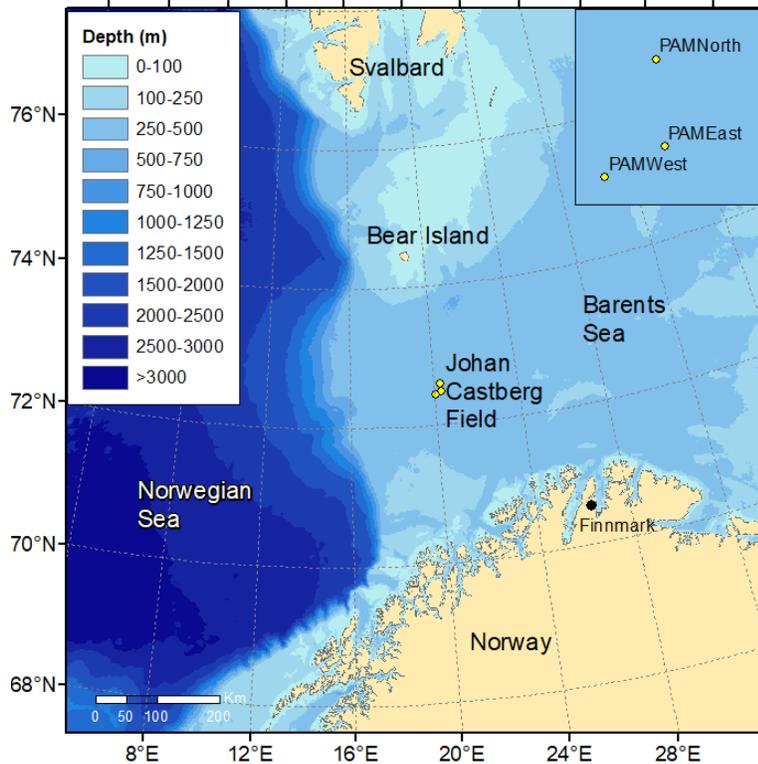
Figure 7. The Johan Castberg field in relation to the surrounding landmasses. The insert map shows the relative position of the three acoustic recorders.

2.2. Ambient Noise

2.2.1. Total Ocean Sound Levels

The first stage of the total sound level analysis involves computing the peak and rms sound pressure level (SPL) for each minute of data. This reduces the data to a manageable size without compromising the value for characterizing the soundscape (ISO 2017a, Ainslie et al. 2018, Martin et al. 2019). The SPL analysis is performed by averaging 120 fast-Fourier transforms (FFTs) that each include 1 second of data with a 50% overlap and that use the Hann window to reduce spectral leakage. The 1-minute average data were stored as power spectral densities (1 Hz resolution) and summed over frequency to calculate decidecade band SPL levels. Decidecade band levels are very similar to 1/3-octave-band levels. Table A-1 lists the decidecade band frequencies, and Table A-2 lists the decade-band frequencies. The decidecade analysis sums as many frequencies as contained in the recorded bandwidth in the power spectral density data to a manageable set of up to 45 bands that approximate the critical bandwidths of mammal hearing. The decade bands further summarize the sound levels into four frequency bands for manageability. Detailed descriptions of the acoustic metrics and decidecade analysis can be found in Appendices A.1 and A.2.

The results will be delivered in spreadsheet format and also presented graphically as:

- **Band-level plots**: These strip charts show the averaged received sound pressure levels as a function of time within a given frequency band. We show the total sound levels from 10 up to 63,000 Hz and the levels in the decade bands of 10–100, 100–1000, 1000–10,000, and 10,000–63,000 Hz. The 10–100 Hz band is associated with fin, sei, and blue whales, large shipping vessels, flow and mooring noise, and seismic survey pulses. Sounds within the 100–1000 Hz band are generally associated with the physical environment such as wind and wave conditions but can also include both biological and anthropogenic sources such as minke, right, and humpback whales, fish, nearby vessels, and pile

driving. Sounds above 1000 Hz include high-frequency components of humpback whale sounds, odontocete whistles and echolocation signals, wind- and wave-generated sounds, and sounds from human sources at close range including pile driving, vessels, seismic surveys, and sonars.

- **Long-term Spectral Averages (LTSAs)**: These color plots show power spectral density levels as a function of time (*x*-axis) and frequency (*y*-axis). The frequency axis uses a logarithmic scale, which provides equal vertical space for each decade increase in frequency and allows the reader to equally see the contributions of low and high-frequency sound sources. The LTSAs are excellent summaries of the temporal and frequency variability in the data.

- **Decidecade box-and-whisker plots**: In these figures, the 'boxes' represent the middle 50% of the range of sound pressure levels measured, so that the bottom of the box is the sound level 25th percentile (L_{25}) of the recorded levels, the bar in the middle of the box is the median (L_{50}), and the top of the box is the level that exceeded 75% of the data (L_{75}). The whiskers indicate the maximum and minimum range of the data.

- **Spectral density level percentiles**: The decidecade box-and-whisker plots are representations of the histogram of each band's sound pressure levels. The power spectral density data has too many frequency bins for a similar presentation. Instead colored lines are drawn to represent the L_{eq}, L_5, L_{25}, L_{50}, L_{75}, and L_{95} percentiles of the histograms. Shading is provided underneath these lines to provide an indication of the relative probability distribution. It is common to compare the power spectral densities to the results from Wenz (1962), which documented the variability of ambient spectral levels off the US Pacific coast as a function of frequency of measurements for a range of weather, vessel traffic, and geologic conditions. The Wenz levels are appropriate for approximate comparisons only since the data were collected in deep water before the known increase in low-frequency sound levels attributed to the increase in maritime shipping (Andrew et al. 2011).

- **Daily sound exposure levels (SEL; $L_{E,24h}$)**: The SEL represents the total sound energy received over a 24-hour period, computed as the linear sum of all 1-minute values for each day. During automated analysis, the dominant sound source in each minute of data is classified as "Vessel", "Seismic" or "Ambient". To minimize the influence of anthropogenic sources on ambient sound level estimates, we defined ambient levels from individual minutes of data that did not have an anthropogenic detection within one hour on either side of that minute. This results in more accurate estimates of daily sound exposure levels (SEL) from each source class, cumulative distribution functions of sound pressure levels, and spectra.

2.2.2. Vessel Noise Detection

Vessels are detected in two steps (Martin 2013):

1. Detect constant, narrowband tones produced by a vessel's propulsion system and other rotating machinery (Arveson and Vendittis 2000). These sounds are also referred to as tonals. We detect the tonals as lines in a 0.125 Hz resolution spectrogram of the data (8 s of data, Hann window, 2 s advance).

2. Assess the SPL for each minute in the 40–315 Hz shipping frequency band, which commonly contains most sound energy produced by mid-sized to large vessels. Background estimates of the shipping band SPL and system-weighted SPL are then compared to their mean values over a 12 h window, centered on the current time.

Vessel detections are defined by the following criterion (Figure 8):

1. SPL in the shipping band (40–315 Hz) is at least 3 dB above the 12 h mean for the shipping band for at least 5 min.

2. AND at least three shipping tonals (0.125 Hz bandwidth) are present for at least 1 min per 5 min window. Tonals are difficult to detect during turns and near the closest points of approach (CPA) due to Lloyds' mirror and Doppler effects.

3. AND SPL in the shipping band is within 12 dB of the system weighted SPL.

Any duration during which these constraints are valid is identified as a period with shipping present. A 10 min shoulder period before and after the detection period is also included in the shipping period. The shipping period is searched for the highest 1 min SPL in the vessel detection band, which is then identified as the closest point of approach (CPA) time. This algorithm is designed to find detectable shipping, meaning situations where the vessel noise can be distinguished from the background. It does not identify cases of two vessels moving together or cases of continuous noise from stationary platforms, such as oil and gas drilling and dynamic positioning operations. Those situations are easily identified using other methods such as the daily SEL and long-term spectral average figures.
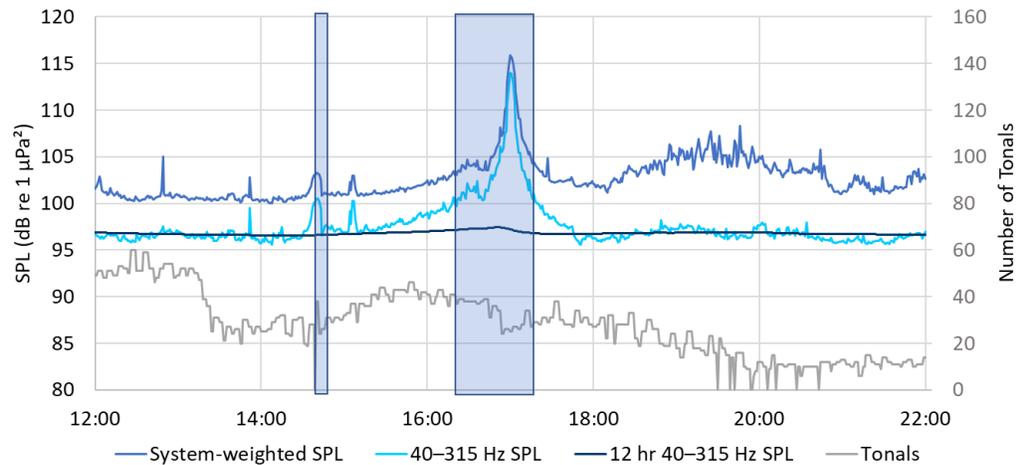
Figure 8. Example of broadband and 40–315 Hz band sound pressure level (SPL), as well as the number of tonals detected per minute as a vessel approached a recorder, stopped, and then departed. The shaded area is the period of shipping detection. Fewer tonals are detected at the vessel's closest point of approach (CPA) at 17:00 because of masking by broadband cavitation noise and due to Doppler shift that affects the tone frequencies.

2.2.3. Seismic Survey Event Detection

Seismic pulse sequences were detected using correlated spectrogram contours. We calculated spectrograms using a 300 s long window with 4 Hz frequency resolution and 0.05 s time resolution (Reisz window). All frequency bins were normalized by their medians over the 300 s window. The detection threshold is three times the median value at each frequency. Contours were created by joining the time-frequency bins above threshold in the 7–1000 Hz band using a 5 × 5 bin kernel. Contours 0.2–6 s in duration with a bandwidth of at least 60 Hz were further analyzed.

An "event" time series was created by summing the normalized value of the frequency bins in each time step that contained detected contours. The event time series was auto-correlated to look for repeated events. The correlated data space was normalized by its median, and a detection threshold of 3 was applied. Peaks larger than their two nearest neighbors were identified, and the list of peaks was searched for entries with a set repetition interval. The allowed spacing between the minimum and maximum time peaks was 4.8 to 65 s, which captures the normal range of seismic pulse periods. Where at least six regularly spaced peaks occurred, the original event time series was searched for all peaks that match the repetition period within a tolerance of 0.25 s. The duration of the 90% SPL window of each peak was determined from the originally sampled time series, and pulses more than 3 s long were rejected.

2.3. Detection Range Modeling

Detection Range Modeling (DRM) was conducted to estimate the detectability of marine mammal vocalizations for the species detected in the study area. DRM considered the following data inputs to estimate species specific detectibly distances:

- Published marine mammal vocalization source level and bandwidth characteristics, as well as vocalization depth (see Appendix B.2),

- Ambient noise percentiles measured in the study area, and

- Local bathymetry, geology, and sound speed profile (see Appendix B.3).

The detection range is defined as the range where the expected sound level of a mammal vocalization is X dB (where X is the detection threshold of the relevant detector for a given species) above the expected noise level. Modeled signal to noise ratios (SNR) were calculated at locations within a three-dimensional (3-D) volume (easting, northing, and depth) to predict a detection range. The detection range, therefore, represents the maximum range at which a signal of a given source level can be identified by a detector in given noise conditions. This underestimates the range to which vocalizations could be detected by experienced human analysts conducting a fine scale analysis.

To compute the detection range an estimate of the sound's propagation loss between the calling animal and our seafloor recorders was required. To perform the propagation loss calculations in a computationally efficient manner, we applied the reciprocity principle which states that an identical signal will be received between a source and receiver pair if their coordinates are inter-changed (Jensen et al. 2011). Rather than performing individual propagation loss calculations for a source at many locations (e.g., an animal) to the receiver (seafloor recorder) to estimate SNR and detectability, the loss between source and receiver is computed by setting the source location for the propagation model to be the location of the seafloor recorder. The propagation loss from this position was then calculated to locations within the ocean interior in a single calculation, thereby reducing the number of individual propagation loss computations that would be required otherwise.

Depending on the frequency characteristics of the marine mammal source level inputs, two potential sound propagation models were used to predict the loss between animal and recorder:

- JASCO's Marine Operations Noise Model (MOMN) a range-dependent parabolic equation model for frequencies up to 2 kHz and/or,

- The BELLHOP Gaussian beam acoustic ray-trace model for frequencies from 2 to 100 kHz.

The MONM and BELLHOP results were combined as required to produce results for the full frequency range for the species of interest. Appendix B.1 contains additional information on the propagation models used for detection range estimation.

Propagation loss was calculated up to a distance of 100 km from a recorder location in each cardinal direction. A horizontal separation of 20 m between receiver points along the modelled radials was used. The sound fields were modeled with a horizontal angular resolution of 10° for a total of 36 radial planes. Receiver depths were chosen to span the entire water column over the modeled areas, from 2 m to a maximum of 1000 m, with step sizes that increased with depth.

Ambient noise percentile information was derived from the measurements performed on the data recorded at PAMNorth. Detection ranges were modeled for May and October. These months were chosen because they had the lowest and highest background noise, respectively, and sound speed profiles at the opposite ends of the observed range. They were thereby expected to provide representative upper and lower bounds for detection ranges (see Appendix B.3.2). The modeling was aimed at the signals targeted by the detectors for all the species detected during the study (fin, humpback, killer and sperm whales and white-beaked dolphins).

We defined two geoaoustic profiles (MZ and MN) based on information provided by Equinor and extracted from published literature. Based on preliminary modeling, the differences in geoacoustic profiles only yielded differences in detection ranges for the low-frequency signals of fin whales. For all other species, the detection ranges were modeled using the geoacoustic profile MN (see Appendix B.3.3).

To evaluate the detection ranges, the following model of the received level, $RL(r)$, measured at the distance r from the source, was used:

$$RL(r) = SL - TL(r), \tag{1}$$

where SL is the source level; and $TL(r)$ is the transmission loss. The detection of sound is the event that satisfies the condition

$$RL(r) \geq NL + c, \tag{2}$$

where NL is the noise level; and c is a constant specifying the detection threshold. $TL(r)$ is a non-random parameter computed by the MONM or BellHop algorithm, such that the models (1) and (2) include two independent random variables, NL and RL.

The joint probability of the events that NL takes some value $NL = NL_i$, and RL takes a value of $RL = RL_j$ is $P(NL_i, RL_j)$. Using Bayes theorem, the joint probability can be represented as a product

$$P(NL_i, RL_j) = P(NL_i|RL_j)P_R(RL_j) = P(RL_j|NL_i)P_N(NL_i), \tag{3}$$

where $P(RL_j|NL_i)$ is a conditional probability, i.e. the likelihood of event $RL = RL_j$ occurring given that $NL = NL_i$; $P_R(RL_j)$ are the probabilities of observing RL_j and NL_i respectively.

Taking into account (3), we may introduce two types of detection probabilities. The conditional probability of detection of a sound at the distance r from the source computed under a certain value of NL is

$$P_{DC}(r|NL) = \sum_{RL<NL+c} P_R(RL(r)) = CDF_R(NL + c), \tag{4}$$

where $CDF_R(x)$ is the is the cumulative distribution function of the received level. The unconditional probability of detection is

$$P_{DU}(r) = 1 - \sum_{NL} P_N(NL) \sum_{RL<NL+c} P_R(RL(r)) = 1 - \sum_{NL} P_N(NL) \, CDF_R(NL + c). \tag{5}$$

The unconditional probability of detection is used to display the detection ranges.

2.4. Marine Mammal Detection Overview

We used a combination of automated detectors and manual review by human analysts to determine the presence of sounds produced by marine mammals. First, automated detectors identified acoustic signals potentially produced by odontocetes and mysticetes (Appendices C.1 and C.2). We then manually reviewed (validated) automated detections within a sample of sound files for each data set (Appendix C.3). The level of validation effort was set at 3% of the data based on the evaluation of divergence curves, which represent the minimum validation effort required to ensure that the sample is representative of the distribution of automated detections throughout each data set (Appendix C.4). Finally, we critically reviewed the results of each automated detector and restricted their output, where necessary, to maximize their performance metrics (Appendix C.5). Automated detector performance metrics are only presented for those species and/or vocalization types exceeding a pre-set precision (P) level (P = 75%), which ensures a level of reliability in the description of marine mammal acoustic occurrence. When the precision was below that threshold, manual detections are presented.

In this report, the term "detector" is used to describe automated algorithms that combine detection and classification steps. A "detection" refers to an acoustic signal that has been automatically flagged as a sound of interest based on spectral features and subsequently classified based on similarities to several templates in a library of marine mammal signals. Detections are reviewed by analysts as part of a process called validation. Manual detections refer to signals detected by an analyst but not the detector during the validation process.

2.4.1. Odontocete Click Detection

Odontocete clicks are high-frequency impulses with energy ranging from ~1 to over 150 kHz (Au et al. 1999, Møhl et al. 2000). JASCO's click detectors are based on zero-crossings in the acoustic time series. Zero-crossings are the rapid oscillations of a click's pressure waveform above and below the signal's normal level. Zero-crossing-based features of detected events are then compared to templates of known clicks for classification (see Appendix C.1 for details). Clicks were classified individually and as trains. Detected clicks that cannot be classified as one of the targeted species are pooled in an "Unidentified Click" category. The suite of click detectors is presented in Table 4.

Table 4. List of automated detectors used to identify clicks produced by odontocetes.

Species targeted	Comments
Sowerby's beaked whales	
Sperm whales	
Killer whales	
Atlantic white-sided dolphins	
Blainville's beaked whales	
Unidentified beaked whales	Targeting long FM clicks, possibly from Gervais' beaked whale
Cuvier's beaked whales	
Dolphins	Generic dolphin click, will capture clicks from a range of dolphin species
Gervais' beaked whales	
Northern bottlenose whales	
Pilot whales	
Risso's dolphins	The detector includes two click types (short and long)
True's beaked whales	
Unidentified beaked whales @ 51 kHz	Could be produced by Gervais' or True's beaked whales

2.4.2. Tonal Signal Detection

Tonal signals are narrowband, often frequency-modulated, signals produced by many species across a range of taxa (e.g., baleen whale moans and delphinids whistles). The signals of some pinniped species, such as bearded seal trills, also have tonal components. Baleen whale moans' frequency range vary among species but is generally below 1 kHz and as low as 17 Hz in blue whales (see e.g., Parks and Tyack 2005, Berchok et al. 2006, Dunlop et al. 2007). Delphinid tonal signals are generally a lot more broadband and range from ~700 Hz up to 18 kHz (see e.g. Steiner 1981, Ford 1989, Rendell et al. 1999, Oswald et al. 2003) but can be as high as 68 kHz in some species (Samarra et al. 2010). The tonal signal detector identified continuous contours of elevated energy and classified them against a library of marine mammal signals (see Appendix C.2 for details). The suite of tonal detectors applied to the data is presented in Table 5.

Table 5. List of automated detectors used to identify tonal signals produced by baleen whales and delphinids. FW: fin whale; SW: sei whale; BW: blue whale; RW: right whale; MW: minke whale.

Detector name	Species targeted	Signal targeted
Atl_BlueWhale_GL_IM	Blue whales	A-B call, tonal song note @ 17 Hz
Atl_BlueWhale_IM	Blue whales	A-B call, tonal song note @ 17 Hz
Atl_BlueWhale_IM2	Blue whales	A-B call, tonal song note @ 17 Hz
Atl_FinWhale_130	Fin whales	130-Hz song note
Atl_FinWhale_21.2	Fin whales	20-Hz pulse
Atl_FinWhale_21	Fin whales	20-Hz pulse
minkeWhalePulses	Minke whales	Pulse train
N_RightWhale_Up1	North Atlantic right whales	Upcall
N_RightWhale_Up2	North Atlantic right whales	Upcall
N_RightWhale_Up3	North Atlantic right whales	Upcall
SW	Sei whales	Broadband downsweep
WhistleLow	Pilot whale/Killer whales	Whistle with energy between 1–10 kHz
WhistleHigh	Other delphinids	Whistle with energy between 4–20 kHz
VLFMoan	Baleen whales, FW/SW/BW	Downsweeps/upsweeps
LFMoan	Baleen whales, SW/BW/RW	Downsweeps/upsweeps
ShortLow	Baleen whales, possibly MW	Moans, pulses
MFMoanLow	Humpbacks	Moans
MFMoanHigh	Humpbacks	Moans

2.4.3. Automated Detector Validation

We develop and test automated detectors with example data files that contain a range of vocalization types and background noise conditions. However, test files cannot cover the full range of possible vocalization types and noise conditions. Therefore, a selection of files representing 3% of each dataset was manually validated to check each detector's performance for a specific location and timeframe to determine how best to refine the detector results, or when to entirely rely on manually validated results, to accurately represent marine mammal occurrence (see details in Appendix C.3).

To determine the per-file performance of each detector and any necessary thresholds, the automated and validated results (excluding files where an analyst indicated uncertainty regarding species identity) were fed to a maximum likelihood estimation algorithm that maximizes the probability of detection and minimizes the number of false alarms using the 'MCC-score' (see Appendix C.5 for details). The algorithm also estimates the precision (*P*) and recall (*R*) of the detector. *P* represents the proportion of files with detections that are true positives. A *P* value of 0.9 means that 90% of the files with detections truly contain the targeted signal, but it does not indicate whether all files containing acoustic signals from the species were identified. *R* represents the proportion of files containing the signal of interest that were identified by the detector. An *R* value of 0.9 means that 90% of files known to contain a target signal had automated detections, but it says nothing about how many files with detections were incorrect. An MCC-score is a combined measure of *P* and *R*, where an MCC-score of 1 indicates perfect performance–all events were detected with no false alarms.

The algorithm determines a threshold for each detector based on detection count per file that maximizes the MCC-score. The resulting thresholds, Ps, and Rs are presented in Section 3.3.1 and described in further detail in Appendix C.5.

3. Results

3.1. Soundscape Characterization

The RTSys recorder deployed at PAMWest recorded for 111 days, less than half the duration of the other stations. Although the measured sound levels were not significantly different from the other two stations, the audio quality of the data was poor. Data were recorded as planned throughout October 2018, but the number of cycles recorded daily fell throughout November and December from 19 (instead of 24, i.e. one per hour) to about 5. In January, recordings were sporadic, with entire days of data missing and generally no more than one or two sound files recorded per day. The poor audio quality of the data yielded high number of false detections which, combined with the erratic recording schedule, and the similarity in marine mammal detections at PAMNorth and PAMEast as well as the proximity of PAMWest to these stations, made the detailed manual analysis of marine mammal data at PAMWest unwarranted.

The figures of all three stations are presented together for comparison. Selected figures are presented for PAMNorth alone (longest recording duration and broadest range of sound levels) for improved readability.

The data recorded at PAMNorth and PAMEast showed noticeable similarities in measured sound levels (Table 6; Figures 9, 10, and 12), which is at least partly attributable to their close proximity (~12 km). The sound levels recorded at PAMWest were generall 3-4 dB lower than at the other stations. Median (L_{50}) broadband sound pressure levels at PAMEast were approximately 112 dB re 1 µPa and were 0.7 dB higher at PAMNorth, but median decade band levels were all within 0.3 dB (Table 6). The range of broadband and decade sound pressure levels was larger at PAMNorth than PAMEast (Figure 9).

The anthropogenic influence on the soundscape was largely restricted to the contribution of vessels in the area. Because of the poor audio quality of data, vessel detections at PAMWest were deemed unusable. Vessels were detected in 4.2 and 4.8% of hours on 36 and 40% of days at PAMNorth and PAMEast, respectively (Figure 14 and Figure 15). Vessels are visible in the long-term spectrograms as horizontal lines between ~50 and 1000 Hz (Figures 10 and 11). The median total daily SEL was 154.4, 156.2 and 152.1 dB re 1µPa^2.s at PAMEast, PAMNorth and PAMWest, respectively (Figure 15). The apparent decline in total daily SEL at PAMWest towards the end of the recording period reflects the decrease in the number of sound files recorded each day.

The other pervasive anthropogenic contributor to underwater soundscapes around the world is seismic surveys. In this study, airgun sound detections were limited to sporadic low-level pulses (Figure 16) recorded on 10–12 and 16–21 May 2019. They are visible as elevated levels in the 100–1000 Hz band in Figures 10 and 11. At the beginning of the recording period at PAMNorth, signals consistent with echosounders were detected for approximately two weeks and are visible as a band of energy around 25 kHz, in conjunction with a more prominent vessel presence (Figure 11).

The only detectable biological contribution to the long-term soundscape was fin whale song notes at 20 Hz and, more faintly, 130 Hz. The occurrence of both notes are visible as energy bands in the long-term spectrograms from the start of the recording until the end of April (Figures 10 and 11). Median power spectral density levels were also elevated by about 10 dB compared to the adjacent frequencies near 20 Hz, but only 2–3 dB at 130 Hz, reflecting the lower intensity of the latter note. The other peak in spectral density levels near 15 Hz is presumably due to vessel or mooring noise.

In the absence of in situ weather data, we obtained wind speed data from the NAVGEM model (https://coastwatch.pfeg.noaa.gov/erddap/griddap/erdNavgem05D10mWind.html). The model produces wind speed data every 6 h. We found a weak but statistically signifcant correlation between wind speed and broaband rms SPL for the corresponding hour (F = 43.16; p = 8.3E-11), indicating that broadband noise levels are higher when wind speeds increase (Figure 17).

Table 6. Broadband and decade band sound pressure levels (dB re 1 µPa) statistics for PAMEast, PAMNorth, and PAMWest.

Sound level statistic	10–63000 Hz			10–100 Hz			100–1000 Hz			1000–10000 Hz			10.0–63.0 kHz		
	East	North	West	East	North	West	East	North	West	East	North	West	East	North	West
L_1	99.4	97.9	98.2	95.7	94.5	96.6	91.6	91.5	87.5	68.4	70.3	79.1	73.2	73	86.2
L_5	106	104.2	102.1	102.3	99.9	100.3	97.1	96.5	92	85.2	84.8	82.8	75.7	76.1	87.3
L_{25}	109.5	109	105.1	107.4	106.4	103.2	100.9	100.6	96.1	96.2	96.3	91.3	87.4	87.6	88.6
L_{50}	111.8	112.5	108.4	110.4	110.7	107.1	103.1	103.1	99.1	100.1	100.2	95.8	90.7	90.8	90.3
L_{75}	115	117.5	118.2	114.3	116.9	118.1	105	105.5	101.5	102.7	102.7	98.9	92.1	92.2	91.4
L_{95}	124.6	124.8	130.2	124.5	124.7	130.2	108.1	111	104.1	105.8	106.3	102.3	93.4	93.8	92.5
L_{99}	145.7	147.6	142.9	145.6	147.6	142.9	133	134.9	120.1	136.2	131	115.7	138.6	119.4	103.8
L_{Mean}	118.9	121.6	124.9	118.6	121.5	124.9	105.2	106.4	100.8	102.6	102.4	97.7	98	91.6	90.4
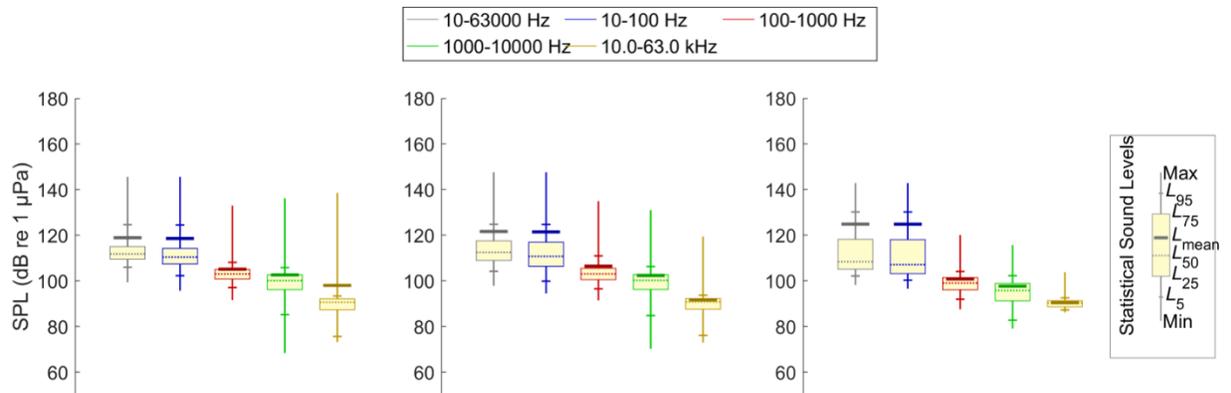
Figure 9. Broadband and decade band sound pressure level boxplots with percentiles. From left to right: PAMEast, PAMNorth, PAMWest.
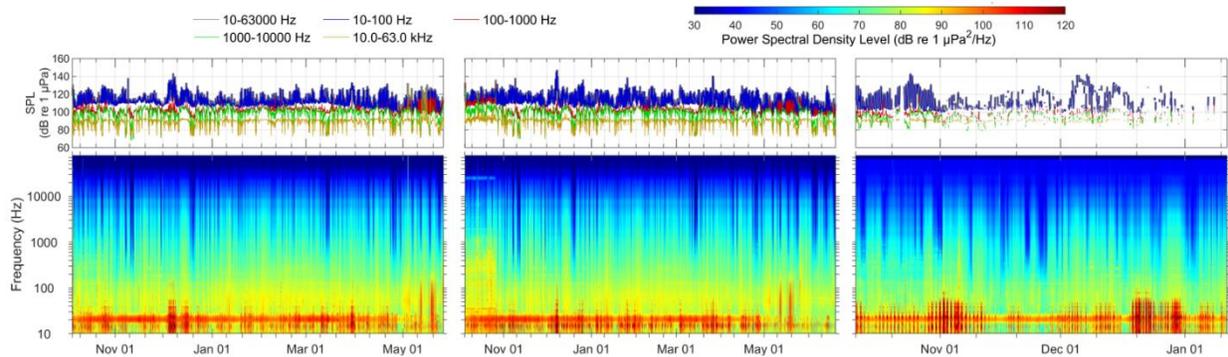
Figure 10. In-band sound pressure level (top panel) and long-term spectral average (bottom panel). From left to right: PAMEast, PAMNorth, PAMWest.
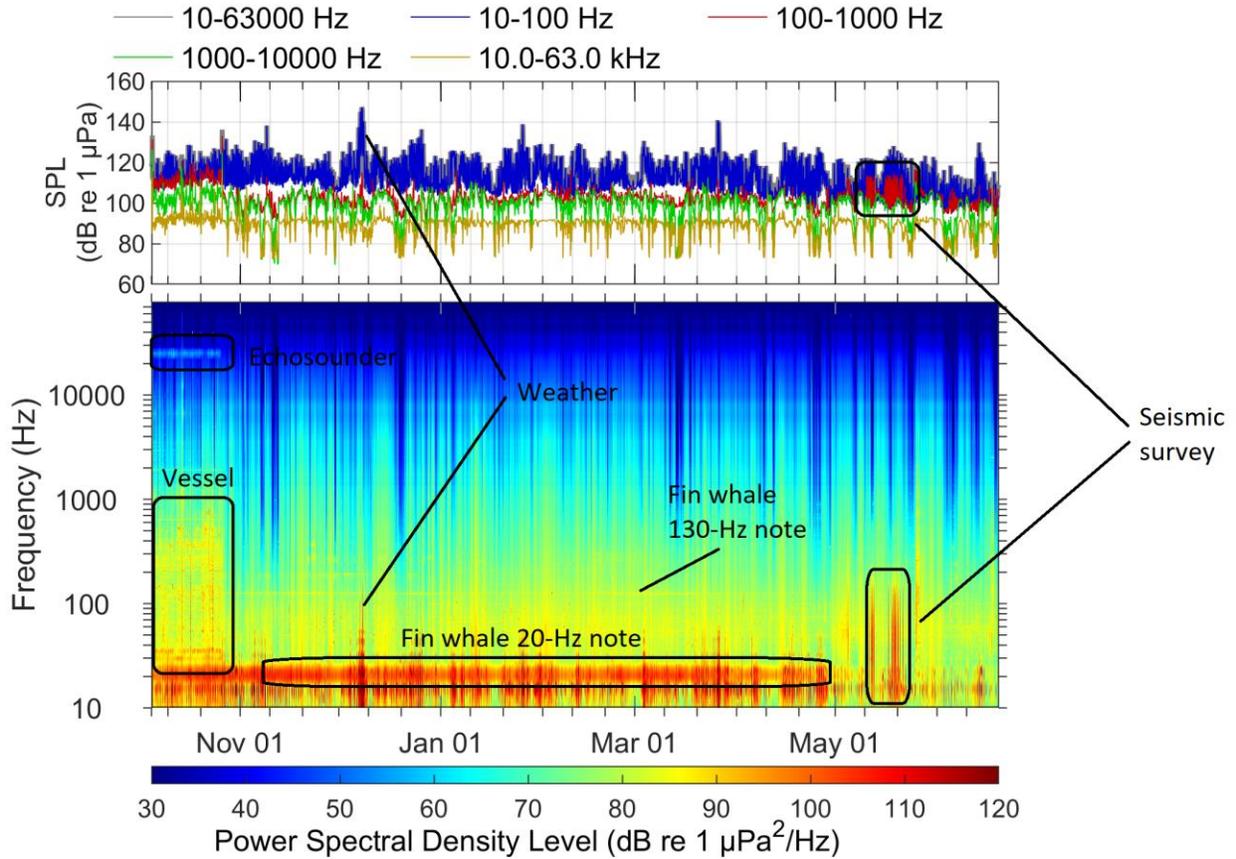
Figure 11. In-band sound pressure level (top panel) and long-term spectral average (bottom panel) for PAMNorth.
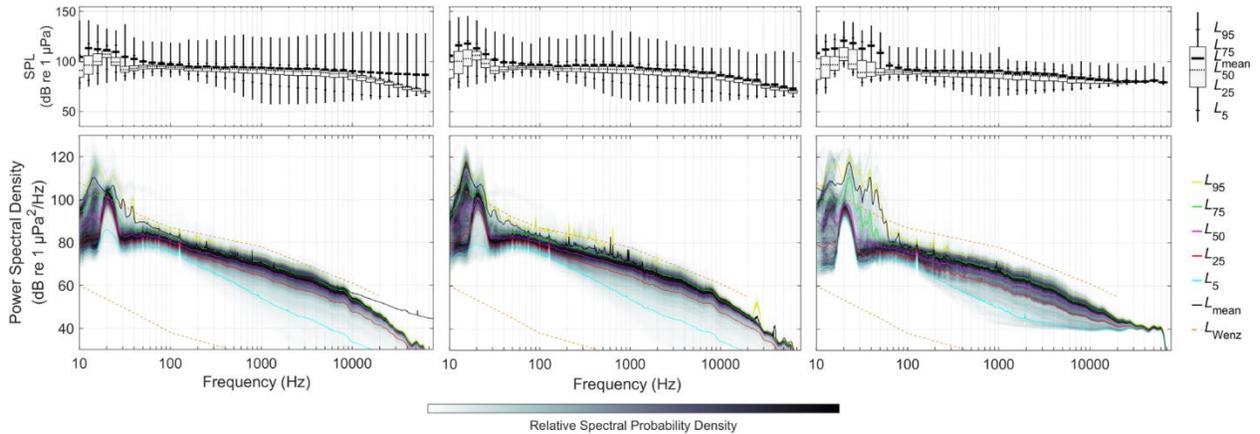
Figure 12. Percentiles and mean of decidecade band sound pressure level (top panel) and percentiles and probability density (bottom panel) of 1-min power spectral density levels compared to the limits of prevailing noise (Wenz 1962). From left to right: PAMEast, PAMNorth, PAMWest.
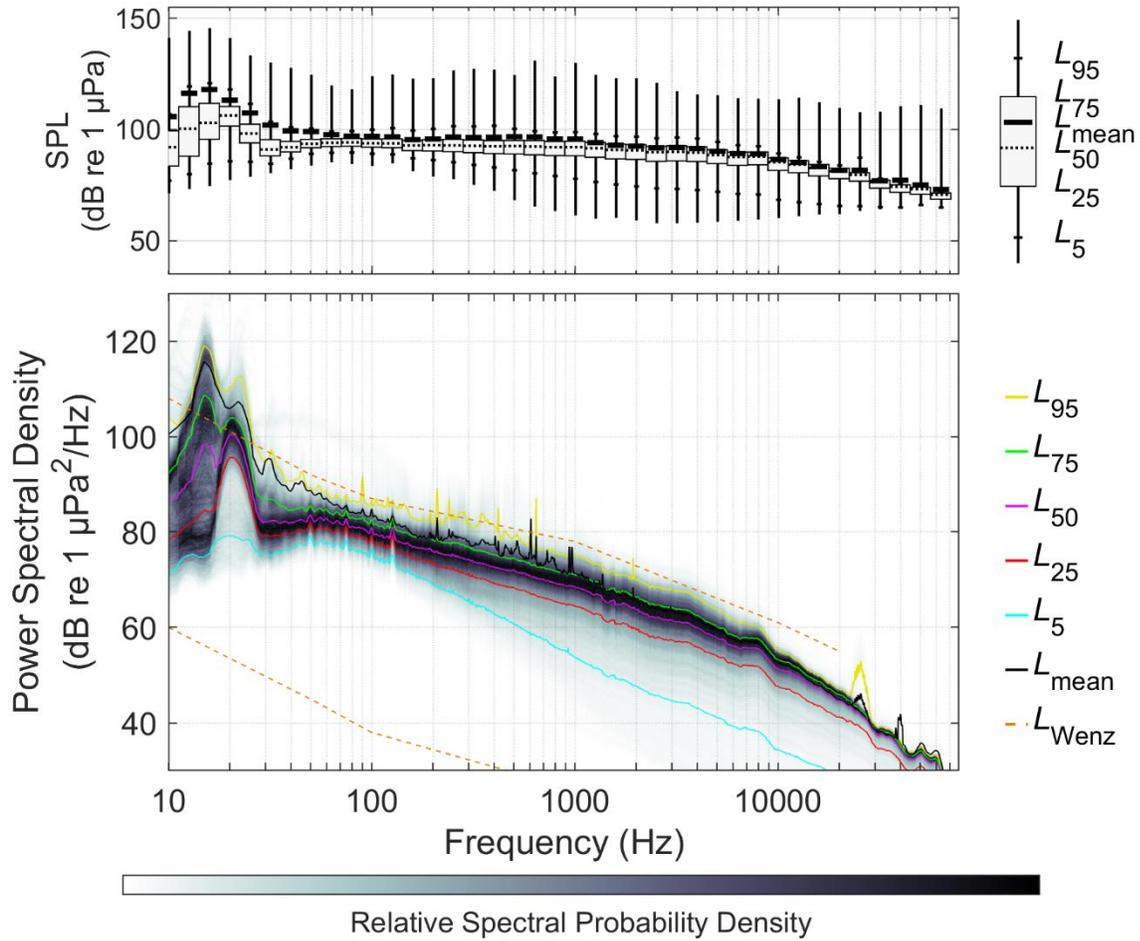
Figure 13. PAMNorth: Percentiles and mean of decidecade band sound pressure level (top panel) and percentiles and probability density (bottom panel) of 1-min power spectral density levels compared to the limits of prevailing noise (Wenz 1962).
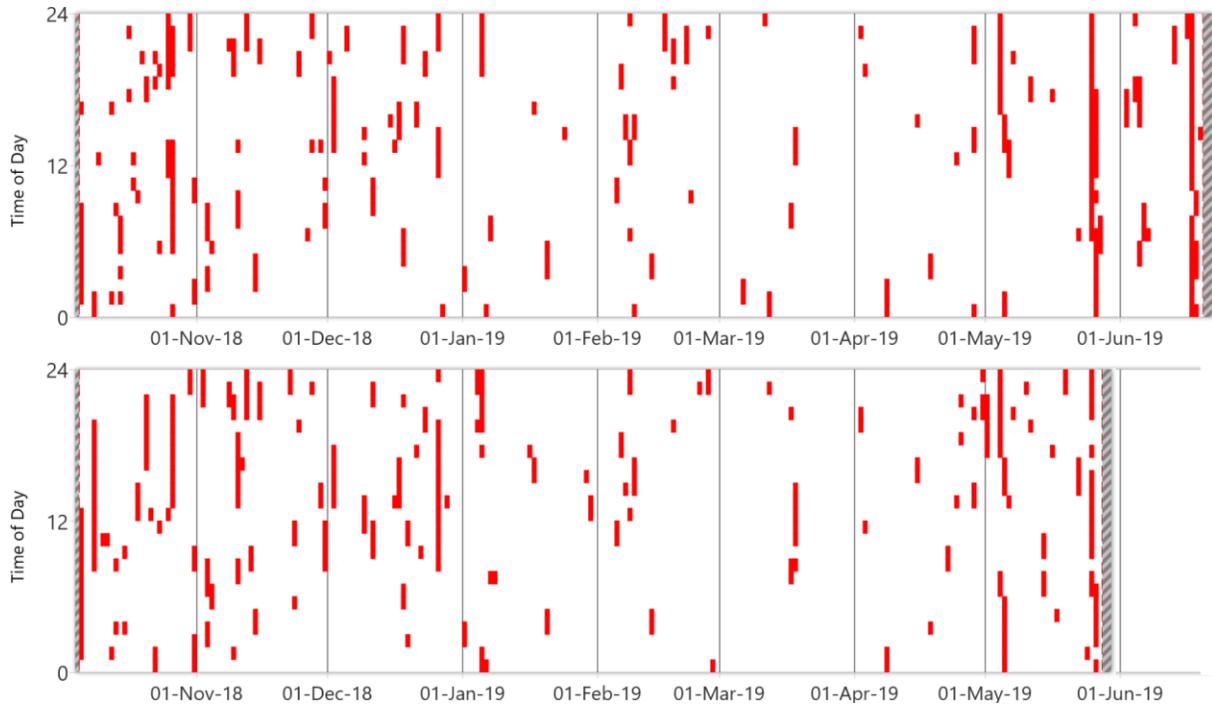
Figure 14. Automated vessel detections at PAMNorth (top) and PAMEast (bottom) between 3 Oct 2019 and 19 Jun 2019. Red lines indicate recorder deployment and retrieval dates or recording end. Hashed lines indicate a lack of recordings. Blue shaded areas indicate hours of darkness.
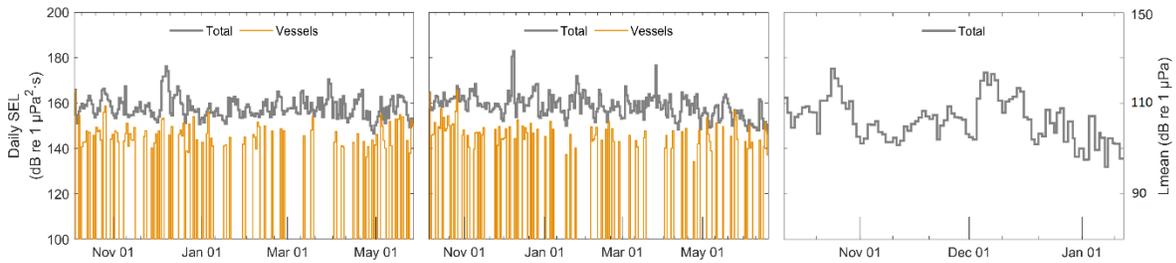
Figure 15. Daily sound exposure level and L_{mean} from overall and vessel-only contributions (Vessel detections were not usable at PAMWest). From left to right: PAMEast, PAMNorth and PAMWest.
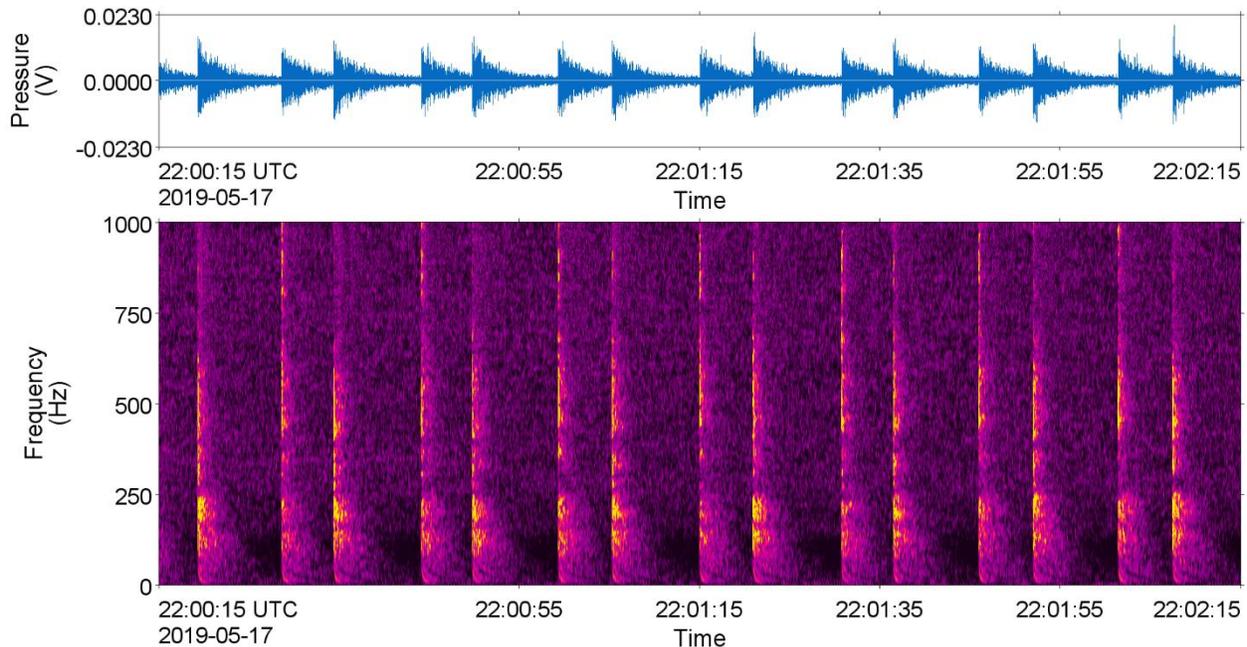
Figure 16. Spectrogram showing seismic airgun sounds recorded at PAMNorth on 17 May 2019 (1.18 Hz frequency resolution, 0.128 s time window, 0.032 s time step, Hamming window).The window length is 2 min.
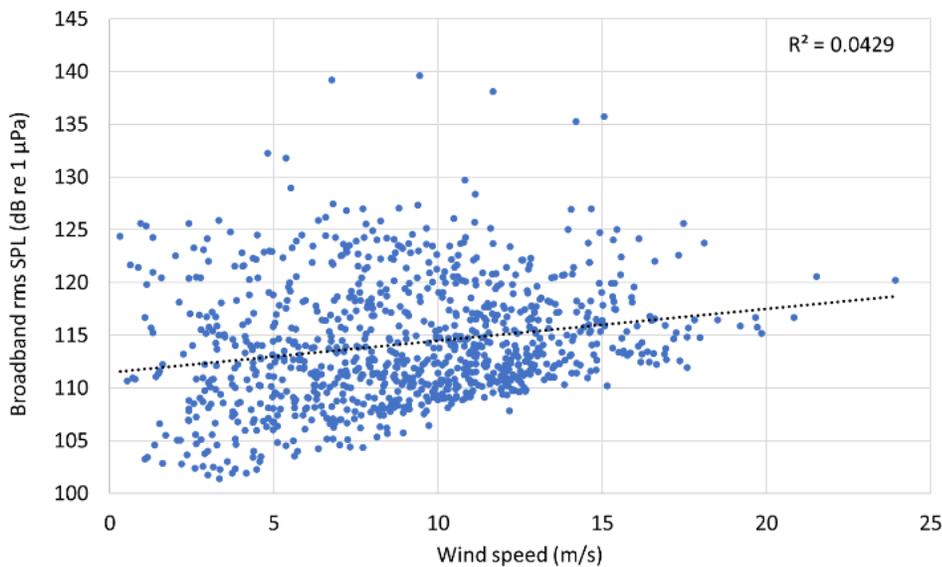
Figure 17. Broadband root-mean-square (rms) sound pressure level (SPL) as a function of wind speed for all data recorded at PAMNorth between 5 Oct 2018 and 19 Jun 2019. The regression line is shown in black.

3.2. Detection Ranges

The choice of animal call source level has a substantial impact on the predicted detection ranges. We modeled fin whale detection ranges using two source levels. The high value (195.4 ± 4.4 dB re 1μPa) was measured in the same are as this study (Garcia et al. 2018) while the low value (185 ± 3 dB re 1μPa) is the midpoint between several published source levels for fin whales worldwide (Weirathmueller et al. 2013a, Wang et al. 2016). The modeled killer whale source level (155 ± 6.5 dB re 1μPa) is the mean of measurements across a range of background noise conditions (Holt et al. 2011). For sperm whale clicks,

we used source levels measured in the Gulf of Alaska (Mathias et al. 2013) that will provide realistic detection ranges for PAM applications but are far from the maximum source levels measured that species (Møhl et al. 2000, Møhl et al. 2003) which would result in substantially longer ranges when realized. Because white-beaked dolphins are presumed to be the most common dolphin species in the area (see section 4.2), we used source level values for that species when modeling detection ranges of delphinid clicks and whistles (Rasmussen et al. 2002, Rasmussen et al. 2006, Atem et al. 2009).

Error! Reference source not found. summarizes the detection ranges for all species and both months. Differences in detection range between May and October are either negligible (baleen whales), slightly longer in October for sperm whale clicks, and negligible or slightly shorter for the other odontocetes. They are not discussed further. We only modelled detection ranges using both geoacoustic profiles for fin whale as it is the only species for which each profile yielded different detection ranges. For all other species, detection ranges were modeled using the geoacoustic profile MN.

Fin whale 20-Hz pulses with a 195 dB source level were detected up to 60-100 km in the best conditions, depending on the geoacoustic profile considered. Geoacoustic profile MN consistently yielded ranges that were 50 to 100 % longer. Under median noise conditions and average source level, these sounds are detectable up to 12.4-23.5 km (Figure 19). Fin whale 20-Hz pulses with a 185 dB source level were detectable up to 36-52 km in the best conditions and up to 4.2-7.6 km under average conditions (Figure 20). In at least one instance, the same calls were heard on the PAMEast and PAMNorth recorders, confirming some of the modeling outputs (Figure 18).
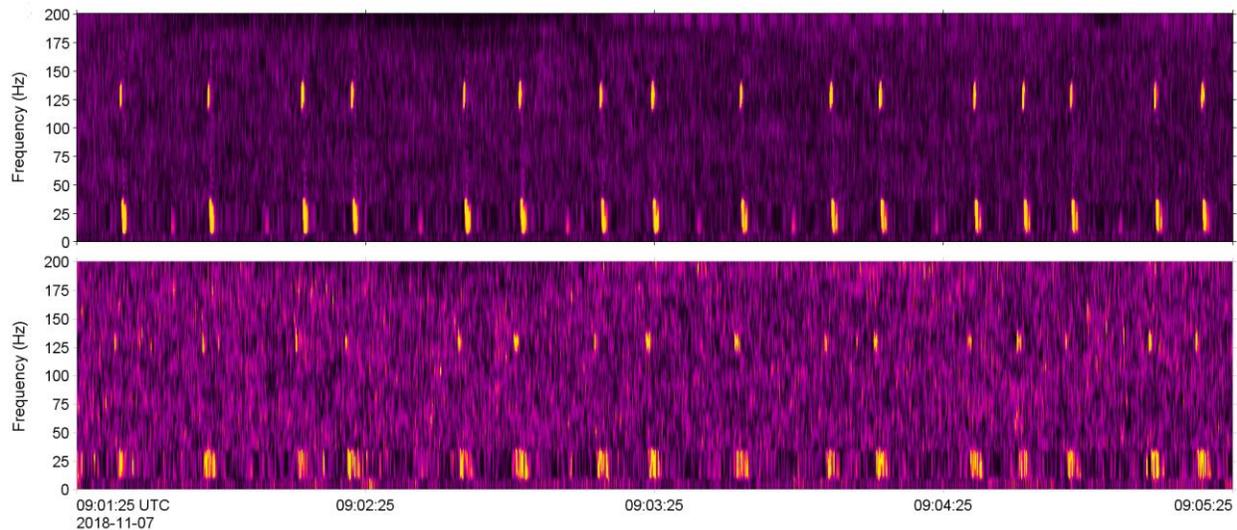
Figure 18. Spectrogram showing a loud fin whale song received at PAMNorth (top) also detected at PAMEast, 12 km away. (1.18 Hz frequency resolution, 0.128 s time window, 0.032 s time step, Hamming window). The window length is 4 min.

Humpback whale song notes were detectable up to 22 km under optimal scenarios and up to 3.5 km under average conditions (Figure 21). Sperm whale clicks were detectable up to 66 km under optimal scenarios and up to 16.8 km under average conditions (Figure 22). Killer whale tonal vocalizations were detectable up to 8.5 km under optimal scenarios but only up to 600 m under average conditions (Figure 23). White-beaked dolphin whistles were detectable up to 8.6 km under optimal scenarios but generally not detectable under median noise conditions. It should be noted that the whistle detections presented in this report are all based on manual detections. Manually detected calls can be expected to have longer detection ranges than presented here because the detection threshold of a human analyst is lower than that of an algorithm (DT=3 in this study). White-beaked dolphin clicks were detectable up to 3.8 km under optimal scenarios and up to 2.4 km under average conditions (Figure 24).

Table 7. Detection ranges for species and signals most likely to be encountered in the Johan Castberg oil field modeled based on two geoacoustic profiles (MN and MZ, where applicable) and background noise conditions for May and October. The range of distances represent minimum and maximum detection ranges across all modeled azimuths. Pd: Probability of detection. Bold values show the most likely detection ranges, under median noise conditions (NL50) for average source levels.

Species and vocalization type	Ambient noise percentile	Pd=0.1				Pd=0.5				Pd=0.9			
		May (MZ)	May (MN)	Oct (MZ)	Oct (MN)	May (MZ)	May (MN)	Oct (MZ)	Oct (MN)	May (MZ)	May (MN)	Oct (MZ)	Oct (MN)
Fin whale 20-Hz pulse 195 dB	NL10	44.8-58.1	86.9-100	43.1-55.7	84.2-100	33.3-40.7	60.6-80.1	33.5-39.6	59.5-78.5	23.0-27.4	40.2-53.1	23.2-28.6	40.6-56.2
	NL50	16.9-20.1	30.9-36.9	16.6-20.3	30.3-37.1	**10.3-12.4**	**18.4-23.3**	**10.2-12.1**	**18.8-23.5**	6.6-7.6	11.1-14.2	6.7-7.7	11.0-14.0
	NL90	5.7 - 6.2	8.8 - 11.2	5.8 - 6.3	8.4 - 11.2	3.1 - 3.7	4.6 - 5.6	3.1 - 3.7	4.5 - 5.6	1.9 - 2.1	2.4 - 2.7	1.9 - 2.2	2.4 - 2.9
Fin whale 20-Hz pulse 185 dB	NL10	21.3-26.0	39.5-50.3	20.7-26.1	39.6-52.5	16.9-20.4	31.4-37.7	16.7-20.5	31.2-37.8	12.3-14.9	22.7-27.8	11.8-14.9	23.5-28.2
	NL50	6.2 - 6.9	9.9 - 12.2	6.2 - 6.9	9.5 - 11.9	**4.2 - 4.9**	**6.9 - 7.6**	**4.3 - 4.9**	**6.9 - 7.4**	2.7 - 3.1	3.6 - 4.7	2.7 - 3.1	3.6 - 4.7
	NL90	1.8 - 1.9	2.2 - 2.5	1.7 - 1.9	2.2 - 2.7	1.2 - 1.3	1.5 - 1.7	1.2 - 1.3	1.5 - 1.7	0.9 - 0.9	1.0 - 1.2	0.9 - 0.9	1.0 - 1.2
Humpback whale song note	NL10	N/A	19.0- 21.6	N/A	17.0- 22.0	N/A	6.6- 8.1	N/A	6.4- 7.0	N/A	2.6- 2.7	N/A	2.5- 2.6
	NL50	N/A	10.0- 11.7	N/A	8.7 - 10.2	N/A	**3.5 - 3.7**	N/A	**3.4 - 3.6**	N/A	0.9 - 1.0	N/A	0.9 - 1.0
	NL90	N/A	4.2 - 4.4	N/A	4.1 - 4.3	N/A	1.1 - 1.4	N/A	1.1 - 1.4	N/A	0.1 - 0.1	N/A	0.1 - 0.1
Sperm whale click	NL10	N/A	50.3- 61.0	N/A	56.9- 66.2	N/A	44.4- 54.4	N/A	54.2- 61.1	N/A	41.6- 51.3	N/A	49.7- 56.4
	NL50	N/A	12.2- 15.9	N/A	13.4- 18.3	N/A	**8.9 - 14.0**	N/A	**11.0- 16.8**	N/A	7.7 - 12.7	N/A	9.8 - 14.5
	NL90	N/A	5.9 - 10.2	N/A	7.7 - 11.3	N/A	5.1 - 8.3	N/A	6.6 - 10.3	N/A	3.9 - 7.7	N/A	4.0 - 8.6
Killer whale tonal vocalizations	NL10	N/A	6.5 - 8.5	N/A	6.3 - 6.5	N/A	3.4 - 3.5	N/A	3.2 - 3.4	N/A	1.0 - 1.3	N/A	1.1 - 1.3
	NL50	N/A	1.5 - 1.7	N/A	1.5 - 1.7	N/A	**0.2 - 0.5**	N/A	**0.2 - 0.6**	N/A	0.0 - 0.0	N/A	0.0 - 0.0
	NL90	N/A	0.8 - 1.0	N/A	0.8 - 1.1	N/A	0.0 - 0.0	N/A	0.0 - 0.0	N/A	0.0 - 0.0	N/A	0.0 - 0.0
White-beaked dolphin whistles	NL10	N/A	6.8 - 8.6	N/A	6.5 - 6.7	N/A	2.7 - 2.9	N/A	2.4 - 2.7	N/A	0.3 - 0.8	N/A	0.5 - 0.8
	NL50	N/A	1.3 - 1.6	N/A	1.3 - 1.6	N/A	**0.0 - 0.0**	N/A	**0.0 - 0.0**	N/A	0.0 - 0.0	N/A	0.0 - 0.0
	NL90	N/A	0.8 - 1.3	N/A	0.8 - 1.0	N/A	0.0 - 0.0	N/A	0.0 - 0.0	N/A	0.0 - 0.0	N/A	0.0 - 0.0
White-beaked dolphin clicks	NL10	N/A	3.4 - 3.8	N/A	3.4 - 3.7	N/A	2.8 - 3.1	N/A	2.9 - 3.1	N/A	2.3 - 2.6	N/A	2.2 - 2.7
	NL50	N/A	2.5 - 2.7	N/A	2.5 - 2.8	N/A	**2.0 - 2.4**	N/A	**2.0 - 2.4**	N/A	1.4 - 2.0	N/A	1.4 - 2.1
	NL90	N/A	2.2 - 2.6	N/A	2.2 - 2.7	N/A	1.8 - 2.1	N/A	1.8 - 2.3	N/A	1.3 - 1.9	N/A	1.2 - 2.0
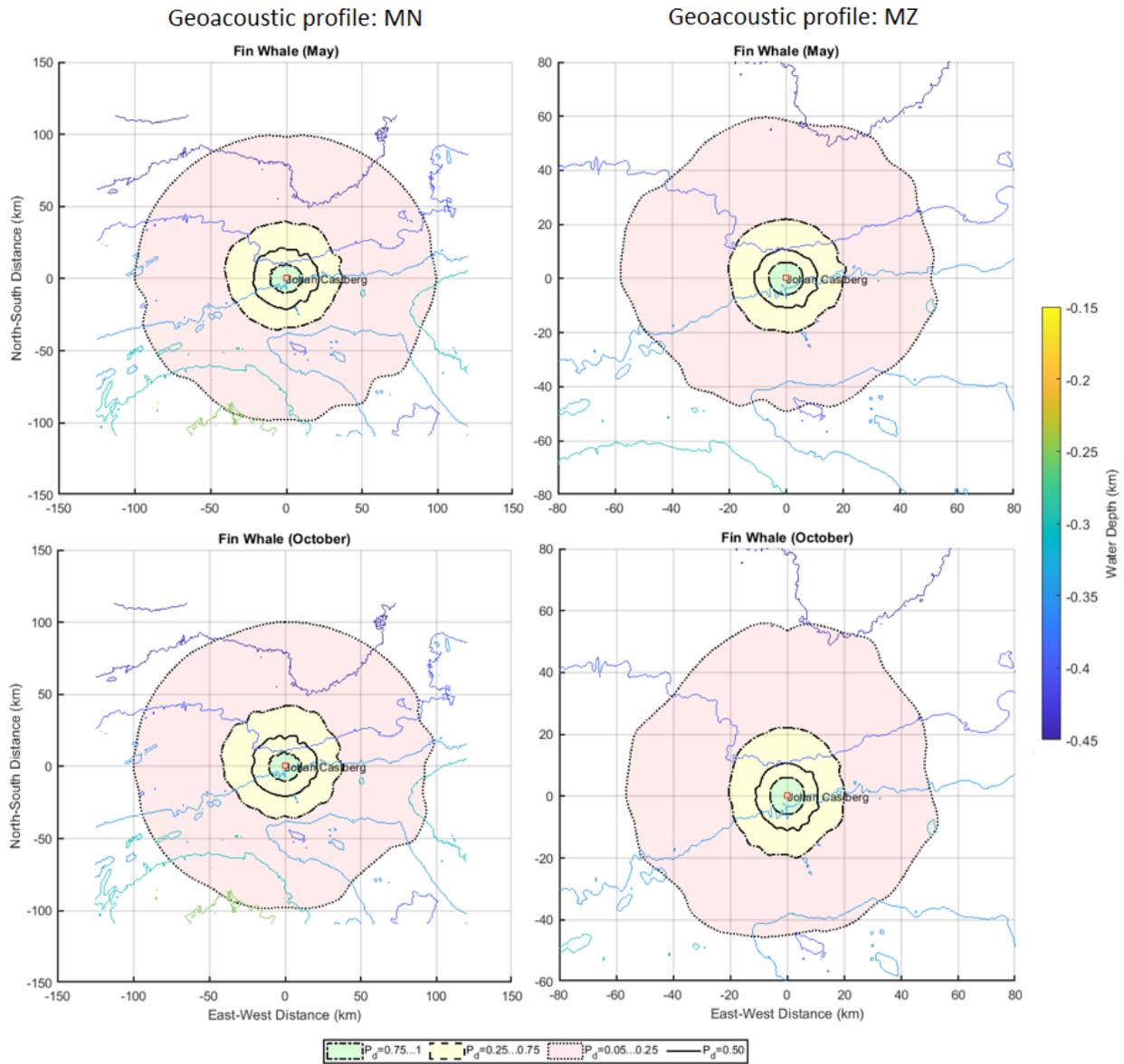
Figure 19. Fin whale 20-Hz call (195 dB source level): Detection ranges associated with various probability of detection under noise conditions recorded at Johan Castberg in May and October for geoacoustic profiles MZ (left) and MN (right). The center of each figures is the Johan Castberg oil field (72.5 N × 20.35 E). The solid black line shows the range for a 50% probability of detection.
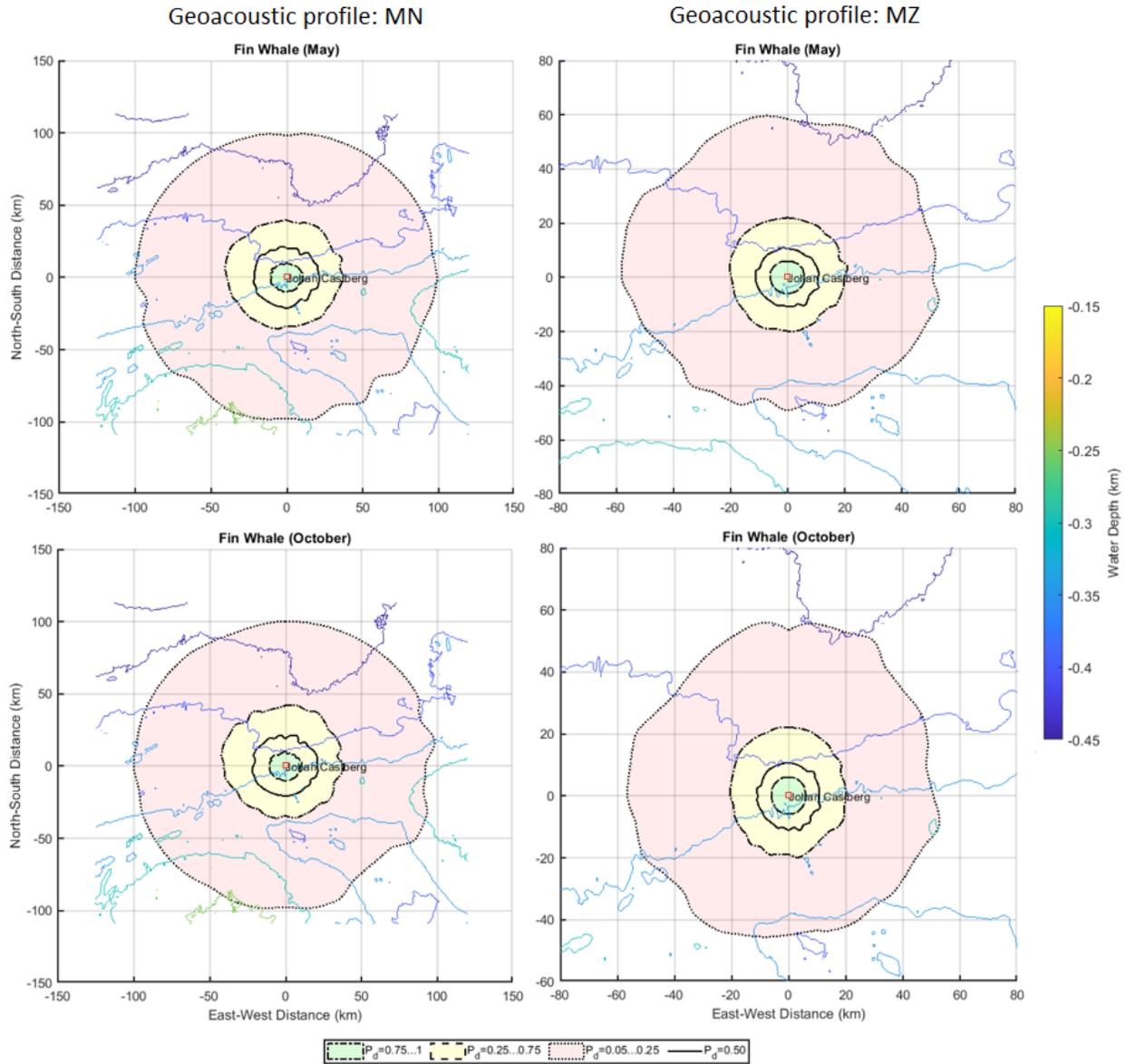
Figure 20. Fin whale 20-Hz call (185 dB source level): Detection ranges associated with various probability of detection under noise conditions recorded at Johan Castberg in May and October for geoacoustic profiles MZ (left) and MN (right). The center of each figures is the Johan Castberg oil field (72.5 N × 20.35 E). The solid black line shows the range for a 50% probability of detection.
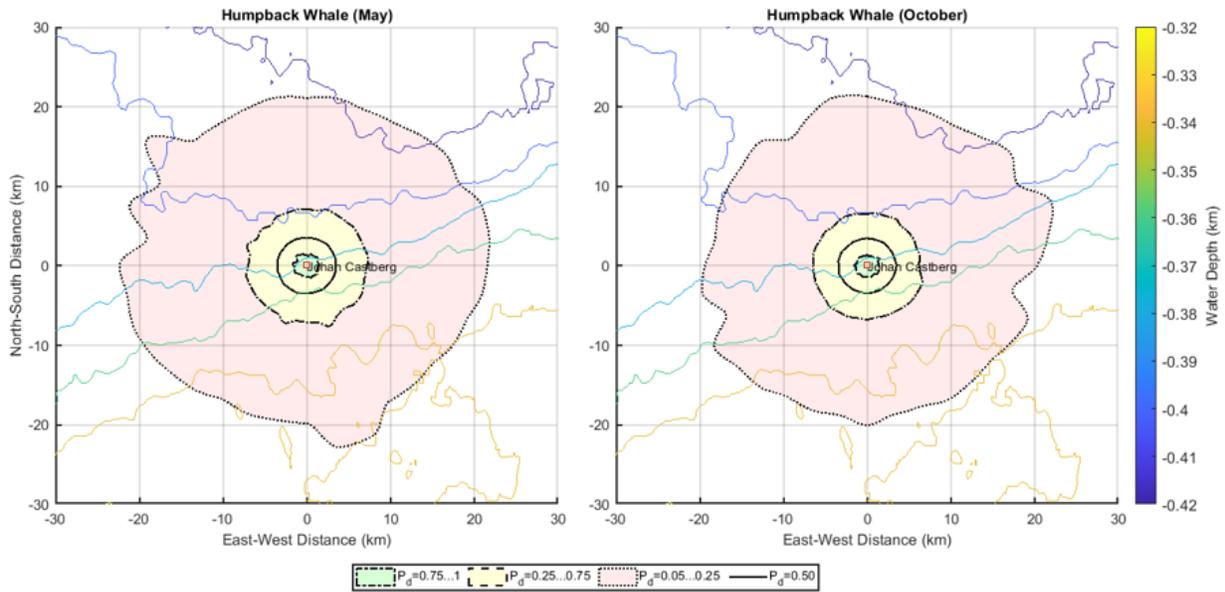
Figure 21. Humpback whale song note: Detection ranges associated with various probability of detection under noise conditions recorded at Johan Castberg in May and October. The center of each figures is the Johan Castberg oil field (72.5 N × 20.35 E). The solid black line shows the range for a 50% probability of detection.
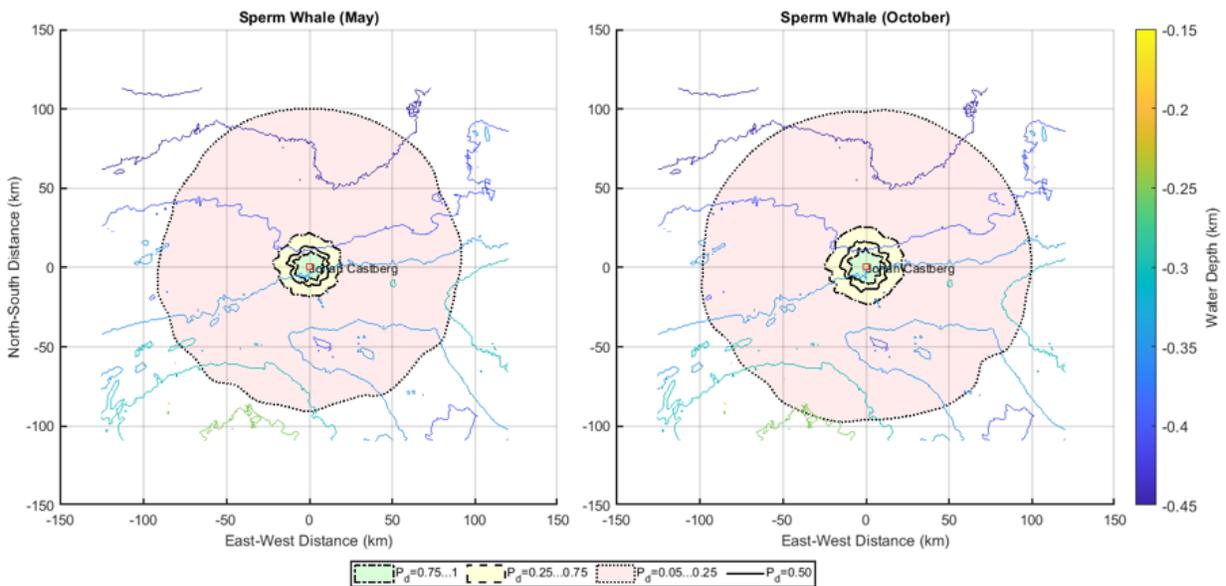
Figure 22. Sperm whale clicks: Detection ranges associated with various probability of detection under noise conditions recorded at Johan Castberg in May and October. The center of each figures is the Johan Castberg oil field (72.5 N × 20.35 E). The solid black line shows the range for a 50% probability of detection.
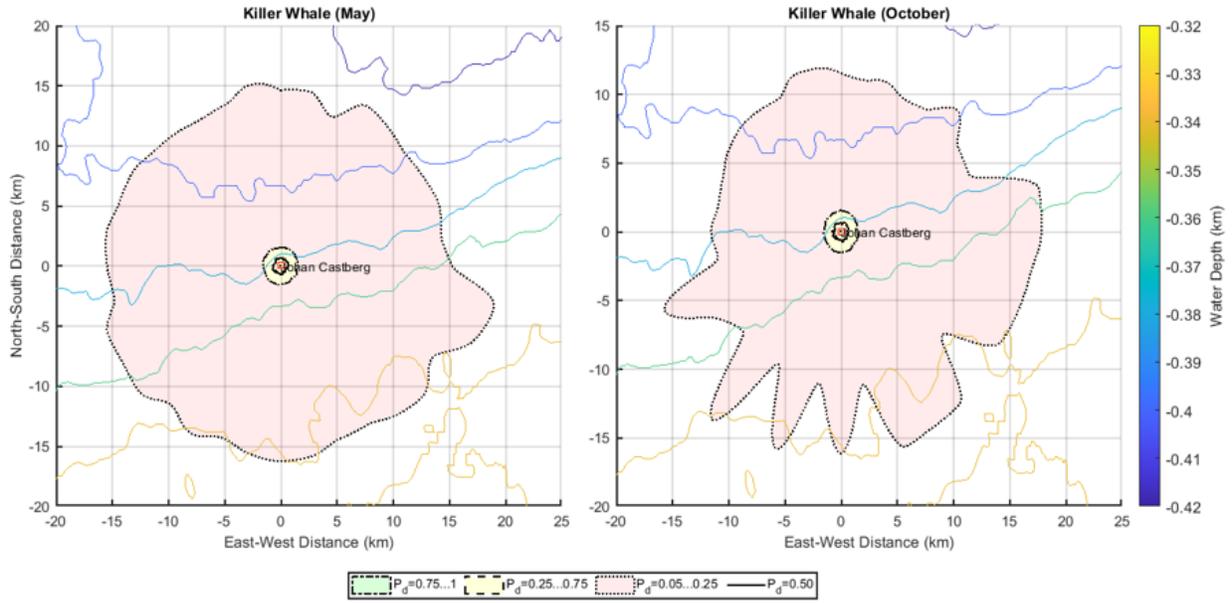
Figure 23. Killer whale tonal vocalization: Detection ranges associated with various probability of detection under noise conditions recorded at Johan Castberg in May and October. The center of each figures is the Johan Castberg oil field (72.5 N × 20.35 E). The solid black line shows the range for a 50% probability of detection.
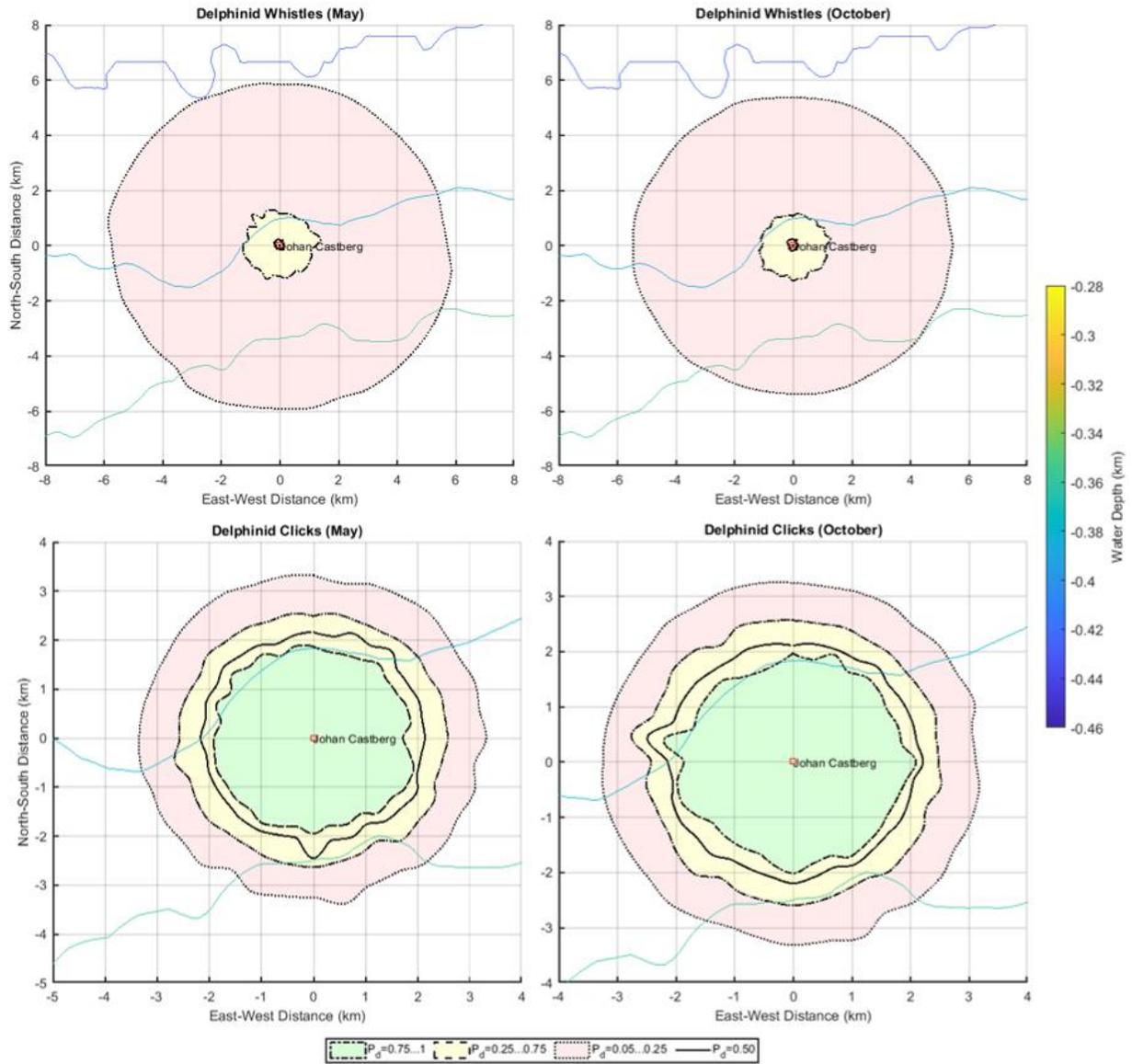
Figure 24. White-beaked dolphin whistles (top) and clicks (bottom): Detection ranges associated with various probability of detection under noise conditions recorded at Johan Castberg in May and October. The center of each figures is the Johan Castberg oil field (72.5 N × 20.35 E). The solid black line shows the range for a 50% probability of detection.

3.3. Marine Mammal Detections

Sound pressure level measurements and initial data quality checks revealed issues with the data recorded at PAMWest (see Section 3.1). The audio quality of the data was poor and although an inspection of the acoustic detector output revealed sporadic marine mammal vocalizations, many were faint or distorted. Based on these observations, the close proximity of the recorders, and the similarity of the detection patterns at PAMEast and PAMNorth, the data recorded at PAMWest were not analyzed for the presence of marine mammals and are not discussed further.

3.3.1. Detector Performance

The assessment of the performance of the detectors is based on a review of automated detections for a sample of files amounting to 3% of the dataset. Table 8 compiles the detector performance metrics for all detectors whose precision exceeded 0.75 (with one exception, see below). This precision value is empirical, based on JASCO's extensive detector development and assessment experience, it provides a good balance between detection accuracy and inclusiveness. Detector performance is always a trade-off between precision and recall. A higher precision cut-off value (i.e., a greater proportion of detections are true positive) generally translates into a lower recall, which means that less true positives are detected. In Table 8, the threshold refers to the minimum number of detections per sound file (the analysis unit) that is required to yield the P, R and MCC values. The exclusion period refers to any range of dates that was, excluded from the sample of validated files because the manual analysis showed an absence of a species in question. Files with a detection count strictly lower than the threshold were excluded from the results presented in Sections 3.3.2 to 3.3.5. When more than one detector was investigated for a given species, the results of the detector with the best scores are presented.

Detector performance is usually assessed for each dataset individually to account for differences in factors that could influence detections, such as species composition or background noise. In some cases, different detectors yielded the best results for PAMEast and PAMNorth, but evaluating both stations together allowed to pick a single detector with high quality results (see e.g., fin whale 20-Hz note or dolphin clicks; Table 8). For the fin whale 130-Hz notes, the detection count threshold was the same and the performance metrics nearly the same when both stations were assessed individually or together.

For sperm whale clicks, the click train detector worked best for PAMEast but despite a good precision (P=0.83), this detector had a low recall (R=0.25), yielding only 26 detection events (i.e., sound files with detection counts above threshold). Its precision was well below the cut-off for PAMNorth (P = 0.5). The combined precision for the click train detector precision was 0.75 but the recall was low (R = 0.15), yielding only 41 detection events for both stations. We therefore elected to use the results of the click detector and assess it for both stations together. Although the combined precision value (P = 0.7) is slightly below our cut-off, the good agreement between manual and automated detections (Figure 35) suggests that the results provide a representative picture of sperm whale occurrence, with about 175 detection events at each station and a recall value of 0.45.

Table 8. Performance of the automated detectors for each location and species including the threshold implemented, the exclusion period implemented, and the original and final detector precision and recall. The final detector performance is calculated after any timeframe and/or threshold restrictions have been applied.

Station	Species/ signal	Original			Exclusion period	Threshold	Threshold			Sample size		
		P	R	MCC			P	R	MCC	Files	Files with annotations	Files with detections
Both	Fin whale, 130 Hz note	0.51	0.78	0.54	None	7	0.85	0.59	0.66	354	58	88
Both	Fin whale, 20-Hz note	0.76	0.63	0.57	None	3	0.88	0.56	0.6	330	102	84
PAMEast	Humpback, moan	0.7	0.27	0.31	Start to 1 Nov; 1 May to end	4	1	0.25	0.43	163	52	20
PAMNorth	Humpback, moan	0.68	0.34	0.37	Start to 1 Nov	3	0.8	0.27	0.38	170	44	22
PAMEast	Killer whale, tonal vocalization	0.69	0.92	0.78	Start to 1 Nov and 1 May to end	2	0.92	0.92	0.91	159	12	16
PAMNorth	Killer whale, tonal vocalization	0.67	0.75	0.69	Start to 1 Nov; 1 Apr to end	2	1	0.75	0.86	182	8	9
Both	SpermWhale, click	0.55	0.51	0.4	None	3	0.7	0.45	0.45	349	80	74
Both	Dolphin, click	0.51	0.81	0.53	None	4	0.87	0.66	0.7	346	68	107

3.3.2. Fin Whales

Fin whale song notes (Figure 25) were the most commonly detected biological signal, with 121 and 127 detection days at PAMEast and PAMNorth, respectively, and 162 unique detection days for the study area as a whole. Considering both stations together, the proportion of days with detections was stable from October to December, declined from January to March and increased from April onward. On the other hand, detection counts peaked in February (Figure 26 and Figure 27). The increase in acoustic occurrence in the spring was not reflected in the number of calls detected, which reflects the decrease in song production in fin whales from April onward. While the total number of detections was similar between both stations, the monthly counts of detections were more variable at PAMNorth, possibly indicating more variability in the number of whales producing song notes near this recorder, or more variability in ambient noise and call detectability as a result, although the latter was not obvious based on the soundscape characterization (Table 9).

Because the 20 and 130 Hz notes of fin whale songs almost systematically co-occur, there were no days with 130-Hz note detections that were not also identified by the 20-Hz note detector. The precision and recall of the detectors for these two notes were comparable. The results indicate that they accurately classified 85-88% and captured 56 to 59% of these vocalizations (Figure 26).
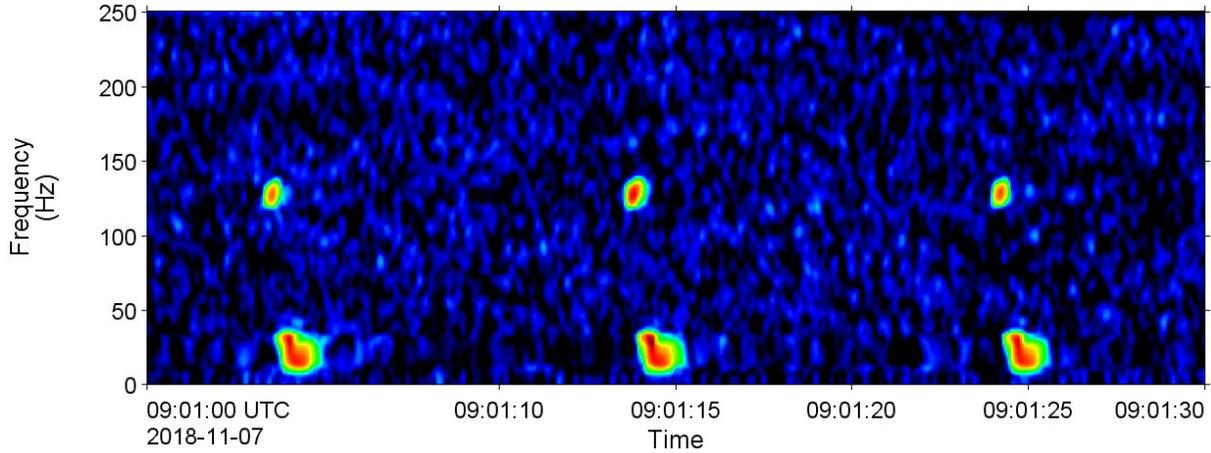
Figure 25. Spectrogram showing fin whale 20-Hz and the 130-Hz song notes recorded at PAMNorth on 7 Nov 2018. (1.18 Hz frequency resolution, 0.128 s time window, 0.032 s time step, Hamming window).The window length is 1.5 min.
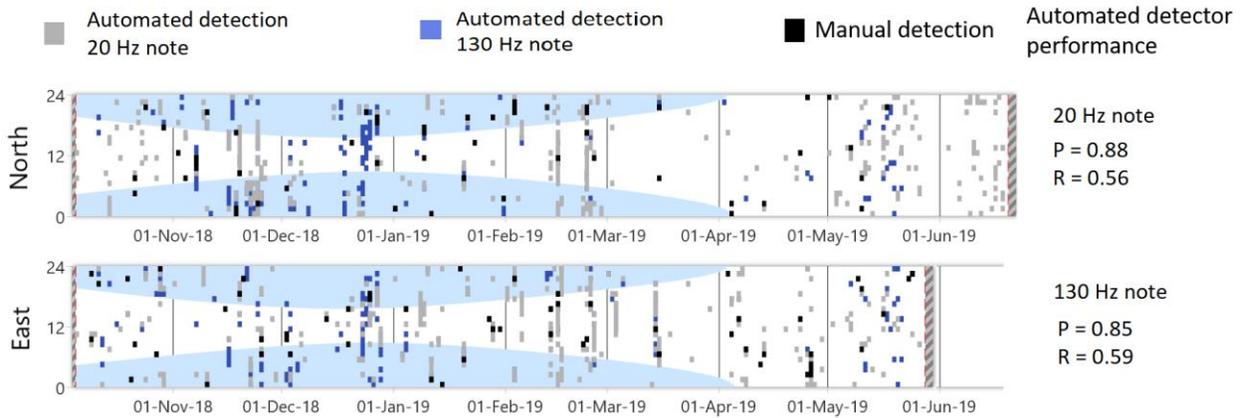
Figure 26. Daily and hourly occurrence of automatically and manually detected fin whale song notes. Red dashed lines indicate recorder deployment and retrieval dates or recording end. Hashed lines indicate a lack of recordings. Blue shaded areas indicate hours of darkness.
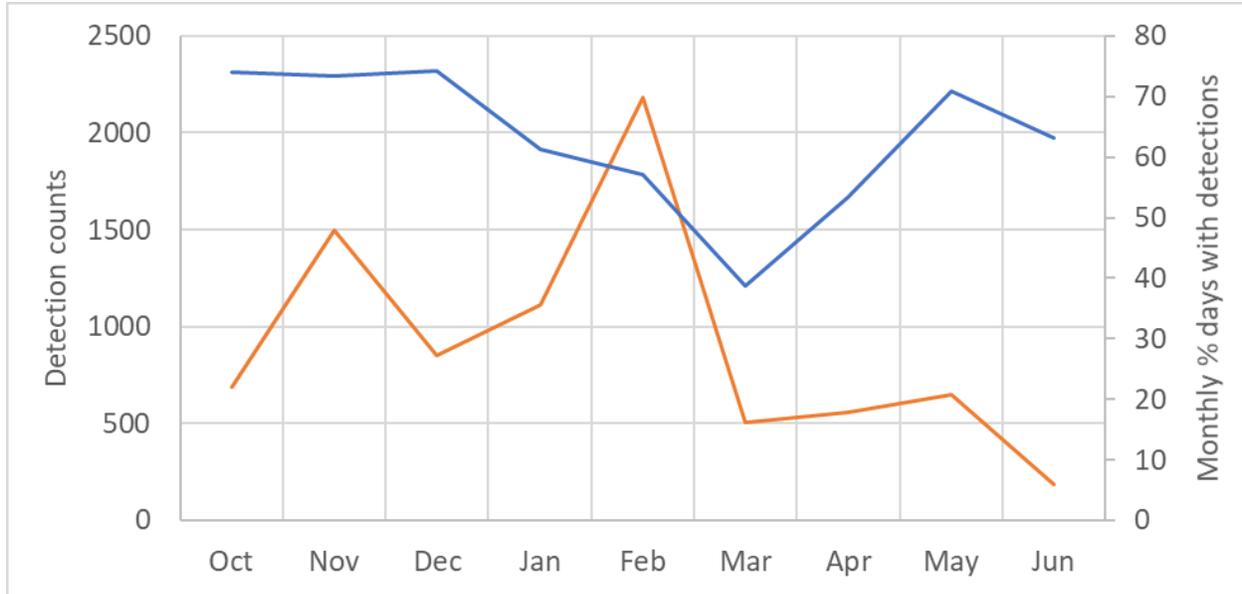
Figure 27. Fin whales: Monthly percent days with detections (blue) and detection counts (orange) by month for PAMEast and PAMNorth combined.

Table 9. Fin whale 20-Hz calls: Percent of days for each month with automated detections, detection counts by month and total number of automated detection days and counts at PAMEast, PAMNorth, and for the study area as a whole between 5 Oct 2018 and 19 Jun 2019. D: Detections.

Month	PAMEast		PAMNorth		Combined	
	% days with D	D counts	% days with D	D counts	% days with D	D counts
October	63	431	56	257	74	688
November	50	313	53	1185	73	1498
December	55	512	61	338	74	850
January	52	809	45	302	61	1111
February	50	987	57	1195	57	2182
March	35	445	16	60	39	505
April	47	430	37	128	53	558
May	65	233	61	419	71	652
June	n/a		63	188	63	188
Total detection days/counts	121	4160	127	4072	162	8232

3.3.3. Humpback Whales

Humpback whale vocalizations were detected at both stations in all months, except in October at both stations and in May at PAMEast. Both stations had similar number of detection days, for a combined total of 73 detection days. However, PAMNorth had nearly 50% more detections. Considering both stations

together, we observed an increase in detection days from October to the peak in March (58% of days had detections). Detections decreased in April, remained stable in May and declined significantly in June at PAMNorth (no data in June at PAMEast) (Figure 28 and Figure 29; Table 10). Most detections consisted of songs or song fragments (Figure 30).

Analysts identified 22 and 18 days at PAMEast and PAMNorth, respectively, that had no automated detections. This is primarily due to the generally low received levels of humpback whale vocalizations in these data. Vocalizations with low signal-to-noise ratio are harder for the detector to identify than for experienced analysts. The precision of the tonal detector targeting humpback whale moans was good for both stations (80-100%), but its recall was low (R ~0.25, Figure 28), suggesting that the automated detections alone underestimate the true occurrence of humpbacks.
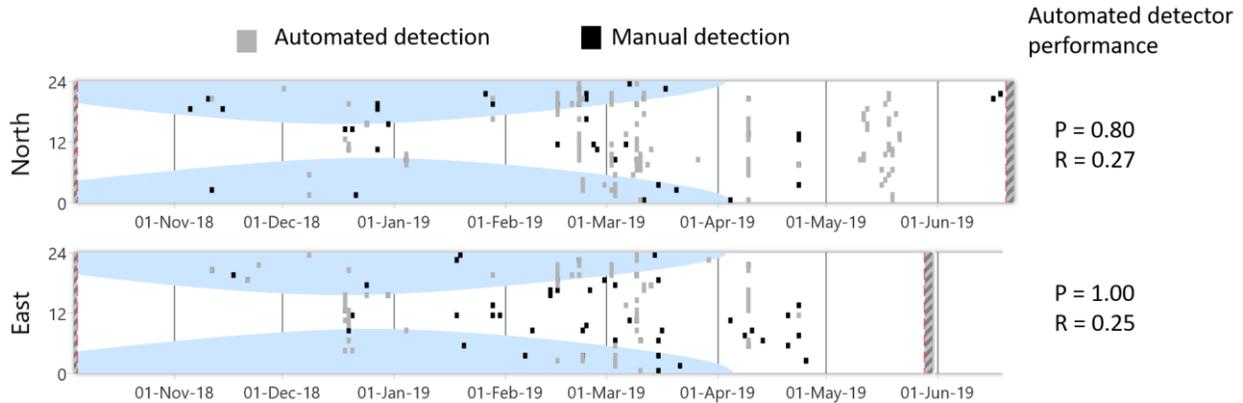
Figure 28. Daily and hourly occurrence of automatically and manually detected humpback whale vocalizations. Red dashed lines indicate recorder deployment and retrieval dates. Hashed lines indicate a lack of recordings. Blue shaded areas indicate hours of darkness.
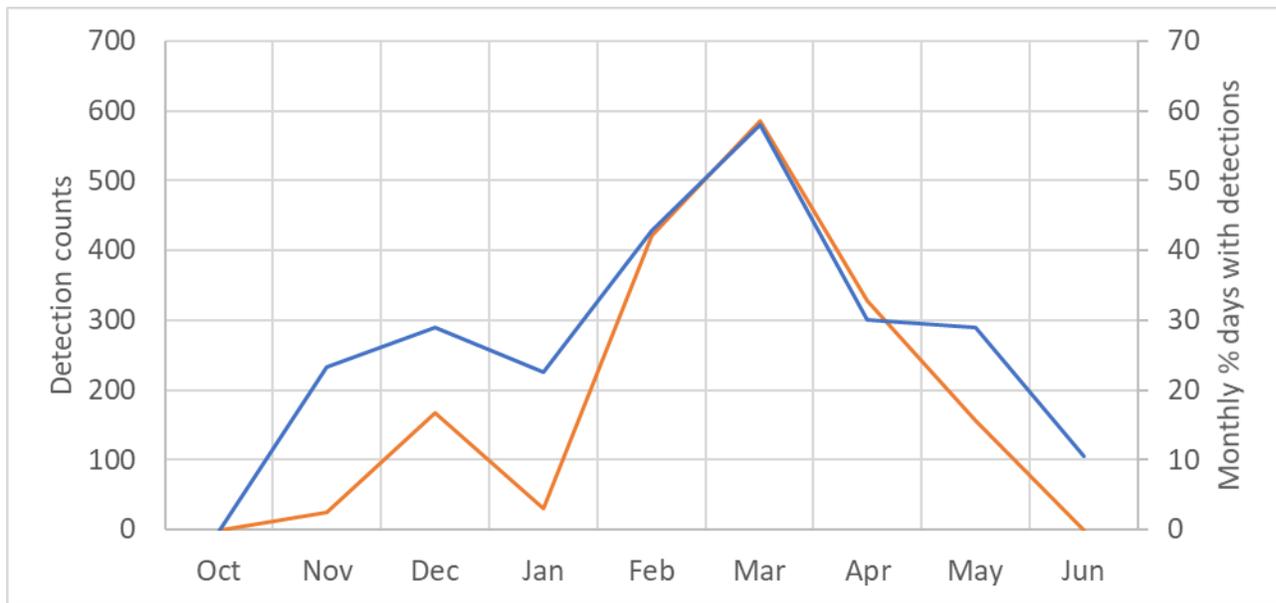
Figure 29. Humpback whales: Monthly percent days with detections (blue) and detection counts (orange) by month for PAMEast and PAMNorth combined.

Table 10. Humpback whale vocalization: Percent of days for each month with automated detections, detection counts by month and total number of automated detection days and counts at PAMEast, PAMNorth, and for the study area as a whole between 5 Oct 2018 and 19 Jun 2019. D: Detections.

Month	PAMEast		PAMNorth		Combined	
	% days with D	D counts	% days with D	D counts	% days with D	D counts
October	0	0	0	0	0	0
November	13	21	13	4	23	25
December	19	124	29	44	29	168
January	19	11	10	20	23	31
February	36	137	29	285	43	422
March	42	267	45	318	58	585
April	27	136	13	192	30	328
May	0	0	29	156	29	156
June	n/a		11	0	11	0
Total detection days/counts	47	696	53	1019	73	1715
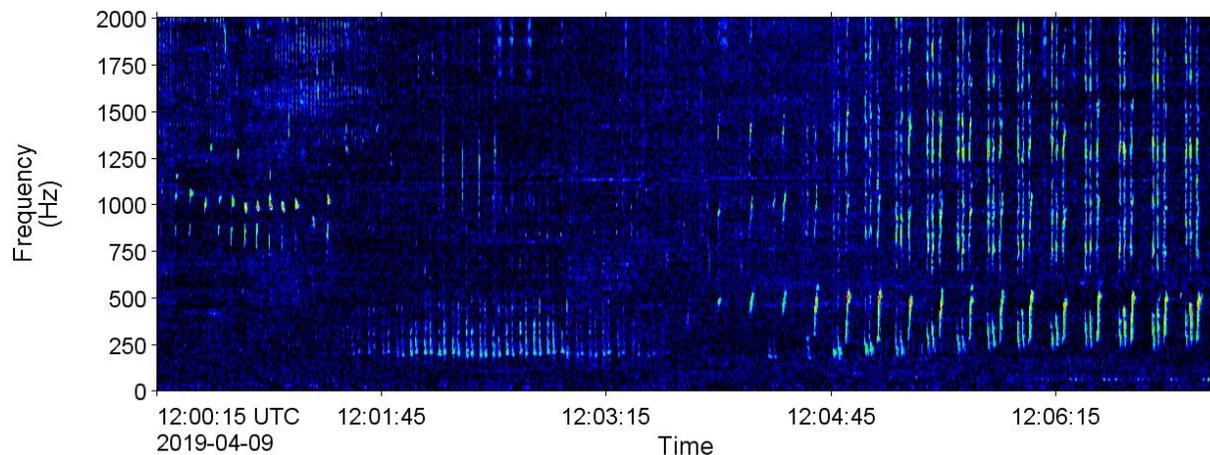
Figure 30. Spectrogram showing a segment of humpback whale song recorded at PAMNorth on 9 Apr 2019. (1.18 Hz frequency resolution, 0.128 s time window, 0.032 s time step, Hamming window). The window length is 7 min.

3.3.4. Killer Whales

Killer whale detections occurred sporadically throughout the recording period at both stations, over a combined total of 26 unique days (Figure 31; Table 11). The months with the highest proportion of days with detections was November. There were no detections in October, May and June. There were only 2 detections (1 at each station) between 4 January and 3 March (Table 11). PAMEast had higher number of detection days and detections, but the bulk of these detections occurred in December and March, with low or no detections in the other months (Figure 32). The precision and recall values were comparable for

both stations and indicate that the automated detections offer an accurate description of the acoustic occurrence of killer whales in the study area.

The detected vocalizations consisted of whistles and pulsed vocalizations, often associated with echolocation clicks (Figure 33).
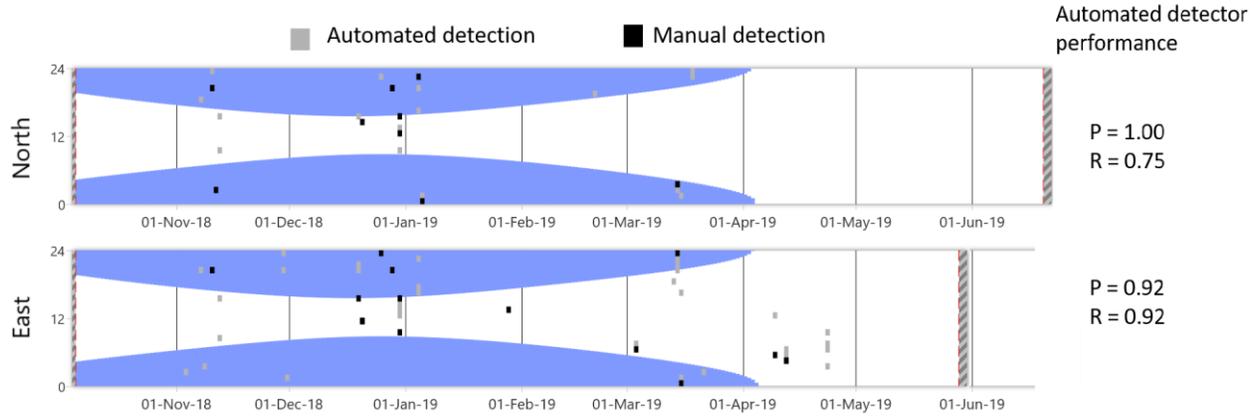
Figure 31. Daily and hourly occurrence of automatically and manually detected killer whale vocalizations. Red dashed lines indicate recorder deployment and retrieval dates. Hashed lines indicate a lack of recordings. Blue shaded areas indicate hours of darkness.
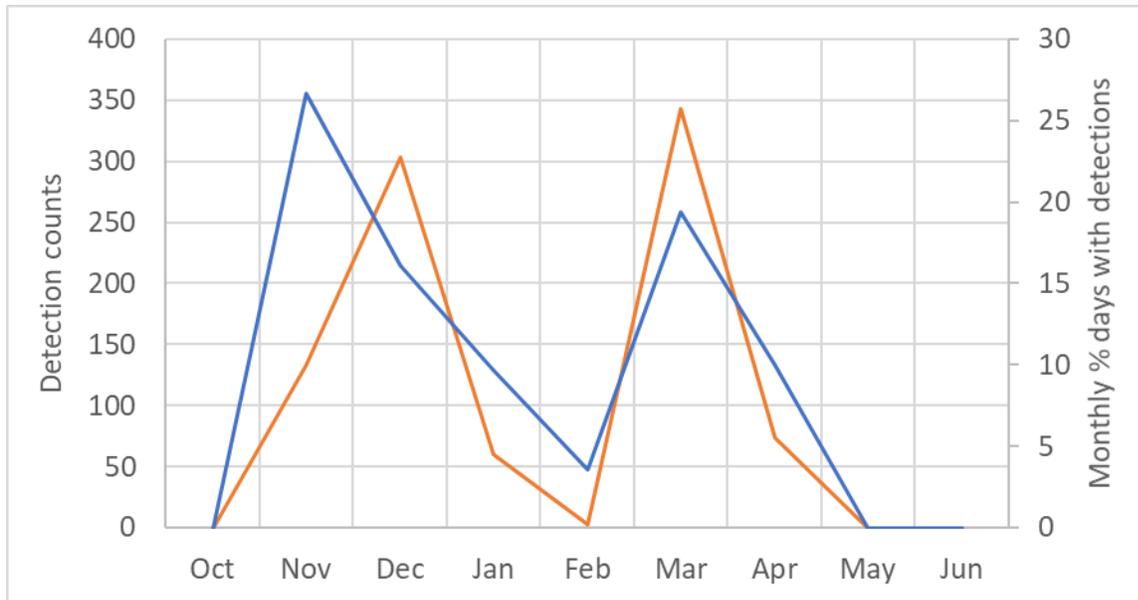
Figure 32. Killer whales: Monthly percent days with detections (blue) and detection counts (orange) by month for PAMEast and PAMNorth combined.

Table 11. Killer whale vocalization: Percent of days for each month with automated detections, detection counts by month and total number of automated detection days and counts at PAMEast, PAMNorth, and for the study area as a whole between 5 Oct 2018 and 19 Jun 2019. D: Detections.

Month	PAMEast		PAMNorth		Combined	
	% days with D	D counts	% days with D	D counts	% days with D	D counts
October	0	0	0	0	0	0
November	23	53	13	80	27	133
December	16	205	16	98	16	303
January	6	12	6	48	10	60
February	0	0	4	3	4	3
March	16	306	10	37	19	343
April	10	74	0	0	10	74
May	0	0	0	0	0	0
June	n/a		0	0	0	0
Total detection days/counts	**22**	**650**	**15**	**266**	**26**	**916**
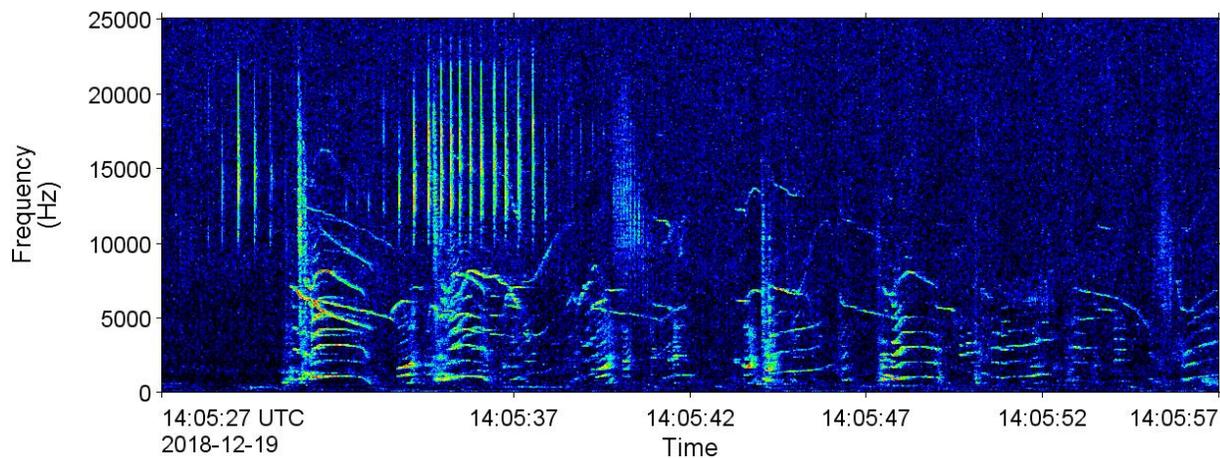
Figure 33. Spectrogram showing killer whale vocalizations recorded at PAMEast on 19 Dec 2018. (38 Hz frequency resolution, 0.01 s time window, 0.005 s time step, Hamming window).The window length is 30 s.

3.3.5. Sperm Whales

Sperm whale clicks (Figure 34) were the third most commonly detected biological signal during the study. They were recorded on 79 and 78 days at PAMEast and PAMNorth, respectively, for a combined total of 118 unique detection days (Table 12). The proportion of days with detections was highest in November, lowest in February and reached another peak in May (Figure 36). PAMEast had approximately twice as many click detections than PAMNorth, but this was almost entirely driven by high click counts in May. In other months, click counts were similar at both stations (Table 12; Figure 35). As discussed in Section

3.3.1, although the precision value (P = 0.7) of the sperm whale click detector is slightly below the cut-off value (P=0.75) that we usually apply to decide whether to consider automated detections or not, the good agreement between manual and automated detections (Figure 35) suggests that the results provide a representative, although underestimated (R=45%), picture of sperm whale occurrence. The precision was presumably affected by the presence of killer whale clicks which can overlap in frequency with those from sperm whales.
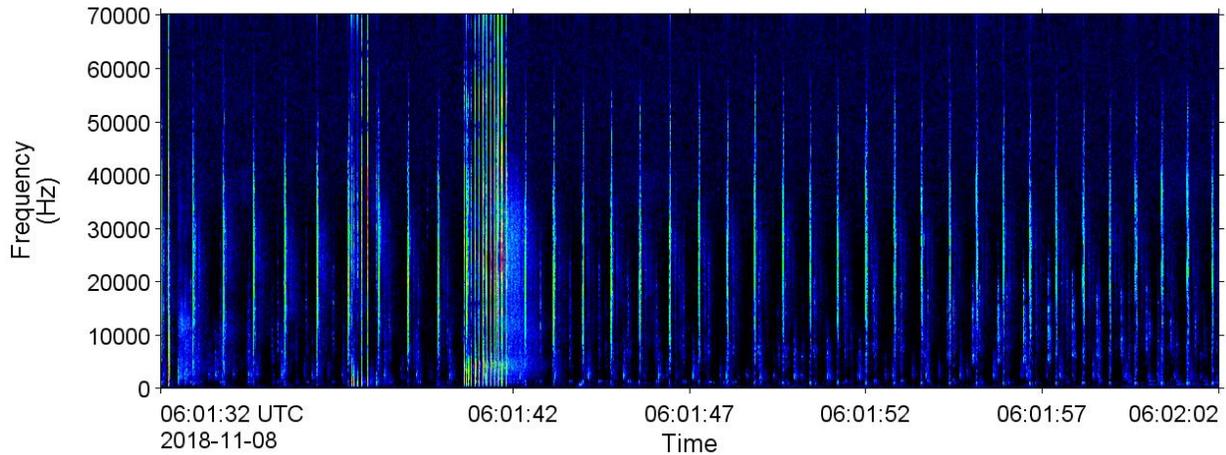
Figure 34. Spectrogram showing sperm whale clicks recorded at PAMEast on 19 Dec 2018. (38 Hz frequency resolution, 0.01 s time window, 0.005 s time step, Hamming window). The window length is 30 s.
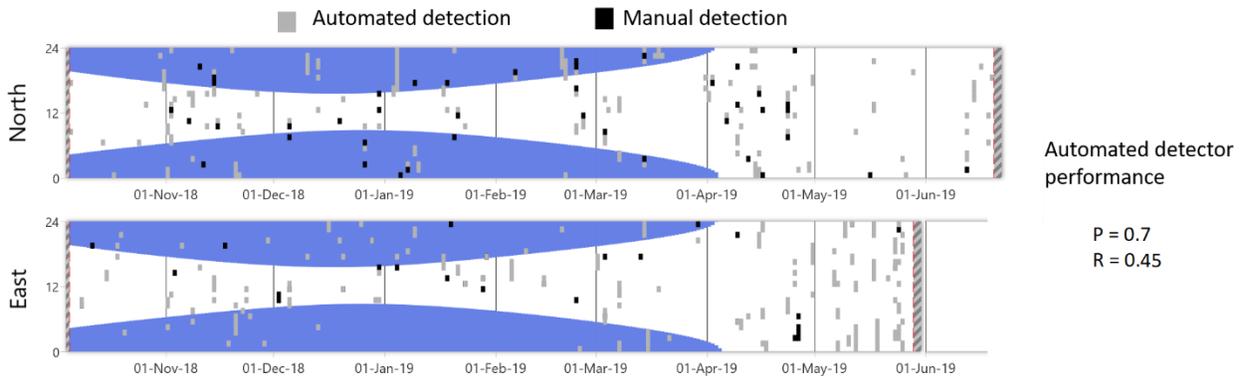

Figure 35. Daily and hourly occurrence of automatically and manually detected sperm whale clicks. Red dashed lines indicate recorder deployment and retrieval dates. Hashed lines indicate a lack of recordings. Blue shaded areas indicate hours of darkness.
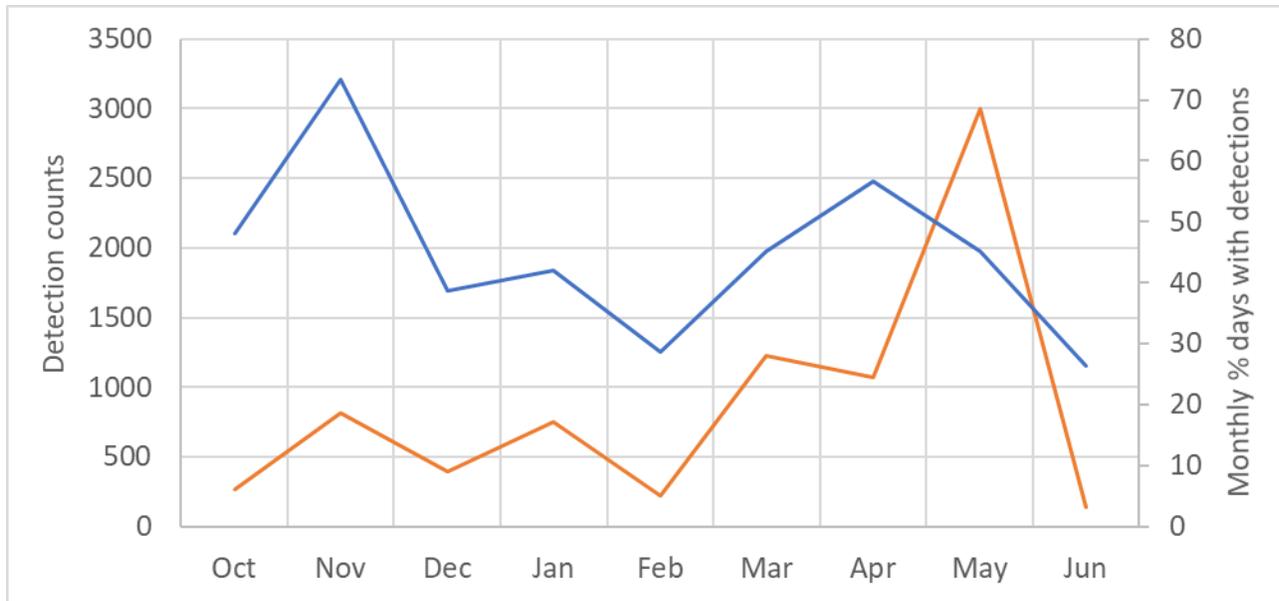
Figure 36. Sperm whales: Monthly percent days with detections (blue) and detection counts (orange) by month for PAMEast and PAMNorth combined.

Table 12. Sperm whale vocalizations: Percent of days for each month with automated detections, detection counts by month and total number of automated detection days and counts at PAMEast, PAMNorth, and for the study area as a whole between 5 Oct 2018 and 19 Jun 2019. D: Detections.

Month	PAMEast		PAMNorth		Combined	
	% days with D	D counts	% days with D	D counts	% days with D	D counts
October	22	106	26	160	48	266
November	50	319	50	497	73	816
December	35	234	23	162	39	396
January	32	125	32	630	42	755
February	18	90	18	130	29	220
March	32	915	26	315	45	1230
April	33	480	53	593	57	1073
May	46	2933	16	65	45	2998
June	n/a		26	139	26	139
Total detection days/counts	79	5202	78	2691	118	7893

3.3.6. Delphinids

The acoustic occurrence of delphinids was assessed by searching for echolocation clicks and whistles (Figure 37). White-beaked dolphins are the dominant species in this area (Øien 1996) and produce both types of signals (Rasmussen and Miller 2002). The whistle detector did not perform satisfactorily on these data. On the other hand, the click detector (for Atlantic white-sided dolphin click; see Table 4) had good precision and recall values. Delphinid clicks were recorded nearly two times more often at PAMNorth than PAMEast (101 versus 48 days) for a combined total of 121 detections days in the study area, making them the second most commonly detected signals (Table 13). At both stations, detections followed a clear seasonal trend. The combined number of detections days was highest in October, decreased in November and was lowest from December to February. Detection days increased in March and stabilized near their October level from April until the end of the recording period, although detection counts remained lower in the spring than in the fall (Table 13; Figure 38 and Figure 39).
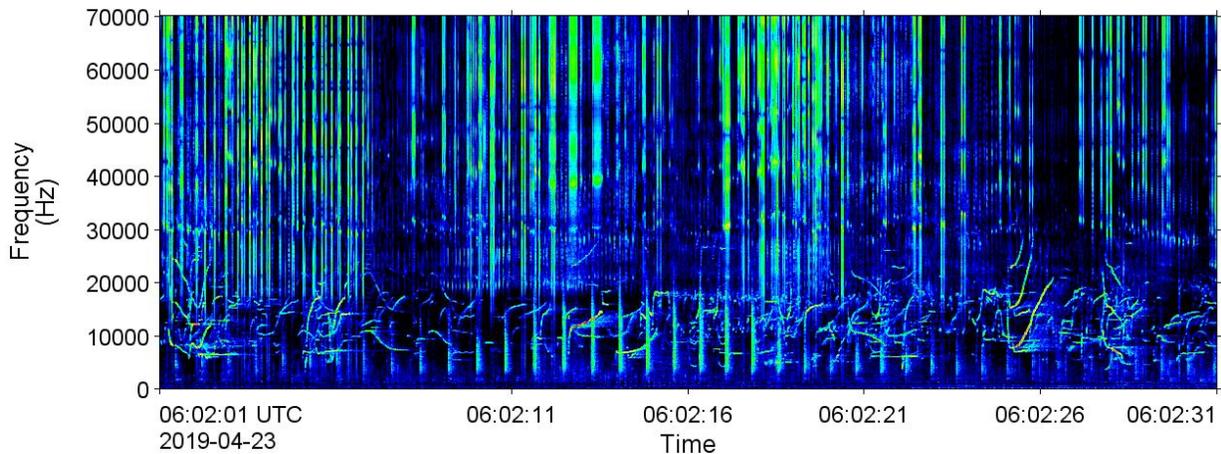
Figure 37. Spectrogram showing delphinid clicks and whistles recorded at PAMEast on 23 Apr 2019. (38 Hz frequency resolution, 0.01 s time window, 0.005 s time step, Hamming window).The window length is 30 s. Sperm whale clicks are also visible below 20 kHz.
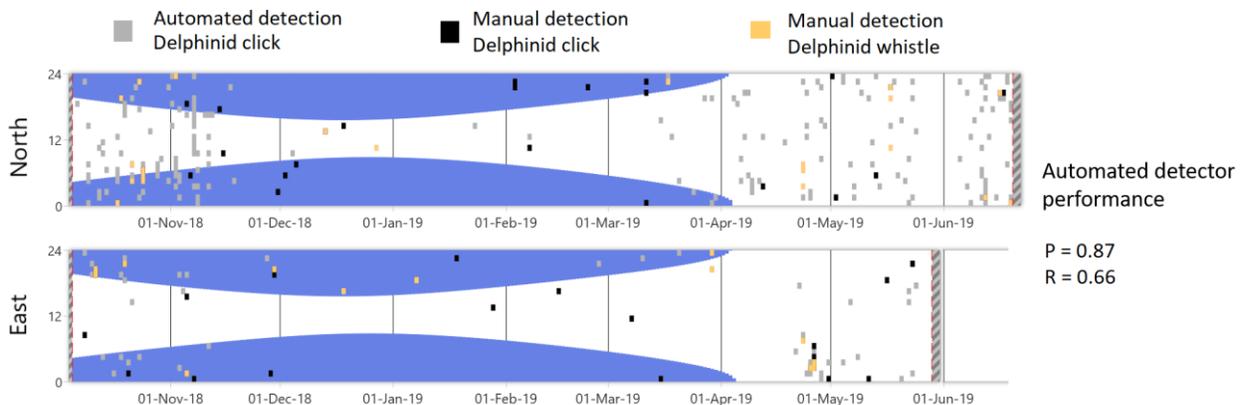

Figure 38. Daily and hourly occurrence of automatically and manually detected delphinid signals. Red dashed lines indicate recorder deployment and retrieval dates. Hashed lines indicate a lack of recordings. Blue shaded areas indicate hours of darkness.
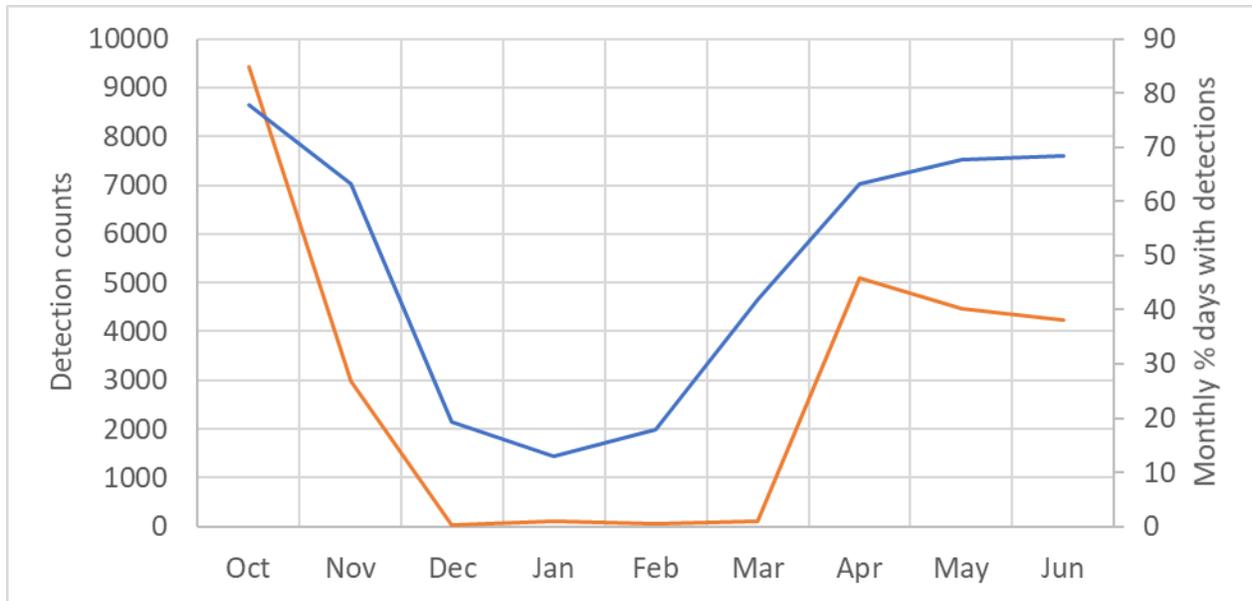
Figure 39. Delphinid clicks: Monthly percent days with detections (blue) and detection counts (orange) by month for PAMEast and PAMNorth combined.

Table 13. Delphinid vocalizations: Percent of days for each month with automated detections, detection counts by month and total number of automated detection days and counts at PAMEast, PAMNorth, and for the study area as a whole between 5 Oct 2018 and 19 Jun 2019. D: Detections.

Month	PAMEast		PAMNorth		Combined	
	% days with D	D counts	% days with D	D counts	% days with D	D counts
October	37	3696	67	5729	78	9425
November	27	699	50	2281	63	2980
December	3	0	19	34	19	34
January	10	67	3	43	13	110
February	7	4	11	52	18	56
March	16	69	35	46	42	115
April	33	4735	50	356	63	5091
May	35	664	61	3803	68	4467
June	n/a		68	4246	68	4246
Total detection days/counts	**48**	**9934**	**101**	**16590**	**121**	**26524**

4. Discussion and Conclusion

4.1. The Soundscape

The soundscape characterization revealed obvious similarities between PAMNorth and PAMEast. This is due to their close proximity (~12 km) and the similar influence of natural and anthropogenic sources as a result. The soundscape saw limited influence from anthropogenic activities besides fishing operations in the vicinity of the oil field. Ultimately, the detected vessels (presumably fishing vessels) had a limited impact on daily SEL (Figure 15). This appears to be consistent with the limited number of distinct tracks (i.e., vessels) recorded on AIS each month near Johan Castberg (Figure 4).

There were no activities connected to the development of the Johan Castberg oil field until May 2019. A seabed profiling survey for a fiber optic cable route from Melkøya to Johan Castberg operated briefly near the outer edges of the field on three occasions in May 2019. The sporadic seismic airgun detections on 10–12 and 16–19 May are presumably connected to subbottom profiling operations.

Despite the limited influence of anthropogenic activities on the measured noise levels, they were high in comparison to other areas monitored over comparable length of time by JASCO in the North Atlantic, particularly at low frequencies (Figure 40). The 20-Hz peak in spectral levels attributed to fin whales was much higher than in many other areas. This may be because source levels in the Barents Sea are higher than in others as suggested by Garcia et al. (2018), song notes thereby contributing more acoustic energy to the soundscape. The detection period of fin whale song notes (October through May) was also longer than in many other north Atlantic areas, including the high Arctic, where song production declines significantly in April and songs are rare from May to August (Klinck et al. 2012, Moore et al. 2012, Morano et al. 2012, Nieukirk et al. 2012, Delarue et al. 2018). This could be why power median spectral density levels near 20 Hz are higher than in other areas when considering long-term datasets, but comparable when considering the month of November (Figure 41) when fin whales can be expected to produce songs at similar rate in most areas.

Sound levels remained higher than in other areas above 30 Hz at PAMNorth and PAMEast. It is unclear why this is so. Although all efforts have been made to ensure that the calibration curves were correctly applied to the data, issues with calibration or the recorders cannot be entirely ruled out by JASCO. Interestingly, the recorder that suffered technical issues (PAMWest) is that which yielded sound levels most consistent with other North Atlantic areas (Figure 40) at higher frequencies.
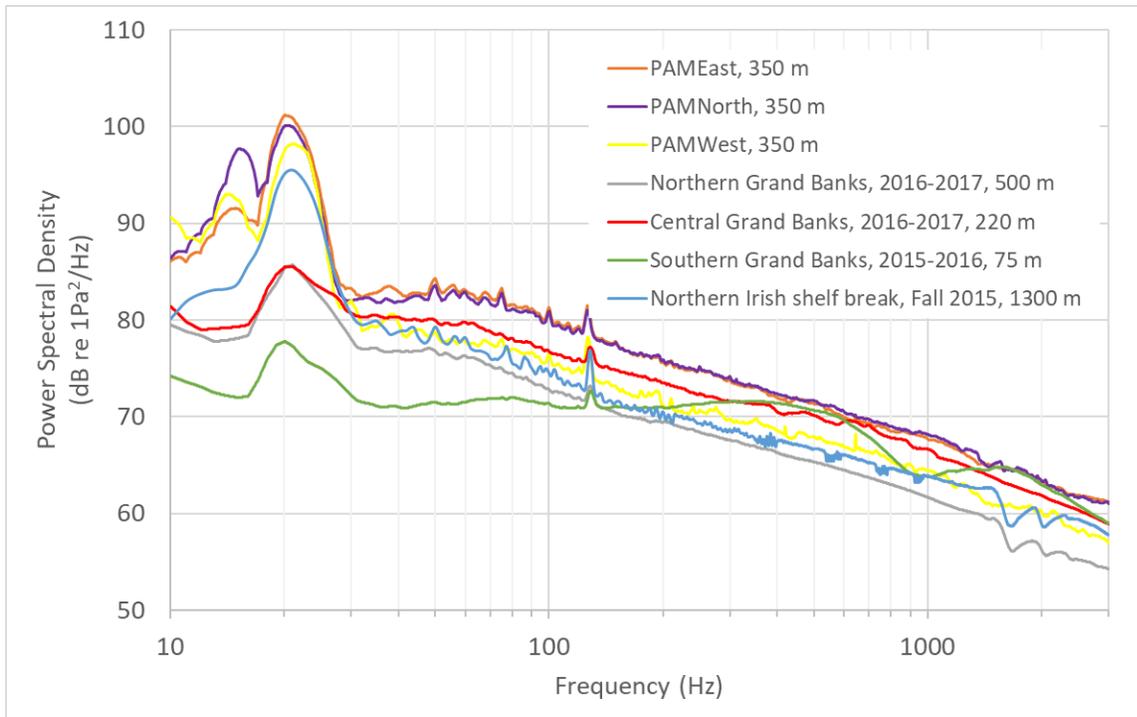
Figure 40. Median of 1-min power spectral density levels for several North Atlantic areas in comparison to those measured at PAMEast, PAMNorth and PAMWest.
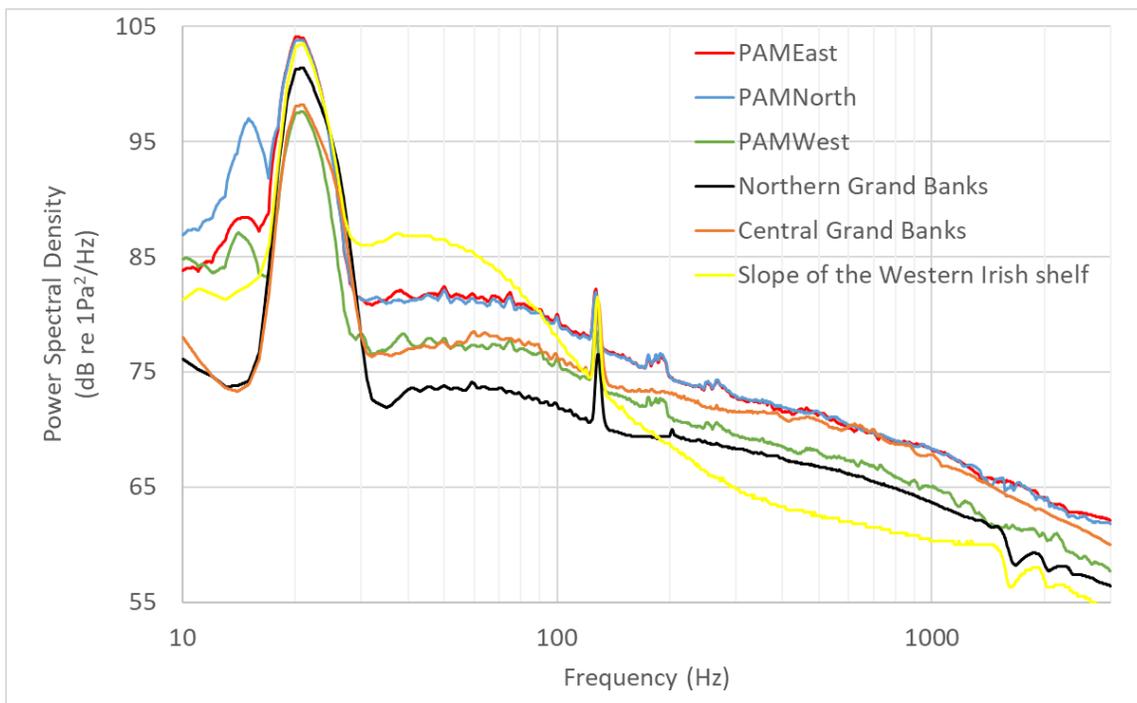
Figure 41. Median of 1-min power spectral density levels in November 2016 at Newfoundland Grand Banks locations and in October 2016 at one location along the continental slope of the Irish shelf in comparison to those measured in November 2018 at PAMEast, PAMNorth and PAMWest.

4.2. Marine Mammals

Thanks to the lack of activities linked to the development of the Johan Castberg oil field during the recording period, the results presented in this report provide a baseline against which to assess the occurrence of marine mammals in the study area in the future. Species diversity was relatively low compared to areas to the north (e.g., Svalbard) or west (continental slope) (Kovacs et al. 2009). This may be the result of a lack of prominent bathymetric (such as banks or seamounts) or oceanographic (such as thermal front, like the polar front located near Svalbard (Skern-Mauritzen et al. 2011)) features in and around the oil field, which tend to increase biological productivity, as well as the absence of sea ice in winter, which concentrates pagophilic pinnipeds and cetaceans such as ringed seals, bowhead (*Balaena mysticetus*) and beluga whales (*Delphinapterus leucas*).

All species showed some seasonal patterns of occurrence. With the exception of October and May-June, all species were detected on at least one day in each month. For all species but fin whales, the lowest acoustic occurrence generally happened during the peak winter months. Humpback whale occurrence peaked in March, possibly coinciding with the northern migration to their Barents Sea feeding grounds. The nearest known feeding ground from the study area is Bear Island, where humpback whales target spring spawning herring and euphausiids in spring and early summer (Christensen et al. 1990, Jourdain and Vongraven 2017). The rise in detections in the fall is likely associated with whales migrating south towards the breeding grounds. Killer whales showed two distinct occurrence peaks in November and March. It is unclear whether this reflects a seasonal migration pattern or whether the detected killer whales may be of the marine mammal-eating ecotype and time their presence in the area to coincide with the presumed migratory waves of potential cetacean preys {Ferguson, 2010 #29810}. Fin whale acoustic occurrence was lowest in March when other species appear to return to the area, but this may reflect acoustic behavior more than a lower presence of the species. Indeed, song production typically declines in March and April at the end of the breeding season (Klinck et al. 2012).
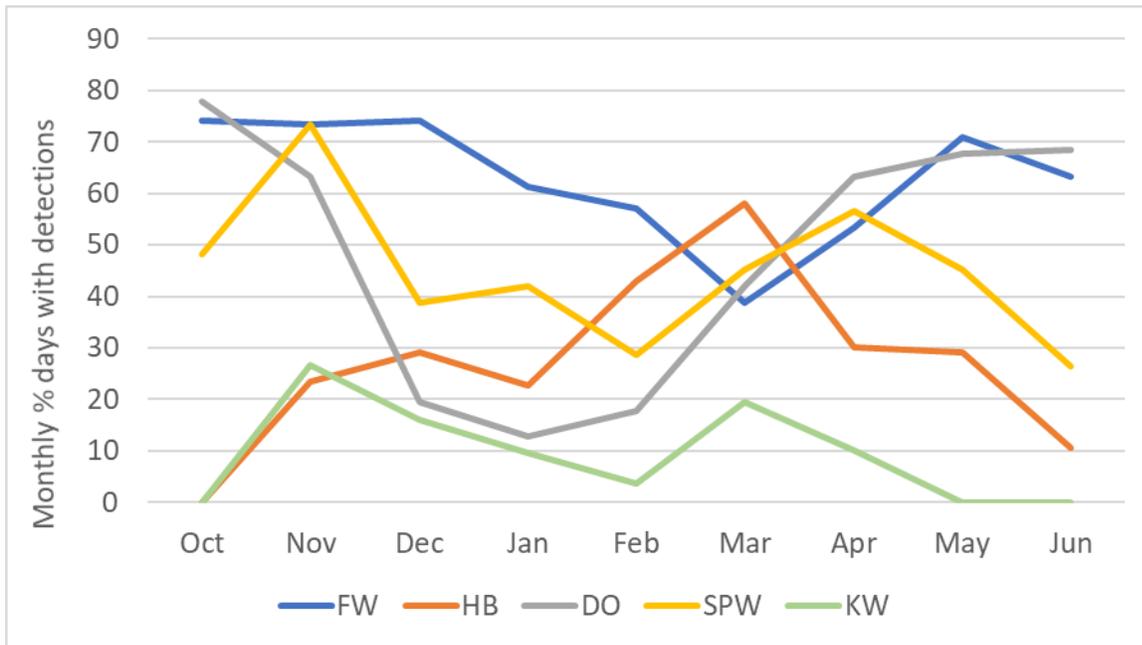
Figure 42. Monthly percent days with detections by month for PAMEast and PAMNorth combined for fin whales (FW), humpback whales (HB), dolphins (DO), sperm whales (SPW) and killer whales (KW).

The acoustic detections of delphinid signals may include a small number of species but the overlap in whistle and click spectral features between many delphinid species did not allow us to identify them acoustically. However, the range of water temperature throughout the year (4.5–7.5°C) and the prevalence of white-beaked dolphins in the sighting records in the Barents Sea suggest that white-beaked

dolphins were the main small delphinid species in the area. White-beaked dolphins are most common in areas with sea surface temperature (SST) less than 13°C off the United Kingdom and Ireland (MacLeod et al. 2008). In the western North Atlantic, white-sided dolphins are typically sighted in SST of 7±3°C, but white-beaked dolphins occur further north and both species have a non-overlapping distribution in eastern Canadian waters (Kingsley and Reeves 1998). The relatively shallow depth in the area (~350 m) and its distance away from the continental slope (~150 km) might also limit the occurrence of species preferring deep water, such as pilot whales. Killer whales, which can be reliably identified acoustically from other delphinids, occurred sporadically. Delphinid detections showed a clear seasonal trend, suggesting that the majority of white-beaked dolphins leave the area in winter.

Because of the high noise levels at low frequencies, the detection range of fin whales was generally low in average conditions. This has the immediate effect of limiting the perceived acoustic occurrence of this species by restricting the monitored area. Our relatively low ranges also contrast with the long detection ranges associated with a 50% probability of detection (PoD) of 20-Hz pulses off Finnmarck with a single hydrophone presented by Garcia et al. (2018). Their 50% PoD range was similar to the detection ranges we obtained under the best conditions. The difference can be explained, for the most part, by the fact that the authors did not use in-situ long-term measurements of ambient noise in their model and may therefore not accurately characterize the soundscape in which the fin whale vocalizations propagate. Even under reduced detection ranges, the persistent presence of fin whale detections throughout the year suggests that they are resident of the area.

The lack of minke whale acoustic detections may be puzzling since they are considered common in the Barents Sea (Kovacs et al. 2009). However, their distribution is strongly biased towards the waters surrounding Svalbard and near the coast of Norway. In addition, minke whales migrate to subtropical or tropical water to breed. The onset of the southern migration is in the fall (Risch et al. 2014), and whales generally return to northern areas in the spring. In Iceland, tagged minke whales started migrating south between early October and early November (Vikingsson and Heide-Jørgensen 2015). The lack of detections could therefore be linked to a lack of, or low occurrence of, minke whales in the study area. In addition, minke whales show evidence of sexual segregation on the feeding grounds, with females found in higher proportion with increasing latitude (Laidre et al. 2009). Since males are believed to produce the signals typically used to monitor this species acoustically, a lack or low proportion of males in the study area would further reduce the likelihood of detecting their calls.

The consistent acoustic occurrence of sperm whales in the study area is noteworthy considering their preferred habitat is generally in deep waters on and off the continental slope {Rogan, 2017 #24821}. However, marine mammal surveys in the Barents Sea have found areas of occurrence well onto the continental shelf in the vicinity of the study area {Storrie, 2018 #29777}.

With the exception of sperm whales whose ranges were comparable to those of fin whales, and which could be substantially longer in the case of the loudest possible clicks, the typical detection range for all species detected was a few kilometers from the recorders. This indicates that the results characterize the acoustic occurrence of marine mammals in the immediate vicinity of the recorders, most of the time.

Overall, at least one species were detected nearly every day of the deployment (Figure 43), suggesting that the southern Barents Sea and Johan Castberg area remain important for a few species of marine mammals year-long. In order to monitor the entire community of species potentially occurring in the area, future studies should use recorders with a sampling rate high enough to capture the clicks of harbor porpoises that may be present in, or transit through, the area. Deploying a recorder away from the Johan Castberg oil field, for instance near the continental slope to the west or close to Bear Island, would allow comparing detections and species diversity to an area not affected by its development and potentially more biologically productive.
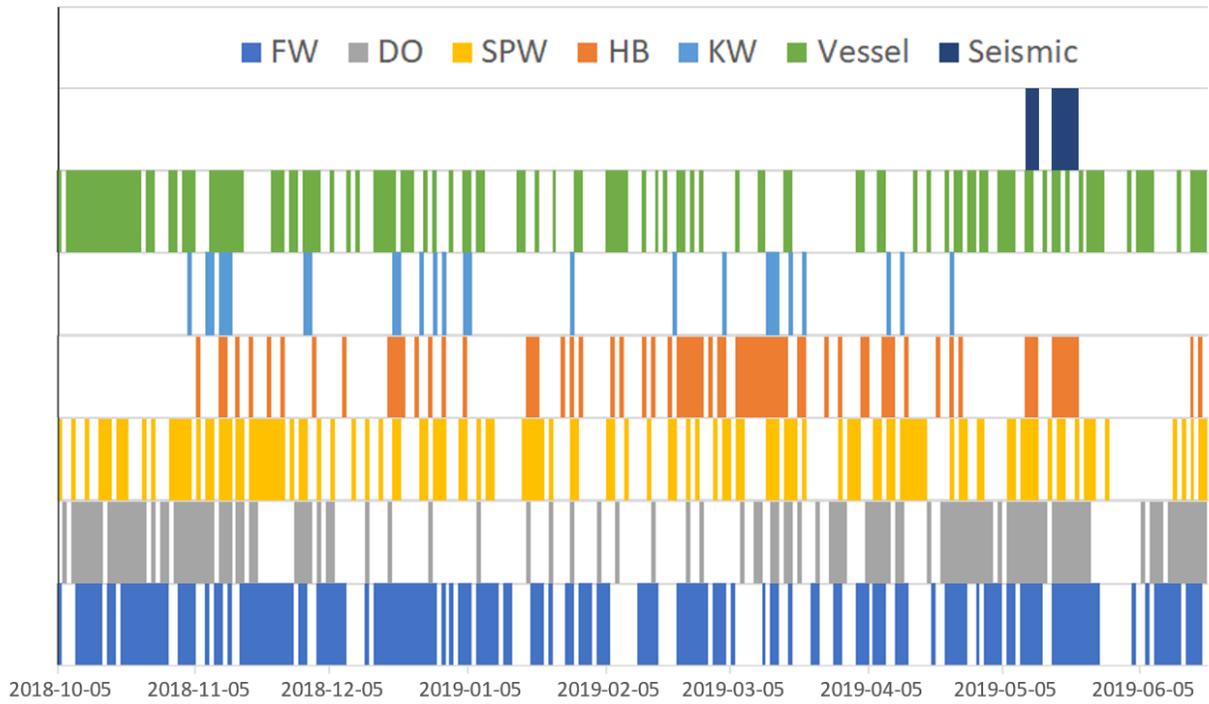
Figure 43. Time series showing the combined daily presence of marine mammal and anthropogenic detections recorded at PAMNorth and PAMEast between 5 Oct 2018 and 19 Jun 2019. FW: fin whale; DO: Dolphins; SPW: sperm whale; HB: humpback whale; KW: killer whale.

Glossary

ambient noise
All-encompassing sound at a given place, usually a composite of sound from many sources near and far (ANSI S1.1-1994 R2004), e.g., shipping vessels, seismic activity, precipitation, sea ice movement, wave action, and biological activity.

Auditory frequency weighting (auditory weighting function, frequency-weighting function)
The process of band-pass filtering sounds to reduce the importance of inaudible or less-audible frequencies for individual species or groups of species of aquatic mammals (ISO 2017b). One example is M-weighting introduced by Southall et al. (2007) to describe "Generalized frequency weightings for various functional hearing groups of marine mammals, allowing for their functional bandwidths and appropriate in characterizing auditory effects of strong sounds".

background noise
Total of all sources of interference in a system used for the production, detection, measurement, or recording of a signal, independent of the presence of the signal (ANSI S1.1-1994 R2004). Ambient noise detected, measured, or recorded with a signal is part of the background noise.

bandwidth
The range of frequencies over which a sound occurs. Broadband refers to a source that produces sound over a broad range of frequencies (e.g., seismic airguns, vessels) whereas narrowband sources produce sounds over a narrow frequency range (e.g., sonar) (ANSI/ASA S1.13-2005 R2010).

box-and-whisker plot
A plot that illustrates the center, spread, and overall range of data from a visual 5-number summary. The ends of the box are the upper and lower quartiles (25th and 75th percentiles). The horizontal line inside the box is the median (50th percentile). The whiskers and points extend outside the box to the highest and lowest observations, where the points correspond to outlier observations (i.e., observations that fall more than 1.5 × IQR beyond the upper and lower quartiles, where IQR is the interquartile range).

broadband sound level
The total sound pressure level measured over a specified frequency range. If the frequency range is unspecified, it refers to the entire measured frequency range.

decade
Logarithmic frequency interval whose upper bound is ten times larger than its lower bound (ISO 2006).

decidecade
One tenth of a decade (ISO 2017b). Note: An alternative name for decidecade (symbol ddec) is "one-tenth decade". A decidecade is approximately equal to one third of an octave (1 ddec ≈ 0.3322 oct) and for this reason is sometimes referred to as a "one-third octave".

decidecade band
Frequency band whose bandwidth is one decidecade. Note: The bandwidth of a decidecade band increases with increasing center frequency.

decibel (dB)
One-tenth of a bel. Unit of level when the base of the logarithm is the tenth root of ten, and the quantities concerned are proportional to power (ANSI S1.1-1994 R2004).

delphinid
Family of oceanic dolphins, or Delphinidae, composed of approximately thirty extant species, including dolphins, porpoises, and killer whales.

frequency
The rate of oscillation of a periodic function measured in cycles-per-unit-time. The reciprocal of the period. Unit: hertz (Hz). Symbol: *f*. 1 Hz is equal to 1 cycle per second.

hearing group
Groups of marine mammal species with similar hearing ranges. Commonly defined functional hearing groups include low-, mid-, and high-frequency cetaceans, pinnipeds in water, and pinnipeds in air.

harmonic
A sinusoidal sound component that has a frequency that is an integer multiple of the frequency of a sound to which it is related. For example, the second harmonic of a sound has a frequency that is double the fundamental frequency of the sound.

hertz (Hz)
A unit of frequency defined as one cycle per second.

high-frequency (HF) cetacean
The functional cetacean hearing group that represents those odontocetes (toothed whales) specialized for hearing high frequencies.

hydrophone
An underwater sound pressure transducer. A passive electronic device for recording or listening to underwater sound.

impulsive sound
Sound that is typically brief and intermittent with rapid (within a few seconds) rise time and decay back to ambient levels (NOAA 2013, ANSI S12.7-1986 R2006). For example, seismic airguns and impact pile driving.

low-frequency (LF) cetacean
The functional cetacean hearing group that represents mysticetes (baleen whales) specialized for hearing low frequencies.

mean-square sound pressure spectral density
Distribution as a function of frequency of the mean-square sound pressure per unit bandwidth (usually 1 Hz) of a sound having a continuous spectrum (ANSI S1.1-1994 R2004). Unit: $\mu Pa^2/Hz$.

median
The 50th percentile of a statistical distribution.

mid-frequency (MF) cetacean
The functional cetacean hearing group that represents those odontocetes (toothed whales) specialized for mid-frequency hearing.

mysticete
Mysticeti, a suborder of cetaceans, use their baleen plates, rather than teeth, to filter food from water. They are not known to echolocate, but they use sound for communication. Members of this group include rorquals (Balaenopteridae), right whales (Balaenidae), and grey whales (*Eschrichtius robustus*).

non-impulsive sound
Sound that is broadband, narrowband or tonal, brief or prolonged, continuous or intermittent, and typically does not have a high peak pressure with rapid rise time (typically only small fluctuations in decibel level) that impulsive signals have (ANSI/ASA S3.20-1995 R2008). For example, marine vessels, aircraft, machinery, construction, and vibratory pile driving (NIOSH 1998, NOAA 2015).

octave
The interval between a sound and another sound with double or half the frequency. For example, one octave above 200 Hz is 400 Hz, and one octave below 200 Hz is 100 Hz.

odontocete
The presence of teeth, rather than baleen, characterizes these whales. Members of the Odontoceti are a suborder of cetaceans, a group comprised of whales, dolphins, and porpoises. The skulls of toothed whales are mostly asymmetric, an adaptation for their echolocation. This group includes sperm whales, killer whales, belugas, narwhals, dolphins, and porpoises.

percentile level, exceedance
The sound level exceeded *n*% of the time during a measurement.

pinniped
A common term used to describe all three groups that form the superfamily Pinnipedia: phocids (true seals or earless seals), otariids (eared seals or fur seals and sea lions), and walrus.

rms
root-mean-square.

sound
A time-varying pressure disturbance generated by mechanical vibration waves travelling through a fluid medium such as air or water.

sound exposure
Time integral of squared, instantaneous frequency-weighted sound pressure over a stated time interval or event. Unit: pascal-squared second ($Pa^2 \cdot s$) (ANSI S1.1-1994 R2004).

sound exposure level (SEL)
A cumulative measure related to the sound energy in one or more pulses. Unit: dB re 1 $\mu Pa^2 \cdot s$. SEL is expressed over the summation period (e.g., per-pulse SEL [for airguns], single-strike SEL [for pile drivers], 24-hour SEL).

sound intensity
Sound energy flowing through a unit area perpendicular to the direction of propagation per unit time.

sound pressure level (SPL)
The decibel ratio of the time-mean-square sound pressure, in a stated frequency band, to the square of the reference sound pressure (ANSI S1.1-1994 R2004).

For sound in water, the reference sound pressure is one micropascal (p_0 = 1 μPa) and the unit for SPL is dB re 1 μPa^2:

$$L_p = 10 \log_{10}(p^2/p_0^2) = 20 \log_{10}(p/p_0)$$

Unless otherwise stated, SPL refers to the root-mean-square (rms) pressure level. See also 90% sound pressure level and fast-average sound pressure level. Non-rectangular time window functions may be applied during calculation of the rms value, in which case the SPL unit should identify the window type.

spectral density level
The decibel level ($10 \cdot \log_{10}$) of the spectral density of a given parameter such as SPL or SEL, for which the units are dB re 1 μPa^2/Hz and dB re 1 $\mu Pa^2 \cdot s$/Hz, respectively.

spectrogram
A visual representation of acoustic amplitude compared with time and frequency.

spectrum

An acoustic signal represented in terms of its power, energy, mean-square sound pressure, or sound exposure distribution with frequency.

temporary threshold shift (TTS)

Temporary loss of hearing sensitivity caused by excessive noise exposure.

Literature Cited

[ISO] International Organization for Standardization. 2006. *ISO 80000-3:2006. Quantities and Units – Part 3: Space and time.* https://www.iso.org/standard/31888.html.

[ISO] International Organization for Standardization. 2017a. *ISO 18406:2017(E). Underwater acoustics— Measurement of radiated underwater sound from percussive pile driving.* Geneva. https://www.iso.org/obp/ui/#iso:std:iso:18406:ed-1:v1:en.

[ISO] International Organization for Standardization. 2017b. *ISO 18405:2017. Underwater acoustics – Terminology.* Geneva. https://www.iso.org/standard/62406.html.

[NIOSH] National Institute for Occupational Safety and Health. 1998. *Criteria for a recommended standard: Occupational noise exposure. Revised Criteria.* Document Number 98-126. US Department of Health and Human Services, NIOSH, Cincinnati, OH, USA. 122 p. https://www.cdc.gov/niosh/docs/98-126/pdfs/98-126.pdf.

[NOAA] National Oceanic and Atmospheric Administration (US). 2013. *Draft guidance for assessing the effects of anthropogenic sound on marine mammals: Acoustic threshold levels for onset of permanent and temporary threshold shifts.* National Oceanic and Atmospheric Administration, U. Department of Commerce, and NMFS Office of Protected Resources, Silver Spring, MD, USA. 76 p.

[NOAA] National Oceanic and Atmospheric Administration (US). 2015. *Draft guidance for assessing the effects of anthropogenic sound on marine mammal hearing: Underwater acoustic threshold levels for onset of permanent and temporary threshold shifts.* NMFS Office of Protected Resources, Silver Spring, MD, USA. 180 p.

[NRC] National Research Council (US). 2003. *Ocean Noise and Marine Mammals.* National Research Council (US), Ocean Studies Board, Committee on Potential Impacts of Ambient Noise in the Ocean on Marine Mammals. The National Academies Press, Washington, DC, USA. https://www.nap.edu/read/10564/chapter/1.

Aerts, L.A.M., M. Blees, S.B. Blackwell, C.R. Greene, Jr., K.H. Kim, D.E. Hannay, and M.E. Austin. 2008. *Marine mammal monitoring and mitigation during BP Liberty OBC seismic survey in Foggy Island Bay, Beaufort Sea, July-August 2008: 90-day report.* Document Number P1011-1. Report by LGL Alaska Research Associates Inc., LGL Ltd., Greeneridge Sciences Inc., and JASCO Applied Sciences for BP Exploration Alaska. 199 p. ftp://ftp.library.noaa.gov/noaa_documents.lib/NMFS/Auke%20Bay/AukeBayScans/Removable%20Disk/P1011-1.pdf.

Ainslie, M.A., J.L. Miksis-Olds, S.B. Martin, K. Heaney, C.A.F. de Jong, A.M. von Benda-Beckmann, and A.P. Lyons. 2018. *ADEON Underwater Soundscape and Modeling Metadata Standard.* Version 1.0. Technical report by JASCO Applied Sciences for ADEON Prime Contract No. M16PC00003.

Amorim, M.C.P. 2006. Diversity of sound production in fish. *In* Ladich, F., S.P. Collin, P. Moller, and B.G. Kapoor (eds.). *Communication in fishes.* Volume 1. Science Publishers. pp. 71-104.

Andrew, R.K., B.M. Howe, and J.A. Mercer. 2011. Long-time trends in ship traffic noise for four sites off the North American West Coast. *Journal of the Acoustical Society of America* 129(2): 642-651. https://doi.org/10.1121/1.3518770.

ANSI S12.7-1986. R2006. *American National Standard Methods for Measurements of Impulsive Noise.* American National Standards Institute, NY, USA.

ANSI S1.1-1994. R2004. *American National Standard Acoustical Terminology*. American National Standards Institute, NY, USA.

ANSI/ASA S1.13-2005. R2010. *American National Standard Measurement of Sound Pressure Levels in Air*. American National Standards Institute and Acoustical Society of America, NY, USA.

ANSI/ASA S3.20-1995. R2008. *American National Standard Bioacoustical Terminology*. American National Standards Institute and Acoustical Society of America, NY, USA.

Atem, A.C.G., M.H. Rasmussen, M. Wahlberg, H.C. Petersen, and L.A. Miller. 2009. Changes in click source levels with distance to targets: studies of free-ranging white-beaked dolphins Lagenorhynchus albirostris and captive harbour porpoises Phocoena phocoena. *Bioacoustics* 19(1-2): 49-65.

Au, W.W.L., R.A. Kastelein, T. Rippe, and N.M. Schooneman. 1999. Transmission beam pattern and echolocation signals of a harbor porpoise (*Phocoena phocoena*). *Journal of the Acoustical Society of America* 106(6): 3699-3705. https://doi.org/10.1121/1.428221.

Austin, M.E. and G.A. Warner. 2012. *Sound Source Acoustic Measurements for Apache's 2012 Cook Inlet Seismic Survey*. Version 2.0. Technical report by JASCO Applied Sciences for Fairweather LLC and Apache Corporation.

Austin, M.E. and L. Bailey. 2013. *Sound Source Verification: TGS Chukchi Sea Seismic Survey Program 2013*. Document Number 00706, Version 1.0. Technical report by JASCO Applied Sciences for TGS-NOPEC Geophysical Company.

Austin, M.E., A. McCrodan, C. O'Neill, Z. Li, and A.O. MacGillivray. 2013. *Marine mammal monitoring and mitigation during exploratory drilling by Shell in the Alaskan Chukchi and Beaufort Seas, July– November 2012: 90-Day Report. In*: Funk, D.W., C.M. Reiser, and W.R. Koski (eds.). Underwater Sound Measurements. LGL Rep. P1272D–1. Report from LGL Alaska Research Associates Inc. and JASCO Applied Sciences, for Shell Offshore Inc., National Marine Fisheries Service (US), and US Fish and Wildlife Service. 266 pp plus appendices.

Austin, M.E. 2014. Underwater noise emissions from drillships in the Arctic. *In*: Papadakis, J.S. and L. Bjørnø (eds.). *UA2014 - 2nd International Conference and Exhibition on Underwater Acoustics*. 22-27 Jun 2014, Rhodes, Greece. pp. 257-263.

Austin, M.E., H. Yurk, and R. Mills. 2015. *Acoustic Measurements and Animal Exclusion Zone Distance Verification for Furie's 2015 Kitchen Light Pile Driving Operations in Cook Inlet*. Version 2.0. Technical report by JASCO Applied Sciences for Jacobs LLC and Furie Alaska.

Austin, M.E. and Z. Li. 2016. *Marine Mammal Monitoring and Mitigation During Exploratory Drilling by Shell in the Alaskan Chukchi Sea, July–October 2015: Draft 90-day report. In*: Ireland, D.S. and L.N. Bisson (eds.). Underwater Sound Measurements. LGL Rep. P1363D. Report from LGL Alaska Research Associates Inc., LGL Ltd., and JASCO Applied Sciences Ltd. For Shell Gulf of Mexico Inc, National Marine Fisheries Service, and US Fish and Wildlife Service. 188 pp + appendices.

Bailey, H., G. Clay, E.A. Coates, D. Lusseau, B. Senior, and P.M. Thompson. 2010. Using T-PODs to assess variations in the occurrence of coastal bottlenose dolphins and harbour porpoises. *Aquatic Conservation: Marine and Freshwater Ecosystems* 20(2): 150-158. https://doi.org/10.1002/aqc.1060.

Ballard, K.A. and K.M. Kovacs. 1995. The acoustic repertoire of hooded seals (*Cystophora cristata*). *Canadian Journal of Zoology* 73(7): 1362-1374. https://doi.org/10.1139/z95-159.

Baumgartner, M.F., S.M. Van Parijs, F.W. Wenzel, C.J. Tremblay, H.C. Esch, and A.M. Warde. 2008. Low frequency vocalizations attributed to sei whales (*Balaenoptera borealis*). *Journal of the Acoustical Society of America* 124(2): 1339-1349. https://doi.org/10.1121/1.2945155.

Becker, J.J., D.T. Sandwell, W.H.F. Smith, J. Braud, B. Binder, J. Depner, D. Fabre, J. Factor, S. Ingalls, et al. 2009. Global Bathymetry and Elevation Data at 30 Arc Seconds Resolution: SRTM30_PLUS. *Marine Geodesy* 32(4): 355-371. https://doi.org/10.1080/01490410903297766.

Berchok, C.L., D.L. Bradley, and T.B. Gabrielson. 2006. St. Lawrence blue whale vocalizations revisited: Characterization of calls detected from 1998 to 2001. *Journal of the Acoustical Society of America* 120(4): 2340-2354. https://doi.org/10.1121/1.2335676.

Bjørge, A., H. Aarefjord, S. Kaarstad, L. Kleivane, and N. Øien. 1991. *Harbor porpoise (Phocoena phocoena) in Norwegian waters*. ICES.

Carnes, M.R. 2009. *Description and Evaluation of GDEM-V 3.0*. US Naval Research Laboratory, Stennis Space Center, MS. NRL Memorandum Report 7330-09-9165. 21 p. https://apps.dtic.mil/dtic/tr/fulltext/u2/a494306.pdf.

Christensen, I., T. Haug, and N. Øien. 1990. *A review of the distribution, migrations, food, reproduction, exploitation and present abundance of humpback whales (Megatera novaeangliae) in the northeast Atlantic*. ICES.

Clark, C.W. 1990. Acoustic behaviour of mysticete whales. *In* Thomas, J. and R.A. Kastelein (eds.). *Sensory Abilities of Cetaceans*. Springer, Boston, MA. pp. 571-583. https://doi.org/10.1007/978-1-4899-0858-2_40.

Collins, M.D. 1993. A split-step Padé solution for the parabolic equation method. *Journal of the Acoustical Society of America* 93(4): 1736-1742. https://doi.org/10.1121/1.406739.

Collins, M.D., R.J. Cederberg, D.B. King, and S. Chin-Bing. 1996. Comparison of algorithms for solving parabolic wave equations. *Journal of the Acoustical Society of America* 100(1): 178-182. https://doi.org/10.1121/1.415921.

Coppens, A.B. 1981. Simple equations for the speed of sound in Neptunian waters. *Journal of the Acoustical Society of America* 69(3): 862-863. https://doi.org/10.1121/1.382038.

Croll, D.A., C.W. Clark, A. Acevedo-Gutiérrez, B. Tershy, S. Flores, J. Gedamke, and J. Urban. 2002. Only male fin whales sing loud songs. *Nature* 417(6891): 809. http://www.nature.com/articles/417809a.

Deane, G.B. 2000. Long time-base observations of surf noise. *Journal of the Acoustical Society of America* 107(2): 758-770. https://doi.org/10.1121/1.428259.

Deecke, V.B., J.K.B. Ford, and P.J.B. Slater. 2005. The vocal behaviour of mammal-eating killer whales: Communicating with costly calls. *Animal Behaviour* 69(2): 395-405. https://doi.org/10.1016/j.anbehav.2004.04.014.

Delarue, J., K.A. Kowarski, E.E. Maxner, J.T. MacDonnell, and S.B. Martin. 2017. *Acoustic Monitoring Along Canada's East Coast: August 2015 to July 2016*. Document Number 01279. Technical report by JASCO Applied Sciences for Environmental Studies Research Fund.

Delarue, J., K.A. Kowarski, E.E. Maxner, J.T. MacDonnell, and S.B. Martin. 2018. *Acoustic Monitoring Along Canada's East Coast: August 2015 to July 2017*. Document Number 01279, Environmental Studies Research Funds Report Number 215, Version 1.0. Technical report by JASCO Applied

Sciences for Environmental Studies Research Fund, Dartmouth, NS, Canada. 120 pp + appendices.

Dunlop, R.A., M.J. Noad, D.H. Cato, and D. Stokes. 2007. The social vocalization repertoire of east Australian migrating humpback whales (*Megaptera novaeangliae*). *Journal of the Acoustical Society of America* 122(5): 2893-2905. https://doi.org/10.1121/1.2783115.

Dunlop, R.A., D.H. Cato, and M.J. Noad. 2008. Non-song acoustic communication in migrating humpback whales (*Megaptera novaeangliae*). *Marine Mammal Science* 24(3): 613-629. https://doi.org/10.1111/j.1748-7692.2008.00208.x

earth.nullschool.net. 2020. EarthWindMap. (c) Cameron Beccario. https://earth.nullschool.net/ (Accessed 13 May 2020).

Edds-Walton, P.L. 1997. Acoustic communication signals of mysticetes whales. *Bioacoustics* 8(1-2): 47-60. https://doi.org/10.1080/09524622.2008.9753759.

Erbe, C., A. Verma, R. McCauley, A. Gavrilov, and I. Parnum. 2015. The marine soundscape of the Perth Canyon. *Progress in Oceanography* 137: 38-51. https://doi.org/10.1016/j.pocean.2015.05.015.

Fisher, F.H. and V.P. Simmons. 1977. Sound absorption in sea water. *Journal of the Acoustical Society of America* 62(3): 558-564. https://doi.org/10.1121/1.381574.

Ford, J.K.B. 1989. Acoustic behaviour of resident killer whales (*Orcinus orca*) off Vancouver Island, British Columbia. *Canadian Journal of Zoology* 67(3): 727-745. https://doi.org/10.1139/z89-105.

Freedman, D. and P. Diaconis. 1981. On the histogram as a density estimator: L_2 theory. *Probability theory* 57(4): 453-476. https://doi.org/10.1007/BF01025868.

Frouin-Mouy, H., K.A. Kowarski, B. Martin, and K. Bröker. 2017. Seasonal Trends in Acoustic Detection of Marine Mammals in Baffin Bay and Melville Bay, Northwest Greenland + Supplementary Appendix 1. *Arctic* 70(1): 59-76. https://doi.org/10.14430/arctic4632.

Funk, D., D.E. Hannay, D.S. Ireland, R. Rodrigues, and W.R. Koski (eds.). 2008. *Marine mammal monitoring and mitigation during open water seismic exploration by Shell Offshore Inc. in the Chukchi and Beaufort Seas, July–November 2007: 90-day report*. LGL Report P969-1. Prepared by LGL Alaska Research Associates Inc., LGL Ltd., and JASCO Research Ltd. for Shell Offshore Inc., National Marine Fisheries Service (U.S.), and U.S. Fish and Wildlife Service. 218 p.

Garcia, H.A., C. Zhu, M.E. Schinault, A.I. Kaplan, N.O. Handegard, O.R. Godø, H. Ahonen, N.C. Makris, D. Wang, et al. 2018. Temporal–spatial, spectral, and source level distributions of fin whale vocalizations in the Norwegian Sea observed with a coherent hydrophone array. *ICES Journal of Marine Science*: fsy127. https://doi.org/10.1093/icesjms/fsy127.

Girola, E., M.J. Noad, R.A. Dunlop, and D.H. Cato. 2019. Source levels of humpback whales decrease with frequency suggesting an air-filled resonator is used in sound production. *The Journal of the Acoustical Society of America* 145(2): 869-880.

Hannay, D.E. and R.G. Racca. 2005. *Acoustic Model Validation*. Document Number 0000-S-90-04-T-7006-00-E, Revision 02. Technical report by JASCO Research Ltd. for Sakhalin Energy Investment Company Ltd. 34 p.

Hannay, D.E., J. Delarue, X. Mouy, B.S. Martin, D. Leary, J.N. Oswald, and J. Vallarta. 2013. Marine mammal acoustic detections in the northeastern Chukchi Sea, September 2007–July 2011. *Continental Shelf Research* 67: 127-146. https://doi.org/10.1016/j.csr.2013.07.009.

Hawkins, A.D., L. Casaretto, M. Picciulin, and K. Olsen. 2002. Locating Spawning Haddock by Means of Sound. *Bioacoustics* 12(2-3): 284-286. https://doi.org/10.1080/09524622.2002.9753723.

Helweg, D.A., D.H. Cat, P.F. Jenkins, C. Garrigue, and R.D. McCauley. 1998. Geographic variation in south pacific humpback whale songs. *Behaviour* 135(1): 1-27. https://doi.org/10.1163/156853998793066438.

Herman, L.M., A.A. Pack, S.S. Spitz, E.Y. Herman, K. Rose, S. Hakala, and M.H. Deakos. 2013. Humpback whale song: Who sings? *Behavioral Ecology and Sociobiology* 67(10): 1653-1663. https://doi.org/10.1007/s00265-013-1576-8.

Holt, M.M., D.P. Noren, and C.K. Emmons. 2011. Effects of noise levels and call types on the source levels of killer whale calls. *Journal of the Acoustical Society of America* 130(5): 3100-3106. https://doi.org/10.1121/1.3641446.

Hooker, S.K. and H. Whitehead. 2002. Click characteristics of northern bottlenose whales (*Hyperoodon ampullatus*). *Marine Mammal Science* 18(1): 69-80. https://doi.org/10.1111/j.1748-7692.2002.tb01019.x.

Ireland, D.S., R. Rodrigues, D. Funk, W.R. Koski, and D.E. Hannay. 2009. *Marine mammal monitoring and mitigation during open water seismic exploration by Shell Offshore Inc. in the Chukchi and Beaufort Seas, July–October 2008: 90-Day Report.* Document Number P1049-1. 277 p.

Jensen, F.B., W.A. Kuperman, M.B. Porter, and H. Schmidt. 2011. *Computational Ocean Acoustics.* 2nd edition. AIP Series in Modern Acourics and Signal Processing. AIP Press - Springer, New York. 794 p.

Jourdain, E. and D. Vongraven. 2017. Humpback whale (Megaptera novaeangliae) and killer whale (Orcinus orca) feeding aggregations for foraging on herring (Clupea harengus) in Northern Norway. *Mammalian Biology* 86(1): 27-32.

Kingsley, M.C.S. and R.R. Reeves. 1998. Aerial surveys of cetaceans in the Gulf of St. Lawrence in 1995 and 1996. *Canadian Journal of Zoology* 76(8): 1529-1550. https://doi.org/10.1139/z98-054.

Klinck, H., S.L. Nieukirk, D.K. Mellinger, K. Klinck, H. Matsumoto, and R.P. Dziak. 2012. Seasonal presence of cetaceans and ambient noise levels in polar waters of the North Atlantic. *Journal of the Acoustical Society of America, Express Letters* 132(3): 176-181. https://doi.org/10.1121/1.4740226.

Kovacs, K.M., T. Haug, and C. Lydersen. 2009. Marine mammals of the Barents Sea. *In Ecosystem Barents Sea.* pp. 453-496.

Kowarski, K.A., C. Evers, H. Moors-Murphy, B. Martin, and S.L. Denes. 2018. Singing through winter nights: Seasonal and diel occurrence of humpback whale (*Megaptera novaeangliae*) calls in and around the Gully MPA, offshore eastern Canada. *Marine Mammal Science* 34(1): 169-189. https://doi.org/10.1111/mms.12447.

Laidre, K.L., P.J. Heagerty, M.P. Heide-Jørgensen, L. Witting, and M. Simon. 2009. Sexual segregation of common minke whales (Balaenoptera acutorostrata) in Greenland, and the influence of sea temperature on the sex ratio of catches. *ICES Journal of Marine Science* 66(10): 2253-2266.

Lillis, A. and T.A. Mooney. 2016. The snapping shrimp conundrum: Spatial and temporal complexity of snapping sounds on coral reefs. *Journal of the Acoustical Society of America* 140(4): 3071-3071. https://doi.org/10.1121/1.4969566.

Lind, S., R.B. Ingvaldsen, and T. Furevik. 2018. Arctic warming hotspot in the northern Barents Sea linked to declining sea-ice import. *Nature Climate Change* 8(7): 634-639.

Loeng, H. 1991. Features of the physical oceanographic conditions of the Barents Sea. *Polar Research* 10(1): 5-18.

MacGillivray, A.O. 2018. Underwater noise from pile driving of conductor casing at a deep-water oil platform. *Journal of the Acoustical Society of America* 143(1): 450-459. https://doi.org/10.1121/1.5021554.

MacIntyre, K.Q., K.M. Stafford, C.L. Berchok, and P.L. Boveng. 2013. Year-round acoustic detection of bearded seals (*Erignathus barbatus*) in the Beaufort Sea relative to changing environmental conditions, 2008-2010. *Polar Biology* 36(8): 1161-1173. https://doi.org/10.1007/s00300-013-1337-1.

MacLeod, C.D., C.R. Weir, M.B. Santos, and T.E. Dunn. 2008. Temperature-based summer habitat partitioning between white-beaked and common dolphins around the United Kingdom and Republic of Ireland. *Marine Biological Association of the United Kingdom. Journal of the Marine Biological Association of the United Kingdom* 88(6): 1193.

Martin, B. 2013. Computing cumulative sound exposure levels from anthropogenic sources in large data sets. *Proceedings of Meetings on Acoustics* 19(1): 9. https://doi.org/10.1121/1.4800967.

Martin, B., K. Bröker, M.-N.R. Matthews, J.T. MacDonnell, and L. Bailey. 2015. Comparison of measured and modeled air-gun array sound levels in Baffin Bay, West Greenland. *OceanNoise 2015*. 11-15 May 2015, Barcelona, Spain.

Martin, B., J.T. MacDonnell, and K. Bröker. 2017a. Cumulative sound exposure levels—Insights from seismic survey measurements. *Journal of the Acoustical Society of America* 141(5): 3603-3603. https://doi.org/10.1121/1.4987709.

Martin, S.B. and A.N. Popper. 2016. Short- and long-term monitoring of underwater sound levels in the Hudson River (New York, USA). *Journal of the Acoustical Society of America* 139(4): 1886-1897. https://doi.org/10.1121/1.4944876.

Martin, S.B., M.-N.R. Matthews, J.T. MacDonnell, and K. Bröker. 2017b. Characteristics of seismic survey pulses and the ambient soundscape in Baffin Bay and Melville Bay, West Greenland. *Journal of the Acoustical Society of America* 142(6): 3331-3346. https://doi.org/10.1121/1.5014049.

Martin, S.B., C. Morris, K. Bröker, and C. O'Neill. 2019. Sound exposure level as a metric for analyzing and managing underwater soundscapes. *Journal of the Acoustical Society of America* 146(1): 135-149. https://doi.org/10.1121/1.5113578.

Mathias, D., A.M. Thode, J. Straley, and R.D. Andrews. 2013. Acoustic tracking of sperm whales in the Gulf of Alaska using a two-element vertical array and tags. *Journal of the Acoustical Society of America* 134(3): 2446-2461. https://doi.org/10.1121/1.4816565.

Matthews, M.-N.R. and A.O. MacGillivray. 2013. Comparing modeled and measured sound levels from a seismic survey in the Canadian Beaufort Sea. *Proceedings of Meetings on Acoustics* 19(1): 1-8. https://doi.org/10.1121/1.4800553

McCrodan, A., C.R. McPherson, and D.E. Hannay. 2011. *Sound Source Characterization (SSC) Measurements for Apache's 2011 Cook Inlet 2D Technology Test*. Version 3.0. Technical report by JASCO Applied Sciences for Fairweather LLC and Apache Corporation. 51 p.

McPherson, C.R. and G.A. Warner. 2012. *Sound Sources Characterization for the 2012 Simpson Lagoon OBC Seismic Survey 90-Day Report*. Document Number 00443, Version 2.0. Technical report by JASCO Applied Sciences for BP Exploration (Alaska) Inc. http://www.nmfs.noaa.gov/pr/pdfs/permits/bp_openwater_90dayreport_appendices.pdf.

McPherson, C.R., K. Lucke, B.J. Gaudet, B.S. Martin, and C.J. Whitt. 2018. *Pelican 3-D Seismic Survey Sound Source Characterisation*. Document Number 001583. Version 1.0. Technical report by JASCO Applied Sciences for RPS Energy Services Pty Ltd.

McPherson, C.R. and B. Martin. 2018. *Characterisation of Polarcus 2380 in^3 Airgun Array*. Document Number 001599, Version 1.0. Technical report by JASCO Applied Sciences for Polarcus Asia Pacific Pte Ltd.

Mellinger, D.K. and C.W. Clark. 2003. Blue whale (*Balaenoptera musculus*) sounds from the North Atlantic. *Journal of the Acoustical Society of America* 114(2): 1108-1119. https://doi.org/10.1121/1.1593066.

Miksis-Olds, J.L. and S.M. Nichols. 2016. Is low frequency ocean sound increasing globally? *Journal of the Acoustical Society of America* 139(1): 501-511. https://doi.org/10.1121/1.4938237.

Møhl, B., M. Wahlberg, P.T. Madsen, L.A. Miller, and A. Surlykke. 2000. Sperm whale clicks: Directionality and source level revisited. *Journal of the Acoustical Society of America* 107(1): 638-648. https://doi.org/10.1121/1.428329.

Møhl, B., M. Wahlberg, P.T. Madsen, A. Heerfordt, and A. Lund. 2003. The monopulsed nature of sperm whale clicks. *Journal of the Acoustical Society of America* 114(2): 1143-1154. https://doi.org/10.1121/1.1586258.

Moore, S.E., K.M. Stafford, H. Melling, C. Berchok, Ø. Wiig, K.M. Kovacs, C. Lydersen, and J. Richter-Menge. 2012. Comparing marine mammal acoustic habitats in Atlantic and Pacific sectors of the High Arctic: year-long records from Fram Strait and the Chukchi Plateau. *Polar Biology* 35(3): 475-480.

Morano, J.L., D.P. Salisbury, A.N. Rice, K.L. Conklin, K.L. Falk, and C.W. Clark. 2012. Seasonal and geographical patterns of fin whale song in the western North Atlantic Ocean. *Journal of the Acoustical Society of America* 132(2): 1207-1212. https://doi.org/10.1121/1.4730890.

Nemiroff, L. and H. Whitehead. 2009. Structural characteristics of pulsed calls of long-finned pilot whales *Globicephala melas*. *Bioacoustics* 19(1-2): 67-92. https://doi.org/10.1080/09524622.2009.9753615.

Nieukirk, S.L., K.M. Stafford, D.K. Mellinger, R.P. Dziak, and C.G. Fox. 2004. Low-frequency whale and seismic airgun sounds recorded in the mid-Atlantic Ocean. *Journal of the Acoustical Society of America* 115(4): 1832-1843. https://doi.org/10.1121/1.1675816.

Nieukirk, S.L., D.K. Mellinger, S.E. Moore, K. Klinck, R.P. Dziak, and J. Goslin. 2012. Sounds from airguns and fin whales recorded in the mid-Atlantic Ocean, 1999–2009. *Journal of the Acoustical Society of America* 131(2): 1102-1112. https://doi.org/10.1121/1.3672648.

Nordeide, J.T. and E. Kjellsby. 1999. Sound from spawning cod at their spawning grounds. *ICES Journal of Marine Science* 56(3): 326-332. https://doi.org/10.1006/jmsc.1999.0473.

O'Neill, C., D. Leary, and A. McCrodan. 2010. Sound Source Verification. (Chapter 3) *In* Blees, M.K., K.G. Hartin, D.S. Ireland, and D.E. Hannay (eds.). *Marine mammal monitoring and mitigation during open water seismic exploration by Statoil USA E&P Inc. in the Chukchi Sea, August-October 2010: 90-day report*. LGL Report P1119. Prepared by LGL Alaska Research Associates Inc., LGL Ltd.,

and JASCO Applied Sciences Ltd. for Statoil USA E&P Inc., National Marine Fisheries Service (US), and US Fish and Wildlife Service. pp. 1-34.

Øien, N. 1996. Lagenorhynchus species in Norwegian waters as revealed from incidental observations and recent sighting surveys. *International Whaling Commission, Scientific Committee Document SC/48/SM15, Cambridge, UK*.

Øien, N. and S. Hartvedt. 2011. *Northern bottlenose whales Hyperoodon ampullatus in Norwegian and adjacent waters*. Cambridge: International Whaling Commission, IWC SC/63/SM1.

Oswald, J.N., J. Barlow, and T.F. Norris. 2003. Acoustic identification of nine delphinid species in the eastern tropical Pacific Ocean. *Marine Mammal Science* 19(1): 20-37. https://doi.org/10.1111/j.1748-7692.2003.tb01090.x.

Ottersen, G. and N.C. Stenseth. 2001. Atlantic climate governs oceanographic and ecological variability in the Barents Sea. *Limnology and Oceanography* 46(7): 1774-1780. https://doi.org/10.4319/lo.2001.46.7.1774.

Ou, H., W.W. Au, S. Van Parijs, E.M. Oleson, and S. Rankin. 2015. Discrimination of frequency-modulated baleen whale downsweep calls with overlapping frequencies. *The Journal of the Acoustical Society of America* 137(6): 3024-3032.

Parks, S.E. and P.L. Tyack. 2005. Sound production by North Atlantic right whales (*Eubalaena glacialis*) in surface active groups. *Journal of the Acoustical Society of America* 117(5): 3297-3306. https://doi.org/10.1121/1.1882946.

Porter, M.B. and Y.-C. Liu. 1994. Finite-element ray tracing. *In*: Lee, D. and M.H. Schultz (eds.). *International Conference on Theoretical and Computational Acoustics*. Volume 2. World Scientific Publishing Co. pp. 947-956.

Prieto, R., D. Janiger, M.A. Silva, G.T. Waring, and J.M. Goncalves. 2012. The forgotten whale: a bibliometric analysis and literature review of the North Atlantic sei whale Balaenoptera borealis. *Mammal Review* 42(3): 235-272.

Racca, R.G., A.N. Rutenko, K. Bröker, and M.E. Austin. 2012a. A line in the water - design and enactment of a closed loop, model based sound level boundary estimation strategy for mitigation of behavioural impacts from a seismic survey. *11th European Conference on Underwater Acoustics*. Volume 34(3), Edinburgh, UK.

Racca, R.G., A.N. Rutenko, K. Bröker, and G. Gailey. 2012b. Model based sound level estimation and in-field adjustment for real-time mitigation of behavioural impacts from a seismic survey and post-event evaluation of sound exposure for individual whales. *In*: McMinn, T. (ed.). *Acoustics 2012 Fremantle: Acoustics, Development and the Environment. Proceedings of the Annual Conference of the Australian Acoustical Society*. Fremantle, Australia. http://www.acoustics.asn.au/conference_proceedings/AAS2012/papers/p92.pdf.

Racca, R.G., M.E. Austin, A.N. Rutenko, and K. Bröker. 2015. Monitoring the gray whale sound exposure mitigation zone and estimating acoustic transmission during a 4-D seismic survey, Sakhalin Island, Russia. *Endangered Species Research* 29(2): 131-146. https://doi.org/10.3354/esr00703.

Rasmussen, M.H. and L.A. Miller. 2002. Whistles and clicks from white-beaked dolphins, *Lagenorhynchus albirostris*, recorded in Faxafloi Bay, Iceland. *Aquatic Mammals* 28(1): 78-89. https://www.aquaticmammalsjournal.org/share/AquaticMammalsIssueArchives/2002/AquaticMammals_28-01/28-01_Rasmussen.pdf.

Rasmussen, M.H., L.A. Miller, and W.W. Au. 2002. Source levels of clicks from free-ranging white-beaked dolphins (Lagenorhynchus albirostris Gray 1846) recorded in Icelandic waters. *The Journal of the Acoustical Society of America* 111(2): 1122-1125.

Rasmussen, M.H., M. Lammers, K. Beedholm, and L.A. Miller. 2006. Source levels and harmonic content of whistles in white-beaked dolphins (*Lagenorhynchus albirostris*). *Journal of the Acoustical Society of America* 120: 510-517. https://doi.org/10.1121/1.2202865.

Renard, V. and J. Malod. 1974. Structure of the Barents Sea from seismic refraction. *Earth and Planetary Science Letters* 24(1): 33-47.

Rendell, L.E., J.N. Matthews, A. Gill, J.C.D. Gordon, and D.W. MacDonald. 1999. Quantitative analysis of tonal calls from five odontocete species, examining interspecific and intraspecific variation. *Journal of Zoology* 249(4): 403-410. https://doi.org/10.1111/j.1469-7998.1999.tb01209.x.

Risch, D., C.W. Clark, P.J. Corkeron, A. Elepfandt, K.M. Kovacs, C. Lydersen, I. Stirling, and S.M. Van Parijs. 2007. Vocalizations of male bearded seals, *Erignathus barbatus*: Classification and geographical variation. *Animal Behaviour* 73(5): 747-762. https://doi.org/10.1016/j.anbehav.2006.06.012.

Risch, D., C.W. Clark, P.J. Dugan, M. Popescu, U. Siebert, and S.M. Van Parijs. 2013. Minke whale acoustic behavior and multi-year seasonal and diel vocalization patterns in Massachusetts Bay, USA. *Marine Ecology Progress Series* 489: 279-295. https://doi.org/10.3354/meps10426.

Risch, D., M. Castellote, C.W. Clark, G.E. Davis, P.J. Dugan, L.E.W. Hodge, A. Kumar, K. Lucke, D.K. Mellinger, et al. 2014. Seasonal migrations of North Atlantic minke whales: Novel insights from large-scale passive acoustic monitoring networks. *Movement Ecology* 2(24). https://doi.org/10.1186/s40462-014-0024-3.

Ross, D. 1976. *Mechanics of Underwater Noise*. Pergamon Press, NY, USA.

RTsys. 2020. *Underwater acoustic recorders* (webpage). https://rtsys.eu/en/underwater-acoustic-recorders/. (Accessed 13 May 2020).

Samarra, F.I.P., V.B. Deecke, K. Vinding, M.H. Rasmussen, R.J. Swift, and P.J.O. Miller. 2010. Killer whales (*Orcinus orca*) produce ultrasonic whistles. *Journal of the Acoustical Society of America* 128(5): EL205-EL210. https://doi.org/10.1121/1.3462235.

Simon, M., K.M. Stafford, K. Beedholm, C.M. Lee, and P.T. Madsen. 2010. Singing behavior of fin whales in the Davis Strait with implications for mating, migration and foraging. *Journal of the Acoustical Society of America* 128(5): 3200-3210. https://doi.org/10.1121/1.3495946.

Skern-Mauritzen, M., E. Johannesen, A. Bjørge, and N. Øien. 2011. Baleen whale distributions and prey associations in the Barents Sea. *Marine Ecology Progress Series* 426: 289-301.

Smith, W.H.F. and D.T. Sandwell. 1997. Global sea floor topography from satellite altimetry and ship depth soundings. *Science* 277(5334): 1956-1962. https://science.sciencemag.org/content/277/5334/1956.

Southall, B.L., A.E. Bowles, W.T. Ellison, J.J. Finneran, R.L. Gentry, C.R. Greene, Jr., D. Kastak, D.R. Ketten, J.H. Miller, et al. 2007. Marine Mammal Noise Exposure Criteria: Initial Scientific Recommendations. *Aquatic Mammals* 33(4): 411-521. https://doi.org/10.1080/09524622.2008.9753846.

Staaterman, E.R., C.W. Clark, A.J. Gallagher, M.S. Devries, T. Claverie, and S.N. Patek. 2011. Rumbling in the benthos: Acoustic ecology of the California mantis shrimp *Hemisquilla californiensis*. *Aquatic Biology* 13(2): 97-105. https://doi.org/10.3354/ab00361.

Stafford, K.M., D.K. Mellinger, S.E. Moore, and C.G. Fox. 2007. Seasonal variability and detection range modeling of baleen whale calls in the Gulf of Alaska, 1999–2002. *Journal of the Acoustical Society of America* 122(6): 3378-3390. https://doi.org/10.1121/1.2799905.

Steiner, W.W. 1981. Species-specific differences in pure tonal whistle vocalizations of five western North Atlantic dolphin species. *Behavioral Ecology and Sociobiology* 9(4): 241-246. https://doi.org/10.1007/BF00299878.

Storrie, L., C. Lydersen, M. Andersen, R.B. Wynn, and K.M. Kovacs. 2018. Determining the species assemblage and habitat use of cetaceans in the Svalbard Archipelago, based on observations from 2002 to 2014. *Polar Research* 37(1): 1463065.

Sundvor, E. 1975. Thickness and distribution of sedimentary rocks in the southern Barents Sea. *Bulletin-Norges Geologiske Undersøkelse* 29: 237.

Teague, W.J., M.J. Carron, and P.J. Hogan. 1990. A comparison between the Generalized Digital Environmental Model and Levitus climatologies. *Journal of Geophysical Research* 95(C5): 7167-7183. https://doi.org/10.1029/JC095iC05p07167.

Terhune, J.M. 1994. Geographical variation of harp seal underwater vocalizations. *Canadian Journal of Zoology* 72(5): 892-897. https://doi.org/10.1139/z94-121.

Tyack, P.L. and C.W. Clark. 2000. Communication and acoustic behavior of dolphins and whales. *In Hearing by whales and dolphins*. Springer, New York. pp. 156-224.

Urazghildiiev, I.R. and S.M. Van Parijs. 2016. Automatic grunt detector and recognizer for Atlantic cod (*Gadus morhua*). *Journal of the Acoustical Society of America* 139(5): 2532-2540. https://doi.org/10.1121/1.4948569.

Vikingsson, G.A. and M.P. Heide-Jørgensen. 2015. First indications of autumn migration routes and destination of common minke whales tracked by satellite in the North Atlantic during 2001–2011. *Marine Mammal Science* 31(1): 376-385.

Wahlberg, M., K. Beedholm, A. Heerfordt, and B. Møhl. 2012. Characteristics of biosonar signals from the northern bottlenose whale, *Hyperoodon ampullatus*. *Journal of the Acoustical Society of America* 130(5): 3077-3084. https://doi.org/10.1121/1.3641434.

Wang, D., W. Huang, H. Garcia, and P. Ratilal. 2016. Vocalization source level distributions and pulse compression gains of diverse baleen whale species in the Gulf of Maine. *Remote Sensing* 8(11): 881.

Warner, G.A., C. Erbe, and D.E. Hannay. 2010. Underwater Sound Measurements. (Chapter 3) *In* Reiser, C.M., D. Funk, R. Rodrigues, and D.E. Hannay (eds.). *Marine Mammal Monitoring and Mitigation during Open Water Shallow Hazards and Site Clearance Surveys by Shell Offshore Inc. in the Alaskan Chukchi Sea, July-October 2009: 90-Day Report*. LGL Report P1112-1. Report by LGL Alaska Research Associates Inc. and JASCO Applied Sciences for Shell Offshore Inc., National Marine Fisheries Service (US), and Fish and Wildlife Service (US). pp. 1-54.

Warner, G.A., M.E. Austin, and A.O. MacGillivray. 2017. Hydroacoustic measurements and modeling of pile driving operations in Ketchikan, Alaska. *Journal of the Acoustical Society of America* 141(5): 3992. https://doi.org/10.1121/1.4989141.

Watkins, W.A. 1981. Activities and underwater sounds of fin whales. *Scientific Reports of the Whales Research Institute* 33: 83-117.

Watkins, W.A., P.L. Tyack, K.E. Moore, and J.E. Bird. 1987. The 20-Hz signals of finback whales (*Balaenoptera physalus*). *Journal of the Acoustical Society of America* 82(6): 1901–1912. https://doi.org/10.1121/1.395685.

Weirathmueller, M.J., W.S. Wilcock, and D.C. Soule. 2013a. Source levels of fin whale 20 Hz pulses measured in the Northeast Pacific Ocean. *Journal of the Acoustical Society of America* 133(2): 741-749. https://doi.org/10.1121/1.4773277.

Weirathmueller, M.J., W.S.D. Wilcock, and D.C. Soule. 2013b. Source levels of fin whale 20 Hz pulses measured in the Northeast Pacific Ocean. *Journal of the Acoustical Society of America* 133(2): 741-749. https://doi.org/10.1121/1.4773277.

Wenz, G.M. 1962. Acoustic Ambient Noise in the Ocean: Spectra and Sources. *Journal of the Acoustical Society of America* 34(12): 1936-1956. https://doi.org/10.1121/1.1909155.

Zhang, Z.Y. and C.T. Tindle. 1995. Improved equivalent fluid approximations for a low shear speed ocean bottom. *Journal of the Acoustical Society of America* 98(6): 3391-3396. https://doi.org/10.1121/1.413789.

Zykov, M.M. and J.T. MacDonnell. 2013. *Sound Source Characterizations for the Collaborative Baseline Survey Offshore Massachusetts Final Report: Side Scan Sonar, Sub-Bottom Profiler, and the R/V Small Research Vessel experimental*. Document Number 00413, Version 2.0. Technical report by JASCO Applied Sciences for Fugro GeoServices, Inc. and the (US) Bureau of Ocean Energy Management.

Appendix A. Ambient Sound Analysis

A.1. Total Ambient Sound Levels

Underwater sound pressure amplitude is measured in decibels (dB) relative to a fixed reference pressure of p_0 = 1 µPa. Because the perceived loudness of sound, especially impulsive noise such as from seismic airguns, pile driving, and sonar, is not generally proportional to the instantaneous acoustic pressure, several sound level metrics are commonly used to evaluate noise and its effects on marine life. We provide specific definitions of relevant metrics used in this report. Where possible we follow the ANSI and ISO standard definitions and symbols for sound metrics, but these standards are not always consistent.

The zero-to-peak pressure level, or peak pressure level (PK or $L_{p,pk}$; dB re 1 µPa), is the decibel level of the maximum instantaneous sound pressure level in a stated frequency band attained by an acoustic pressure signal, $p(t)$:

$$\text{PK} = L_{p,\text{pk}} = 10\log_{10}\frac{\max|p^2(t)|}{p_0^2} \qquad\qquad \text{(A-1)}$$

PK is often included as criterion for assessing whether a sound is potentially injurious; however, because it does not account for the duration of a noise event, it is generally a poor indicator of perceived loudness.

The sound pressure level (SPL or L_p; dB re 1 µPa) is the decibel level of the root-mean-square (rms) pressure in a stated frequency band over a specified time window (T; s) containing the acoustic event of interest. It is important to note that SPL always refers to an rms pressure level and therefore not instantaneous pressure:

$$\text{SPL} = L_p = 10\log_{10}\left[\frac{1}{T}\int_T p^2(t)\,dt \Big/ p_0^2\right] \qquad\qquad \text{(A-2)}$$

The SPL represents a nominal effective continuous sound over the duration of an acoustic event, such as the emission of one acoustic pulse, a marine mammal vocalization, the passage of a vessel, or over a fixed duration. Because the window length, *T*, is the divisor, events with similar sound exposure level (SEL), but more spread out in time have a lower SPL.

The sound exposure level (SEL or L_E, dB re 1 µPa^2·s) is a measure related to the acoustic energy contained in one or more acoustic events (N). The SEL for a single event is computed from the time-integral of the squared pressure over the full event duration (T):

$$\text{SEL} = L_E = 10\log_{10}\left[\int_T p^2(t)\,dt \Big/ T_0 p_0^2\right] \qquad\qquad \text{(A-3)}$$

where T_0 is a reference time interval of 1 s. The SEL continues to increase with time when non-zero pressure signals are present. It therefore can be construed as a dose-type measurement, so the integration time used must be carefully considered in terms of relevance for impact to the exposed recipients.

SEL can be calculated over periods with multiple events or over a fixed duration. For a fixed duration, the square pressure is integrated over the duration of interest. For multiple events, the SEL can be computed by summing (in linear units) the SEL of the N individual events:

$$L_{E,N} = 10\log_{10}\sum_{i=1}^{N} 10^{\frac{L_{E,i}}{10}} \qquad\qquad \text{(A-4)}$$

To compute the SPL(T_{90}) and SEL of acoustic events in the presence of high levels of background noise, equations A-1 and A-2 are modified to subtract the background noise contribution:

$$\mathrm{SPL}(T_{90}) = L_{p90} = 10 \log_{10}\left[\frac{1}{T_{90}} \int\limits_{T_{90}} \left(p^2(t) - \overline{n^2}\right) dt \Big/ p_0^2 \right] \tag{A-5}$$

$$L_E = 10 \log_{10}\left[\int\limits_{T} \left(p^2(t) - \overline{n^2}\right) dt \Big/ T_0 p_0^2 \right] \tag{A-6}$$

where $\overline{n^2}$ is the mean square pressure of the background noise, generally computed by averaging the squared pressure of a temporally-proximal segment of the acoustic recording during which acoustic events are absent (e.g., between pulses).

Because the SPL(T_{90}) and SEL are both computed from the integral of square pressure, these metrics are related numerically by the following expression, which depends only on the duration of the time window T:

$$L_p = L_E - 10\log_{10}(T) \tag{A-7}$$

$$L_{p90} = L_E - 10\log_{10}(T_{90}) - 0.458 \tag{A-8}$$

where the 0.458 dB factor accounts for the 10% of SEL missing from the SPL(T_{90}) integration time window.

Energy equivalent SPL (dB re 1 µPa) denotes the SPL of a stationary (constant amplitude) sound that generates the same SEL as the signal being examined, $p(t)$, over the same period of time, T:

$$L_{\mathrm{eq}} = 10 \log_{10}\left[\frac{1}{T} \int\limits_{T} p^2(t)\, dt \Big/ p_0^2 \right] \tag{A–9}$$

The equations for SPL and the energy-equivalent SPL are numerically identical; conceptually, the difference between the two metrics is that the former is typically computed over short periods (typically of one second or less) and tracks the fluctuations of a non-steady acoustic signal, whereas the latter reflects the average SPL of an acoustic signal over times typically of one minute to several hours.

A.2. Decidecade-Band Analysis

The distribution of a sound's power with frequency is described by the sound's spectrum. The sound spectrum can be split into a series of adjacent frequency bands. Splitting a spectrum into 1 Hz wide bands, called passbands, yields the power spectral density of the sound. These values directly compare to the Wenz curves, which represent typical deep ocean sound levels (Figure 2) (Wenz 1962). This splitting of the spectrum into passbands of a constant width of 1 Hz, however, does not represent how animals perceive sound.

Because animals perceive exponential increases in frequency rather than linear increases, analyzing a sound spectrum with passbands that increase exponentially in size better approximates real-world scenarios. In underwater acoustics, a spectrum is commonly split into 1/3-octave-bands, which are one-third of an octave wide; each octave represents a doubling in sound frequency. A very similar measure is to logarithmically divide each frequency decade into 10 passbands, which are commonly misnamed the 1/3-octave-bands rather than decidecades; we use this naming in the report. The center frequency of the ith decidecade-band, $f_c(i)$, is defined as:

$$f_c(i) = 10^{\frac{i}{10}}, \tag{A–10}$$

and the low (f_{lo}) and high (f_{hi}) frequency limits of the ith decidecade -band are defined as:

$$f_{\mathrm{lo},i} = 10^{\frac{-1}{20}} f_c(i) \quad \text{and} \quad f_{\mathrm{hi},i} = 10^{\frac{1}{20}} f_c(i) \tag{A–11}$$

The decidecade -bands become wider with increasing frequency, and on a logarithmic scale the bands appear equally spaced (Figure A-1).
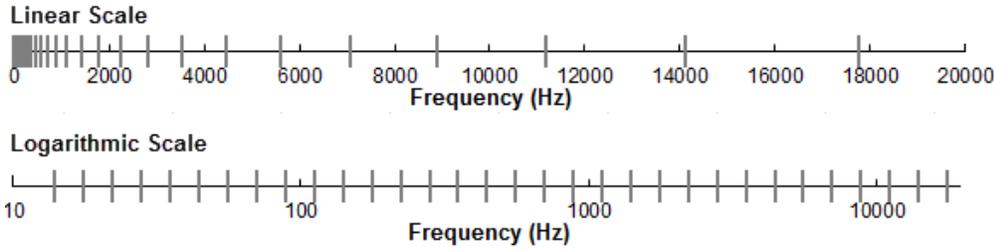
Figure A-1. Decidecade-bands (vertical lines) shown on a linear frequency scale and a logarithmic scale.

The sound pressure level in the ith band ($L_{\mathrm{p},i}$) is computed from the spectrum $S(f)$ between $f_{\mathrm{lo},i}$ and $f_{\mathrm{hi},i}$:

$$L_{\mathrm{p},i} = 10 \log_{10} \int_{f_{\mathrm{lo},i}}^{f_{\mathrm{hi},i}} S(f)\, df \tag{A-12}$$

Summing the sound pressure level of all the decidecade-bands yields the broadband sound pressure level:

$$\text{Broadband SPL} = 10 \log_{10} \sum_{i} 10^{\frac{L_{\mathrm{p},i}}{10}} \tag{A-13}$$

Figure A-2 shows an example of how the decidecade-band sound pressure levels compare to the power spectrum of an ambient noise signal. Because the decidecade-octave-bands are wider with increasing frequency, the decidecade-octave-band SPL is higher than the power spectrum, especially at higher frequencies. Decidecade-octave-band analysis is applied to both continuous and impulsive noise sources. For impulsive sources, the decidecade-octave-band SEL is typically reported.
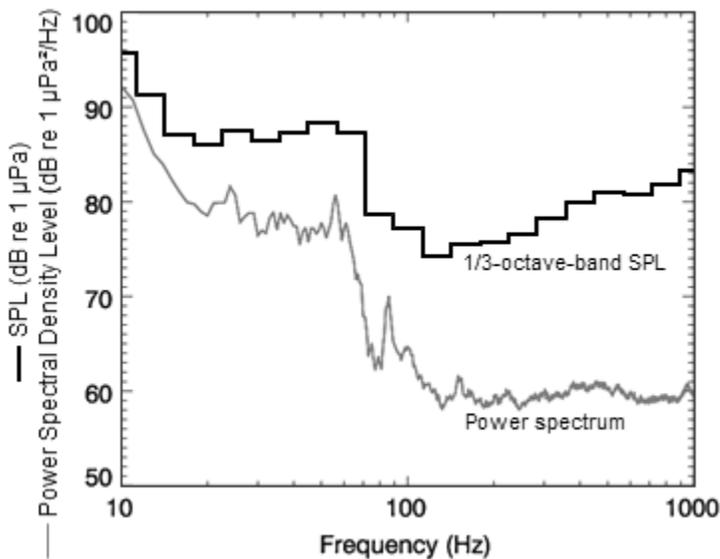
Figure A-2. A power spectrum and the corresponding decidecade-band sound pressure levels of example ambient noise shown on a logarithmic frequency scale. Because the decidecade-octave-bands are wider with increasing frequency, the decidecade-band SPL is higher than the power spectrum.

Table A-1. Decidecade-band frequencies (Hz).

Band	Lower frequency	Nominal center frequency	Upper frequency
10	8.9	10.0	11.2
11	11.2	12.6	14.1
12	14.1	15.8	17.8
13	17.8	20.0	22.4
14	22.4	25.1	28.2
15	28.2	31.6	35.5
16	35.5	39.8	44.7
17	44.7	50.1	56.2
18	56.2	63.1	70.8
19	70.8	79.4	89.1
20	89.1	100.0	112.2
21	112	126	141
22	141	158	178
23	178	200	224
24	224	251	282
25	282	316	355
26	355	398	447
27	447	501	562
28	562	631	708
29	708	794	891
30	891	1000	1122
31	1122	1259	1413
32	1413	1585	1778
33	1778	1995	2239
34	2239	2512	2818
35	2818	3162	3548
36	3548	3981	4467
37	4467	5012	5623
38	5623	6310	7079
39	7079	7943	8913
40	8913	10000	11220
41	11220	12589	14125
42	14260	16000	17952
43	17825	20000	22440
44	22281	25000	28050
45	28074	31500	35344

Band	Lower frequency	Nominal center frequency	Upper frequency
46	35650	40000	44881
47	44563	50000	56101
48	56149	63000	70687

Table A-2. Decade-band frequencies (Hz).

Decade band	Lower frequency	Nominal center frequency	Upper frequency
A	10	50	100
B	100	500	1,000
C	1,000	5,000	10,000
D	10,000	50,000	100,000

Appendix B. Detection Range Modeling

B.1. Sound Propagation Models: MONM-BELLHOP

Long-range sound fields were computed using JASCO's Marine Operations Noise Model (MONM). MONM is well suited for effective longer-range estimation but less accurately predicts steep-angle propagation for environments with higher shear speed. This model computes sound propagation at frequencies of 10 Hz to 2 kHz via a wide-angle parabolic equation solution to the acoustic wave equation (Collins 1993) based on a version of the U.S. Naval Research Laboratory's Range-dependent Acoustic Model (RAM), which has been modified to account for a solid seabed (Zhang and Tindle 1995). For this project, MONM computes sound propagation at frequencies above 2 kHz via the BELLHOP Gaussian beam acoustic ray-trace model (Porter and Liu 1994).

The parabolic equation method has been extensively benchmarked and is widely employed in the underwater acoustics community (Collins et al. 1996). MONM accounts for the additional reflection loss at the seabed, which results from partial conversion of incident compressional waves to shear waves at the seabed and sub-bottom interfaces, and it includes wave attenuations in all layers. MONM incorporates the following site-specific environmental properties: a bathymetric grid of the modeled area, underwater sound speed as a function of depth, and a geoacoustic profile based on the overall stratified composition of the seafloor.

MONM accounts for sound attenuation due to energy absorption through ion relaxation and viscosity of water in addition to acoustic attenuation due to reflection at the medium boundaries and internal layers (Fisher and Simmons 1977). The former type of sound attenuation is significant for frequencies higher than 5 kHz and cannot be neglected without noticeably affecting the model results.

MONM computes acoustic fields in three dimensions by modeling transmission loss within two-dimensional (2-D) vertical planes aligned along radials covering a 360° swath from the source, an approach commonly referred to as N×2-D. These vertical radial planes are separated by an angular step size of $\Delta\theta$, yielding N = 360°/$\Delta\theta$ number of planes (Figure B-1).
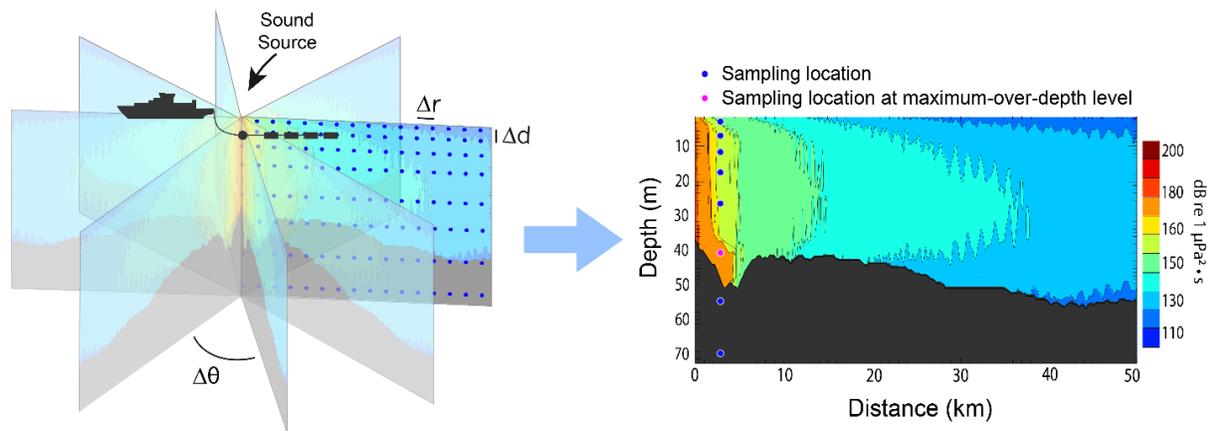
Figure B-1. The N×2-D and maximum-over-depth modeling approach used by MONM.

MONM treats frequency dependence by computing acoustic transmission loss at the center frequencies of decidecade bands. Sufficiently many decidecade bands, starting at 10 Hz, are modeled to include most of the acoustic energy emitted by the source. At each center frequency, the transmission loss is modeled within each of the N vertical planes as a function of depth and range from the source.

B.2. Marine Mammal Parameters

The parameters used as inputs to the Detection Range Modeling (see Section 2.3) are summarized in Table B-1.

Table B-1. Marine mammal input parameters. The detection threshold refers to the threshold of the relevant detectors.

Species	Frequency range (Hz)	Mean source level (dB)	Source level standard deviation	Source depth range (m)	Detection threshold	References
Mysticetes						
Fin Whale 20-Hz calls (Barents)	16–32	195.4	4.4	5–25	4	Garcia et al. (2018)
Fin Whale 20-Hz calls (global)	16–32	185	3	5–25	4	(Weirathmueller et al. 2013b), Wang et al. (2016)
Humpback Whale moans	50-1000	171	6	10–30	3	(Girola et al. 2019)
Odontocetes						
Sperm Whale clicks	2000–16000	186	1	100–1500	14	(Mathias et al. 2013)
Killer whale tonal signals	631–5000	155	6.5	5–50	3	(Holt et al. 2011)
White-beaked dolphin whistles	5000–20000	145	10	5–50	3	(Rasmussen et al. 2006)
White-beaked dolphin clicks	31500–100000	180	5	5–100	14	(Rasmussen et al. 2002, Atem et al. 2009)

B.3. Environmental Parameters

B.3.1. Bathymetry

Water depths throughout the modelled area were extracted from the SRTM15+ grid (Smith and Sandwell 1997, Becker et al. 2009).

B.3.2. Sound speed profile

The sound speed profiles for the modelled site were derived from temperature and salinity profiles from the U.S. Naval Oceanographic Office's Generalized Digital Environmental Model V 3.0 (GDEM; Teague et al. 1990, Carnes 2009). GDEM provides an ocean climatology of temperature and salinity for the world's oceans on a latitude-longitude grid with 0.25° resolution, with a temporal resolution of one month, based on global historical observations from the U.S. Navy's Master Oceanographic Observational Data Set (MOODS). The climatology profiles include 78 fixed depth points to a maximum depth of 6800 m (where the ocean is that deep). The GDEM temperature-salinity profiles were converted to sound speed profiles according to Coppens (1981).

Figure B-2 shows the resulting profiles for May and October used as an input to the sound propagation modelling. These two had represent the most extreme profiles during the study period.
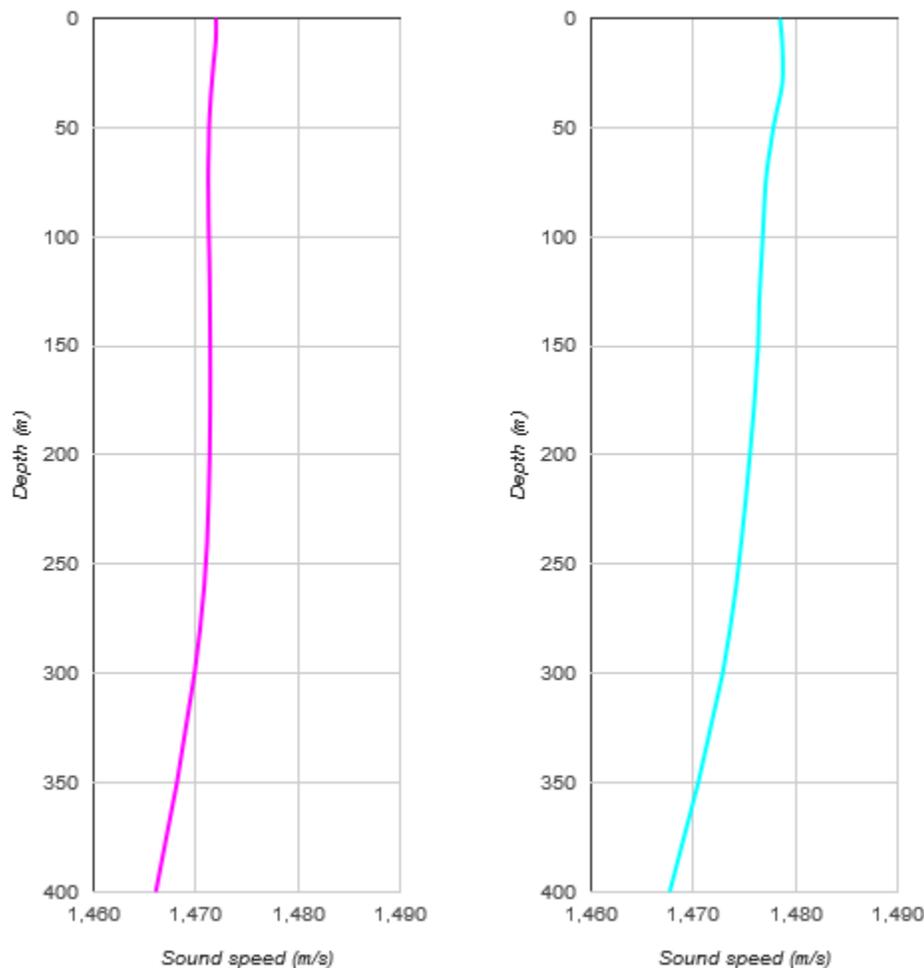
Figure B-2. The sound speed profiles for May (left) and October (right). The profile was calculated from temperature and salinity profiles from GDEM V 3.0 (GDEM; Teague et al. 1990, Carnes 2009).

B.3.3. Geoacoustics

The geoacoustic properties of the modelled area were defined based on published literature describing the bottom properties of the Barents Sea (Renard and Malod 1974, Sundvor 1975) as well as information provided by Equinor (J. Weissenberger, personal communication). Because of the uncertainty in the local geology, we defined two geoacoustic profiles (Figure B-3), which allows evaluating a potential range of detection ranges, if any. The main difference between both profiles is the rapid increase in sound speed at 400 m for profile MZ. This is to account for the superposition of a layer of unconsolidated young sediments above a layer of semi-consolidated sediments, whose sound speed differ (Renard and Malod 1974, Sundvor 1975). Based on preliminary modeling, the differences in geoacoustic profiles only yielded differences in ranges for the low-frequency signals of fin whales. For all other species, the detection ranges were modeled using the geoacoustic profile MZ.
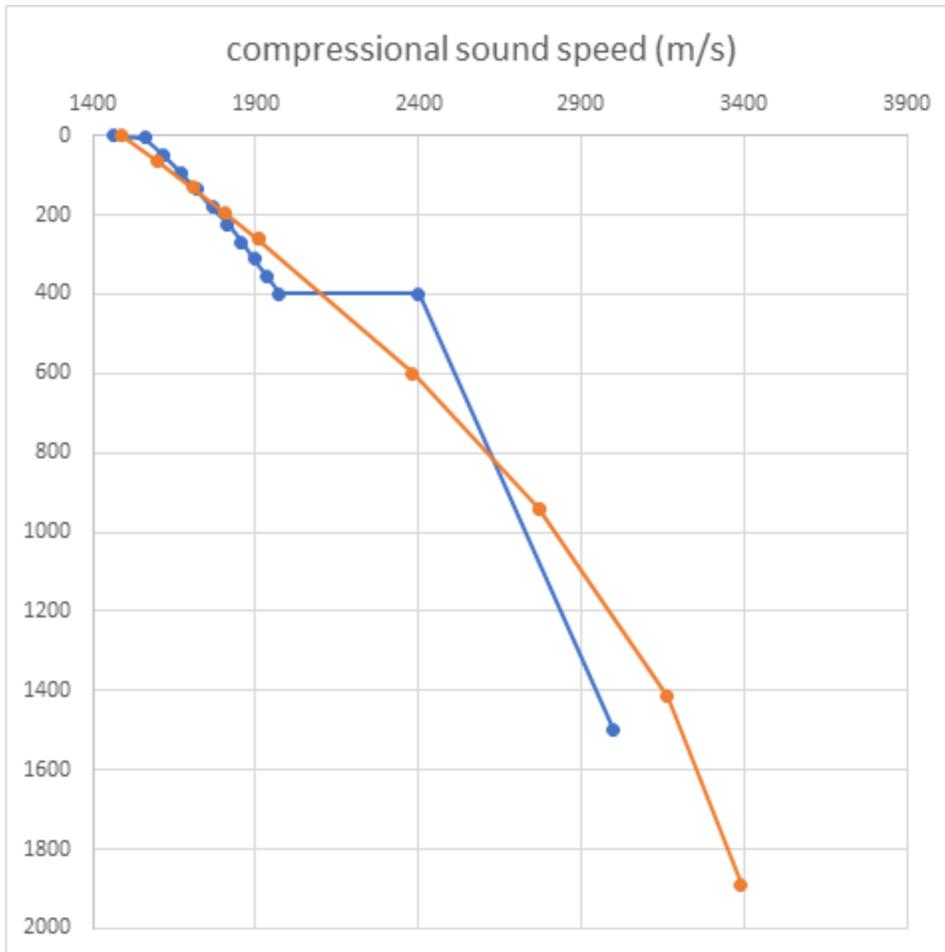
Figure B-3. Compressional sound speed as a function of depth (m) for profile MZ (blue) and MN (orange)

B.4. Model Validation Information

Predictions from JASCO's propagation models (e.g., MONM) have been validated against experimental data from a number of underwater acoustic measurement programs conducted by JASCO globally, including the United States and Canadian Artic, Canadian and southern United States waters, Greenland, Russia and Australia (Hannay and Racca 2005, Aerts et al. 2008, Funk et al. 2008, Ireland et al. 2009, O'Neill et al. 2010, Warner et al. 2010, Racca et al. 2012a, Racca et al. 2012b, Matthews and MacGillivray 2013, Martin et al. 2015, Racca et al. 2015, Martin et al. 2017a, Martin et al. 2017b, Warner et al. 2017, MacGillivray 2018, McPherson et al. 2018, McPherson and Martin 2018).

In addition, JASCO has conducted measurement programs associated with a significant number of anthropogenic activities which have included internal validation of the modeling that supported the detection range assessment (including McCrodan et al. 2011, Austin and Warner 2012, McPherson and Warner 2012, Austin and Bailey 2013, Austin et al. 2013, Zykov and MacDonnell 2013, Austin 2014, Austin et al. 2015, Austin and Li 2016, Martin and Popper 2016).

Appendix C. Marine Mammal Detection Methods

C.1. Automated Click Detector for Odontocetes

We applied an automated click detector/classifier to detect clicks from porpoise and dolphins (Figure C-1.). This detector/classifier is based on the zero-crossings in the acoustic time series. Zero-crossings are the rapid oscillations of a click's pressure waveform above and below the signal's normal level (e.g., Figure C-1.). Clicks are detected by the following steps (Figure C-1.):

1. The raw data is high-pass filtered to remove all energy below 5 kHz. This removes most energy from other sources such as shrimp, vessels, wind, and cetacean tonal calls, yet allows the energy from all marine mammal click types to pass.

2. The filtered samples are summed to create a 0.334 ms rms time series. Most marine mammal clicks have a 0.1–1 ms duration.

3. Possible click events are identified with a split-window normalizer that divides the 'test' bin of the time series by the mean of the 6 'window' bins on either side of the test bin, leaving a 1-bin wide 'notch'.

4. A Teager-Kaiser energy detector identifies possible click events.

5. The high-pass filtered data is searched to find the maximum peak signal within 1 ms of the detected peak.

6. The high-pass filtered data is searched backwards and forwards to find the time span where the local data maxima are within 9 dB of the maximum peak. The algorithm allows for two zero-crossings to occur where the local peak is not within 9 dB of the maximum before stopping the search. This defines the time window of the detected click.

7. The classification parameters are extracted. The number of zero crossings within the click, the median time separation between zero crossings, and the slope of the change in time separation between zero crossings are computed. The slope parameter helps to identify beaked whale clicks, as beaked whales can be identified by the increase in frequency (upsweep) of their clicks.

8. The Mahalanobis distance between the extracted classification parameters and the templates of known click types is computed. The covariance matrices for the known click types, computed from thousands of manually identified clicks for each species, are stored in an external file. Each click is classified as a type with the minimum Mahalanobis distance, unless none of them are less than the specified distance threshold.
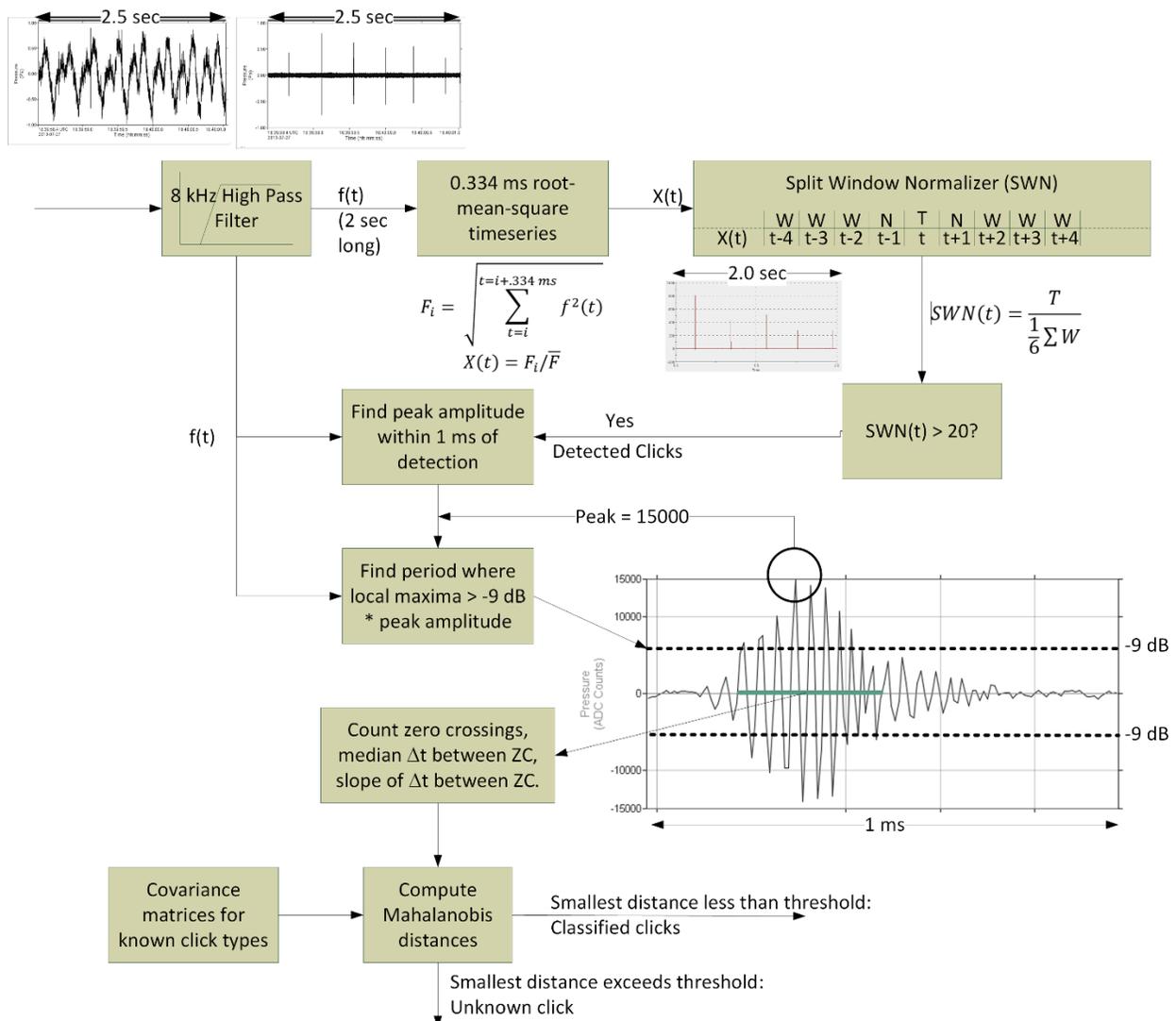
Figure C-1. The click detector/classifier block diagram.

Odontocete clicks occur in groups called click trains. Each species has a characteristic inter-click-interval (ICI) and number of clicks per train. The click detector includes a second stage that associates individual clicks into trains (Figure C-2). The steps of the click train associator algorithm are:

1. Queue clicks for N seconds, where N is twice the maximum number of clicks per train times the maximum ICI.

2. Search for all clicks within the window that have Malahanobis distances less than 11 for the species of interest (this gets 99% of all clicks for the species as defined by the template).

3. Create a candidate click train if:

    a. the number of clicks is greater or equal to the minimum number of clicks in a train;

    b. the maximum time between any two clicks is less than twice the maximum ICI, and

    c. the smallest Malahanobis distance for all clicks in the candidate train is less than 4.1.

4. Create a new 'time-series' that has a value of 1 at the time of arrival of each clicks and zeroes everywhere else.

5.   Apply a Hann window to the timeseries then compute the cepstrum.

6.   A click train is classified if a peak in the cepstrum with amplitude > 5 times the standard deviation of the cepstrum occurs at a quefrency between the minimum maximum ICI.

7.   Queue clicks for N seconds

8.   Search for all clicks within the window that have Malahanobis distances less than 10 (equal to the extent of the variance in the training data set).

9.   If the number of clicks is greater than or equal to 3 and dT is less than 2 * max ICI, make a new time-series at the 0.333 ms rate; where the value is 1 when the clicks occurred and 0 for all other time bins. Perform the following processing on this time series:

     a.   Compute cepstrum

     b.   ICI is the peak of the cepstrum with amplitude > 5 * stdev and searching for quefrency between minICI and maxICI.

     c.   For each click related to the previous Ncepstrum, create a new time series and compute ICI; if we get a good match, extend the click train; find a mean ICI and variance.

10. If the click features, total clicks and mean ICI match the species, output a species_click_train detection.
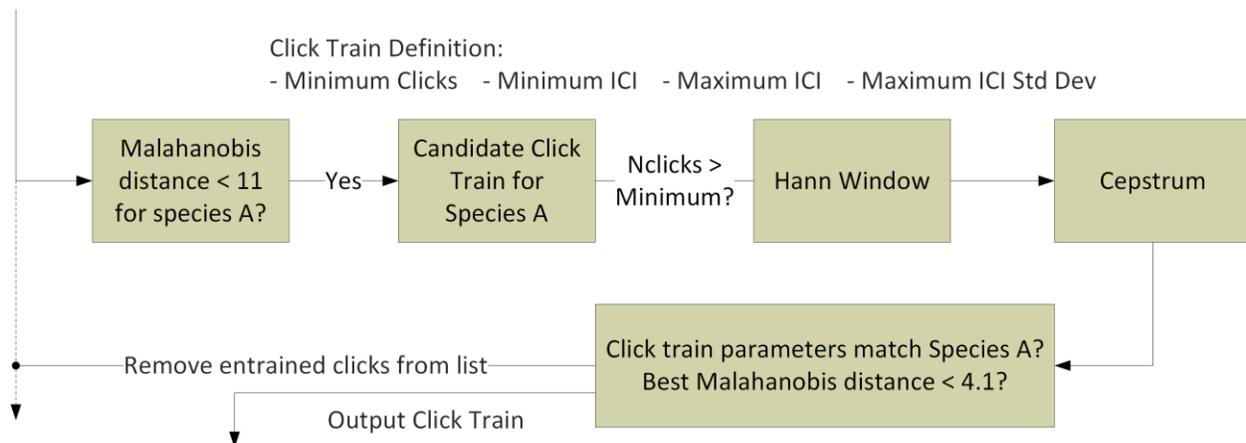
Figure C-2. The click train detector/classifier block diagram.

C.2. Tonal Signal Detection

Marine mammal tonal acoustic signals are detected by the following steps:

1.   Spectrograms of the appropriate resolution for each mammal vocalization type that were normalized by the median value in each frequency bin for each detection window (Table C-1.) were created.

2.   Adjacent bins were joined, and contours were created via a contour-following algorithm (Figure C-3.).

3.   A sorting algorithm determined if the contours match the definition of a marine mammal vocalization (Table C-2.).
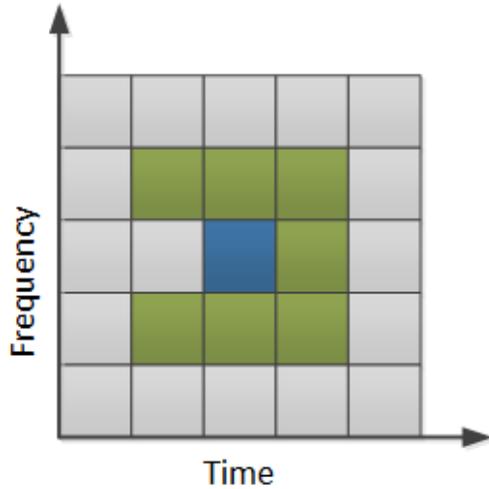
Figure C-3. Illustration of the search area used to connect spectrogram bins. The blue square represents a bin of the binary spectrogram equaling 1 and the green squares represent the potential bins it could be connected to. The algorithm advances from left to right so grey cells left of the test cell need not be checked.

Table C-1. Fast Fourier Transform (FFT) and detection window settings for all contour-based detectors used to detect tonal vocalizations of marine mammal species expected in the data. Values are based on JASCO's experience and empirical evaluation on a variety of data sets.

| Detector	FFT			Detection window (s)	Detection threshold
	Resolution (Hz)	Frame length (s)	Timestep (s)		
Atl_BlueWhale_GL_IM	0.125	2	0.5	40	4
Atl_BlueWhale_IM	0.125	2	0.5	40	4
Atl_BlueWhale_IM2	0.125	2	0.5	120	4
Atl_FinWhale_130	2	0.2	0.05	5	3
Atl_FinWhale_21	1	0.2	0.05	5	1.7
Atl_FinWhale_21.2	1	0.2	0.05	5	4
MinkePulseTrain	8	0.1	0.025	1	40
N_RightWhale_Up1	4	0.128	0.032	8	2.5
N_RightWhale_Up2	4	0.128	0.032	8	3
N_RightWhale_Up3	7	0.17	0.025	10	3
SeiWhale	3.25	0.2	0.035	5	3.5
VLFMoan	2	0.2	0.05	15	4
LFMoan	2	0.25	0.05	10	3
ShortLow	7	0.17	0.025	10	3
MFMoanLow	4	0.2	0.05	5	3
MFMoanHigh	8	0.125	0.05	5	3
WhistleLow	16	0.03	0.015	5	3
WhistleHigh	64	0.015	0.005	5	3

Table C-2. A sample of vocalization sorter definitions for the tonal vocalizations of cetacean species expected in the area.

Detector	Target species	Frequency (Hz)	Duration (s)	Bandwidth (B; Hz)	Other detection parameters
Atl_BlueWhale_GL_IM	Blue whales	14–22	8.00–30.00	1<B<5	minSweepRate= −500 Hz/s; minF<18 Hz 16.5<PeakF<17.5 Hz
Atl_BlueWhale_IM	Blue whales	14–22	8.00–30.00	1<B<5	minSweepRate= −500 Hz/s; minF<18 Hz 16.5<FrequencyOfPeakIntensity<18 Hz
Atl_BlueWhale_IM2	Blue whales	15–22	8.00–30.00	1<B<5	N/A
Atl_FinWhale_130	Fin whales	110–150	0.30–1.50	>6	minF<125 Hz
Atl_FinWhale_21	Fin whales	10–40	0.40–3.00	>6	-100<SweepRate<0 Hz/s; minF<17 Hz 20<FrequencyOfPeakIntensity<22 Hz
Atl_FinWhale_21.2	Fin whales	8–40	0.30–3.00	>6	-100<SweepRate<0 Hz/s; minF<17 Hz
MinkePulseTrain	Minke whales	50–500	0.025–0.3		0.25<PulseGap<2 s; 10<TrainLength<100 s
N_RightWhale_Up1	Right whales	65–260	0.60–1.20	70<B<195	minF<75 Hz 30<SweepRate<290 Hz/s
N_RightWhale_Up2	Right whales	65–260	0.50–1.20	B>25	30<SweepRate<290 Hz/s
N_RightWhale_Up3	Right whales	30–400	0.50–10.00		10<SweepRate<500 Hz/s
SeiWhale	Sei whales	20–150	0.50–1.70	19<B<120	-100<SweepRate<−6 Hz/s InstantaneousBandwidth<100 Hz
VLFMoan	Blue/fin/sei whales	10–100	0.30–10.00	>10	minF<40 Hz
LFMoan	Blue/right/sei whales	40–250	0.50–10.00	>15	InstantaneousBandwidth<50 Hz
ShortLow	Fin/baleen whales	30–400	0.08–0.60	>25	N/A
MFMoanLow	Humpback whales	100–700	0.50–5.00	>50	minF<450 Hz InstantaneousBandwidth<200 Hz
MFMoanHigh	Humpback whales	500–2500	0.50–5.00	>150	minF<1500 Hz InstantaneousBandwidth<300 Hz
WhistleLow	Pilot/killer whales	1000–10000	0.50–5.00	>300	Max Instantaneous Bandwidth = 1000 Hz minF<5000 Hz
WhistleHigh	Other delphinid	4000–20000	0.30–3.00	>700	Max Instantaneous Bandwidth = 5000 Hz

C.3. File Selection Process for Validating Detections

To standardize the file selection process, we developed an algorithm that automatically selects a sample of files for review. The selection process starts by computing the distribution of three variables that describe the detections in the full data set: the diversity of detected species per file, the number of detections per file (per species), and the temporal distribution of each species. The algorithm iteratively removes files from the data set by computing the difference between the original distribution and the distribution without each file—the file whose removal brings the new distribution closest to the original distribution is removed. The process is repeated until the sample size is reduced to N, which was set to 1 or 2% of the total duration of acoustic data. In this description, the term 'species' identifies a marine mammal detector whose performance needs to be assessed. The three variables used by the algorithm are described further below:

1. **Diversity**: Select files representative of the range of species diversity (number of detected species in a file). The diversity of the full data set is log transformed to reduce the skew of the data. After being logged, the histogram bin size of the full data set is calculated using the Freedman-Diaconis rule (Freedman and Diaconis 1981), with a maximum of 20 bins. Sample files are selected such that the distribution of diversity within the sample matches the distribution of logged diversity in the full data set.

2. **Counts**: Select files representative of the range of detection counts (number of detections per file for each species). For each species, the detection counts of the full data set are log transformed to manage the skew of the data. After being logged, the histogram bin size of the full data set is calculated using the Freedman-Diaconis rule (Freedman and Diaconis 1981), with a maximum of 20 bins. Sample files are selected such that the distribution of detection counts within the sample matches the distribution of logged detection counts in the full data set. Files with no detections are not included in the calculation for each species (0-detection count files for a species will naturally be included in files selected for other species).

3. **Temporal distribution**: Select files representative of the temporal range of files containing detections for each species. The time frame of the full data set is divided into 12 equally sized bins. If the bin size is greater than 30 days, then the time frame is divided into 30-day bins. File counts per species for each bin are log transformed to reduce the skew of the data. Sample files are selected such that the distribution of files containing detections for each species within the sample matches the distribution of files containing detections for each species in the full data set.

In each iteration, we remove the file whose omission minimizes the Total Variation (υ_T). The υ_T is the sum of the following:

- Diversity Variation (υ_D),

- Count Variation (υ_C), which is the average of the per species count variations (υ_{C_s}), and

- Temporal Distribution Variation (υ_{TD}), which is the average of the per species temporal variations (υ_{TD_s}).

$$\upsilon_T = \upsilon_D + \upsilon_C + \upsilon_{TD}$$

$$\Delta = \sum_{b=1}^{B} |Pf_b - Ps_b|$$

$$\upsilon_D = \Delta_D$$

$$\upsilon_{C_s} = \Delta_{C_s}$$

$$\upsilon_C = \frac{\sum_{s=1}^{S} \upsilon_{C_s}}{S}$$

$$v_{TD_S} = \Delta_{TD_S}$$

$$v_{TD} = \frac{\sum_{s=1}^{S} v_{TD_s}}{S}$$

where Pf_b is proportion of bin 'b' within the full data set, Ps_b is the proportion of bin 'b' within subset 's', Δ is difference between distributions, B is the total number of bins in the distribution, and S is the number of species. Two final constraints on the algorithm are preserving at least 10 files per species and attempting to have the files for each species at least 6 h apart.

Once the sample size has been reduced to N, the two files with the highest detection counts for each species are added back into the sample, if they were not already included. This can result in the final sample being trivially greater than N.

C.4. Divergence Curves

In order to assess whether the selected validation effort was appropriate to produce accurate detector performance metrics, we calculated the variation of the three variables used to score validation file samples (i.e., Diversity, Counts and Temporal Distribution; see Appendix C.3) plus an aggregate score (labelled 'Overall' in Figure C-4) from the full data set for decreasing sample sizes (N), where low variation (denoted Divergence in Figure C-4) indicates little difference between the sample and the full dataset. The N at which the average variation of the three variables and aggregate score is minimal (distribution of sample does not get closer to that of full data set with further decreases in sample size) can be determined. This N$_{ideal}$ represents the minimum proportion of files to be validated. N$_{ideal}$ can vary across data sets depending on the acoustic environments encountered throughout the data sets and the automated detectors employed.
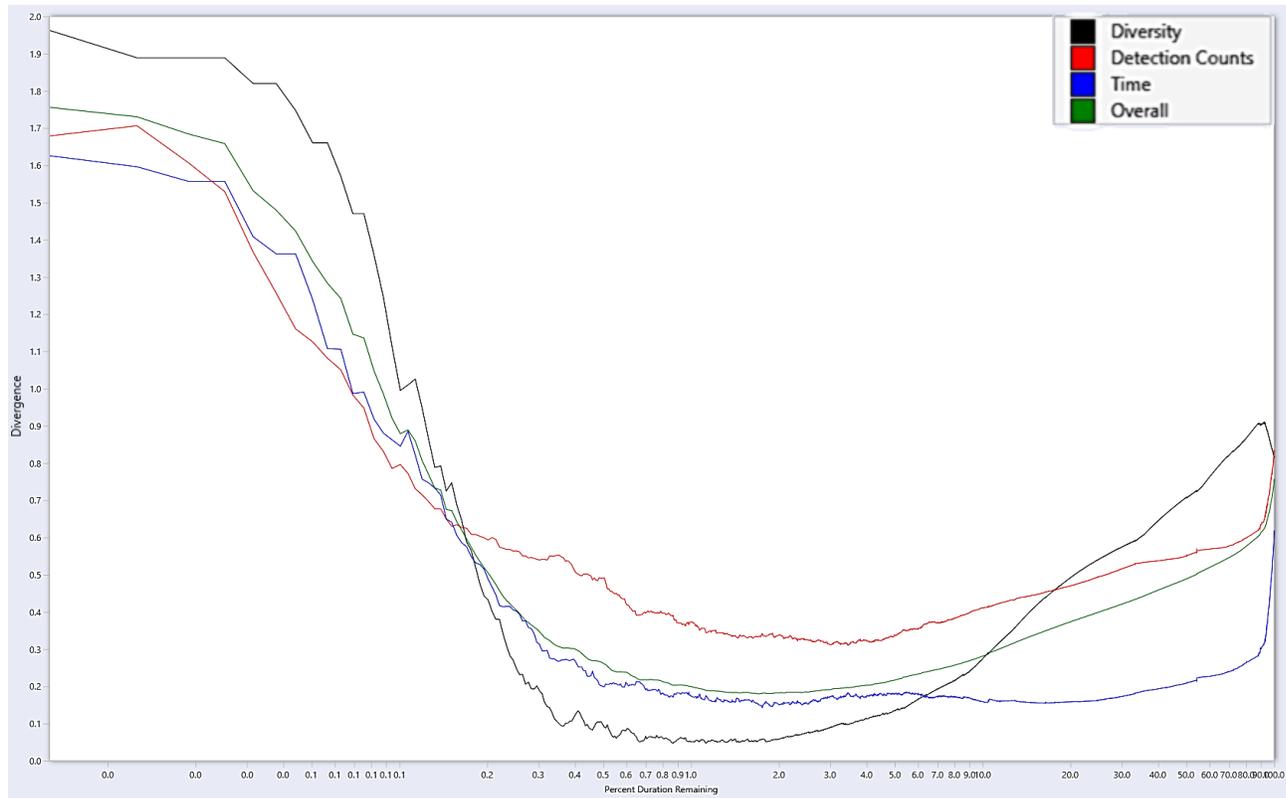

Figure C-4. An example of divergence curves.

C.5. Detector Performance Calculation and Optimization

All files selected for manual validation were reviewed by one of two experienced analysts using JASCO's PAMlab software to determine the presence or absence of every species, regardless of whether a species was automatically detected in the file. Although the detectors classify specific signals, we validated the presence/absence of species at the file level, not the detection level. Acoustic signals were only assigned to a species if the analyst was confident in their assessment. When unsure, analysts would consult one another, peer-reviewed literature, and other experts in the field. If certainty could not be reached, the file of concern would be classified as possibly containing the species in question or containing an unknown acoustic signal. A sample of manually validated vocalizations were reviewed by a senior analyst for all stations to look for erroneous records or assign unidentified signals to a known species. Next, the validated results were compared to the raw detector results in three phases to refine the results and ensure they accurately represent the occurrence of each species in the study area.

In phase 1, the validated versus detector results were plotted as time series and critically reviewed to determine when and where automated detections should be excluded. Questionable detections that overlap with the detection period of other species were scrutinized. By restricting detections spatially and temporally where appropriate, we can maximize the reliability of the results. The following restrictions were applied to our detector results:

1. If a species was automatically detected at a location, but was never manually validated, all automated detections were considered false and the species was considered absent.

2. If a species was automatically detected over a specific timeframe, but manual validation revealed all detections to be falsely triggered by another sound source or species, all automated detections during that period were excluded. Any time frame restrictions employed are described in the results section.

In phase 2, the performance of the detectors was calculated based on the phase 1 restrictions and optimized for each species using a threshold, defined as the number of detections per file at and above which detections of species were considered valid.

To determine the performance of each detector and any necessary thresholds, the automated and validated results (excluding files where an analyst indicated uncertainty in species occurrence) were fed to a maximum likelihood estimation algorithm that maximizes the probability of detection and minimizes the number of false alarms using the MCC:

$$MCC = \frac{TPxTN - FPxFN}{\sqrt{(TP + FP)(TP + FN)(TN + FP)(TN + FN)}}$$

$$P = \frac{TP}{TP + FP}; R = \frac{TP}{TP + FN}$$

where *TP* (true positive) is the number of correctly detected files, *FP* (false positive) is the number of files that are false detections, and *FN* (false negatives) is the number of files with missed detections.

Where the number of validated files was too low, and/or the overlap between manual and automated detections was too limited for the calculation of *P*, *R*, and MCC, automated detections were ignored, and only validated results were used to describe the acoustic occurrence of a species.